

Thèse de doctorat
Pour obtenir le grade de Docteur de l'Université de
VALENCIENNES ET DU HAINAUT-CAMBRESIS
et l'Université de MONS

Discipline, spécialité selon la liste des spécialités pour lesquelles l'Ecole Doctorale est accréditée :
Sciences et Mécanique

Ecole doctorale :

Sciences Pour l'Ingénieur (SPI)

Laboratoires :

Laboratoire d'Automatique, de Mécanique et d'Informatique Industrielles et Humaines (LAMIH)
Service des Matériaux Polymères et Composites (SMPC)

**Elaboration of Polylactide-based materials for automotive application: Study
of structure-process-properties interactions**

**Elaboration des matériaux à base de l'acide polylactique pour application
automobile: Etude des interactions entre structure-process-propriétés**

par Amani BOUZOUITA

A soutenu le 12/10/2016, à Valenciennes, devant le Jury composé de :

Rapporteurs

- Mme Sandra Domenek, Professeure des Universités, Agro ParisTech.
- M. Yves Grohens, Professeur des Universités, LIMATB. **Président du jury**

Examineurs

- M. Marius Murariu, Chercheur Senior, centre de recherche Materia Nova.
- M. Philippe Dubois, Professeur, centre de recherche LIST.
- M. Cyrille Sollogoub, Maître de conférences, Art et Métiers PariTech CNAM.

Directeurs de thèse

- M. Franck Lauro, Professeur des Universités, Université de Valenciennes - LAMIH
- M. Jean-Marie Raquez, Chercheur qualifié FNRS, Université de Mons - SMPC

Co-encadrante :

- Mme Delphine Notta-Cuvier, Maître de Conférences, Université de Valenciennes - LAMIH

REMERCIEMENTS

Je fais partie des personnes qui croient qu'il n'y a de force ni de puissance que par Dieu. Cela étant, je commence par le remercier d'avoir eu la bonté de m'entourer de personnes formidables qui ont, chacune à leur façon, et ce, à différentes étapes de mon cheminement, contribué, d'une manière ou d'une autre, à la réalisation de cette thèse de doctorat.

Je souhaite remercier Pr. Philippe Dubois, pour la confiance qu'il m'a témoignée en m'accueillant dans son service SMPC ainsi que Pr. Franck Lauro de m'avoir permis de réaliser cette thèse au sein du laboratoire LAMIH.

Je tiens à remercier la région Nord-Pas-de-Calais ainsi que la région wallonne et la communauté européenne (FEDER, FSE) pour le financement de cette thèse.

Je tiens à remercier mes directeurs de thèse Franck Lauro et Jean Marie Raquez, ainsi que ma co-encadrante Delphine Notta-Cuvier pour la confiance qu'ils m'ont accordée en acceptant d'encadrer ce travail doctoral, pour leurs multiples conseils et pour toutes les heures qu'ils ont consacrées à diriger cette recherche. J'aimerais également leur dire à quel point j'ai apprécié leur grande disponibilité et leur respect sans faille des délais serrés de relecture des documents que je lui ai adressés. Enfin, j'ai été extrêmement sensible à leurs qualités humaines d'écoute et de compréhension tout au long de ce travail doctoral.

Je remercie les membres du jury Messieurs Cyrille Sollogoub, Yves Grohens, Marius Murariu et Philippe Dubois et Madames Sandra Domenek et Delphine Notta-Cuvier d'avoir accepté de juger ce travail.

Je tiens à remercier tous les membres du centre de la recherche Materia Nova et plus particulièrement M.Yoann Paint, Mme. Lisa Dangreau, M. Marius Murariu, Mme. Oltea Murariu pour votre aide, vos formations ainsi que les nombreuses analyses effectuées au sein de votre service.

Je tiens à remercier aussi les membres du laboratoire LAMIH plus particulièrement M. Rémi Dellile et M. Gregory Haugou, M. Bruno Bennani ainsi que M. Christophe Germain le responsable de notre partenaire industriel Reydel et toute leur équipes pour leurs échanges et collaborations au cours de ma thèse.

Merci à nos post-doc Dr. Cédric Samuel et Dr. Jérémy Odent, qui ont assisté à mes débuts comme nouvelle doctorante, merci pour votre training très pédagogique et votre assistance dans le démarrage de mon aventure au sein du laboratoire.

Réaliser ce travail n'aurait pas été possible sans ma famille qui a toujours encouragé et soutenu toutes mes idées et mes projets, aussi loin qu'ils peuvent être parfois. Je souhaite remercier ma mère Nassima et mon père Nouredine, mon mari Kaies ainsi que mon frère Ahmed, ma belle-sœur Amel, mon neveu Iskander, mes tantes, ma grand mère et surtout mes cousins et mes cousines (Ines, Marwa, Kikou, Souheyla, Asma,

Farah, Souheyel, Hosny...) pour l'intérêt qu'ils ont toujours porté à ce que je réalise. Merci d'avoir toujours été là et de m'avoir tant aidé. Vous avez su me donner toutes les chances pour réussir. Que vous trouvez, dans la réalisation de ce travail, l'aboutissement de vos efforts ainsi que l'expression de ma plus affectueuse gratitude.

Ben, merci pour ta disponibilité, ta sensibilité aux contextes personnels à travers lesquels tes étudiants tentent d'atteindre tous les objectifs d'un doctorat, merci pour ton ouverture à nos caractères et à notre touche propres en recherche, merci pour la liberté que tu nous laisses en nous témoignant ta confiance dans notre travail. Ce sont cette confiance et cette liberté qui, à mon avis, nous laissent spontanément faire ressortir le meilleur de nous-même dans notre travail et comme personnes. Merci de reconnaître nos efforts et nos difficultés. Merci pour la relation que nous avons pu développer depuis mon arrivée au labo (*Ben's Angels*). Merci enfin pour ton soutien incroyablement solide, attentif, fiable, cordial dans mon sprint final des dernières semaines... Tu as beaucoup facilité la longue traversée de mes années de doctorat, comme d'ailleurs mes chers collègues de bureau avec qui j'ai créé des liens plus que professionnels.

Je remercie du fond du cœur l'ensemble des membres du Service des Matériaux Polymères et Composites (SMPC): Florence, Sutima, Michèle, Alex, Lucie, Benjamin, Riccardo, Antoniya, Bertrand, Hamid, Giada, Valentina, Mounch, Nicolas, Ali, Rémi, Bastien, Noémie, Jin, Samira, Rosica, Leila et Xavier. Merci pour le bel esprit de solidarité dans le bureau, de soutien et de compréhension, de sensibilité envers les autres, d'encouragements mutuels, merci pour tout le côté social et l'humour qui rend la vie tellement plus légère au quotidien! J'ai apprécié toutes nos discussions. Je tiens à remercier The Scientific workshop pour la bonne ambiance et les bons moments passés ensemble. Ce fut une chance de partager avec vous pendant ces trois ans nos vies, nos ambitions, nos rêves, nos soirées et surtout les repas préparés avec beaucoup d'amour et de passion. Vous étiez et vous resterez pour toujours ma famille.

« Les vrais amis ne sont jamais loin, peut-être dans la distance, mais pas dans le cœur ». Mejda, Molka et Abir, je vous remercie pour le soutien et l'attention que vous m'avez accordés et qui ont été très importants pour me permettre d'aller au bout de cette thèse. Sans oublier aussi mes amis Ameni, Matou, Achref, Anis, Amine, Maynou, Rami, Salah, Rim et Mariem, pour ces trois années durant lesquelles on a créé une belle amitié, tant d'ambiances et tant de souvenirs. Je ne pourrais jamais assez les remercier.

Finalement, je remercie tout le monde de m'avoir donné l'opportunité de découvrir à la fois deux pays si proche en distance mais si loin en habitudes et traditions. Et entre la Belgique et la France je préfère bien sûr ma chère Tunisie où on peut profiter du beau temps ensoleillé toute l'année.

"Believe in yourself and all that you are. Know that there is something inside you that is greater than any obstacle."

Table of contents

Chapter I: General introduction	1
I.1 (Bio)plastics in the automotive industry	1
I.1.1. Technical requirements for plastics used in car applications	2
I.1.2. Why PLA is being viewed as key-material for cars?	4
I.2 Aim of the work	8
Chapter II: State of art-Development of high-performance PLA-based materials	12
II.1 Highly tough and/or ductile PLA-based blends	12
II.1.1. Plasticized PLA blends	13
II.1.2. Rubber-toughened PLA blends	16
II.1.3. Annealing process	20
II.2 Heat resistance PLA-based blends	21
II.2.1. Highly thermal PLA-based nanocomposites	22
II.2.2. PLA/petro-sourced polymer blends of high thermal stability	25
II.2.3. Heat-resistance PLA-based stereocomplexes	26
II.3 Mold-injected PLA-materials for automotive applications	29
II.4. Durable PLA/polymer blends	33
Research Strategies	45
Chapter III: Design of highly tough poly(L-lactide)-based ternary blends for automotive applications	47
III.1. Miscibility of ternary blends	51
III.2. Mechanical properties of PLA-based blends	54
III.3 Morphology of rubber-toughened blends	58
Chapter IV: Improving crystallinity of highly tough poly(L-Lactide)-based ternary blends	70
IV.1 Annealing	74
IV.2 Stereocomplexing PLA-based materials	81
IV.3 Combination of Nucleating agent and nanoparticles	88
Chapter V: Highly tough poly(L-Lactide)-based ternary blends toward industrialization	98
V.1 Industrialization of Processes	101
V.2 Quasi-Static and Dynamic Tensile Tests at ambient temperature	104

V.3 Quasi-static tensile tests at high temperature	113
V.4 Dynamic mechanical analysis of PLA based materials	115
V.4.1 Evolution of dynamic mechanical properties of PLA-PMMA-BS as a function of frequency for all test temperatures	116
V.4.2 Comparison of PLA/PMMA/BS blends with PLA/BS blends	117
V.4.3 Comparison of PLA/PMMA/BS blends with ABS/PC blends	120
V.5 Study of durability of PLA based blends	122
Conclusion and outlooks	133

CHAPTER I

GENERAL INTRODUCTION

General Introduction

I.1 (Bio)plastics in the automotive industry

The plastics industry plays a significant role on the environmental, societal and economic dimensions of sustainable development. Plastics meet the societal demands of today's products in terms of packaging, lightweight components in cars and aircraft, electronic housing, insulating materials in buildings, medical devices, etc. Yet, plastics industry has still to face up to great challenges dealing with the improvement of safety, protection of the environment and energy-saving in plastics manufacturing processes as well as during their lifetime. In automotive sector, plastics and polymer composites are more and more appealing in order to decrease the fuel-consumption of vehicles, without hampering the safety issues. Indeed, automotive manufacturers tend to replace traditional materials such as metals and metal alloys by lightweight materials such as plastics and composites[1,2]. As an illustration, the contribution of plastics to the average weight of a vehicle is presented in Figure I.1. Today, plastics typically make up 16 % of the average weight of a new vehicle and will account for 18% by 2020, which renders cars lighter and more fuel efficient, resulting to lower greenhouse gas-emissions[3,4].

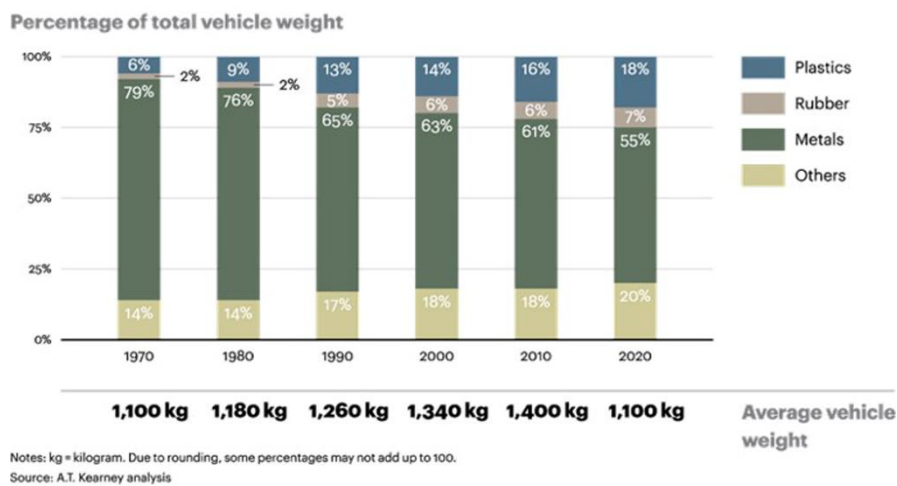


Figure I.1. Evolution of plastics' weight percentage in vehicle [10]

Furthermore, a main challenge of twenty-first century is undoubtedly a sustainable management of resources that is accompanied by new environmental regulations and the take-off of

bioeconomy. This later refers to the sustainable production and conversion of renewable resources from agriculture into a large range of food, health, fiber and industrial products and energy[5]. This trend is pushing automotive manufacturers to propose renewable alternatives to traditional petroplastics, while fulfilling the current and new specification sets of the automotive parts, in order to produce smarter, lighter, greener and, if possible, low cost cars. In that context, bioplastics meet these requirements since they may have similar structural and functional characteristics than their petro-sourced counterparts. We must highlight that the term bioplastics covers materials that are partially or fully biosourced. Beyond their initial use for packaging applications [6-8], bioplastics have reached a very high level of maturity for a large range of automotive applications, offering high performance together with a reduced environmental impact. It is therefore not surprising that the automotive market is becoming one of the major application fields for the bioplastics industry (Figure I.2).

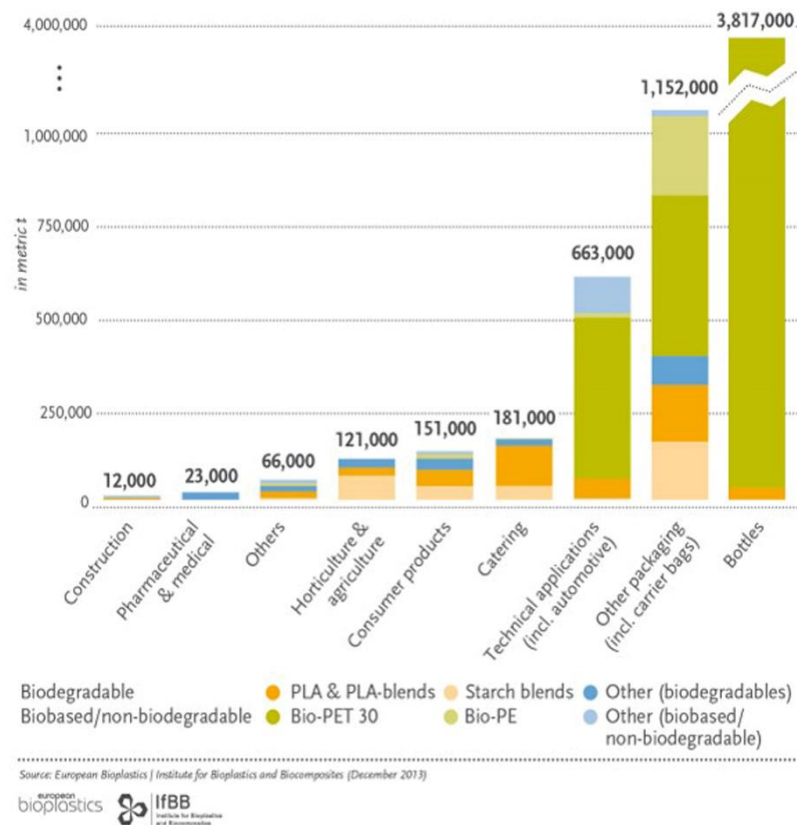


Figure I.2. Global production capacities of bioplastics 2017 by market segment [9]

I.1.1. Technical requirements for plastics used in car applications

Today, plastics are employed to build not only the internal parts as well as the external components in automotive like bumpers to body panels, laminated safety glasses, trims and

many other components (Figure I.3). In the exterior applications, plastics are not used only for their lightweightness but also because they give the freedom to designers for creating innovative concepts, for instance parts of complex shape that could not be massively manufactured using other materials. In other terms, plastics have been nothing less than being revolutionary. They have proven to be great materials for creating comfortable, durable and aesthetically pleasing interior components, while preserving occupant protection, reducing noise and vibration levels. Finally, for electrical, powertrain, fuel, chassis and engine applications, they have proven to be strong, durable, corrosion-resistant and able to withstand high temperatures in harsh engine environments.

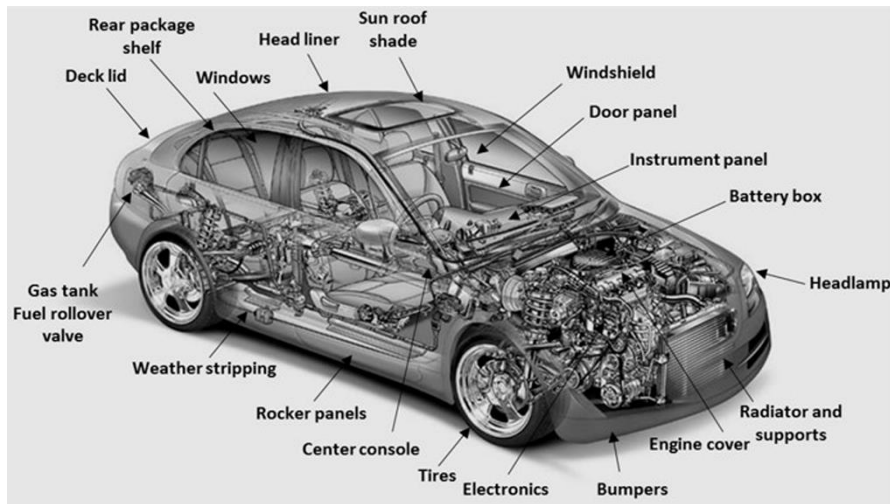


Figure I. 3. Auto part for lightweight plastics and rubber

Usually, the choice of materials made by vehicle manufacturers depends on a combination of several criteria. Some of the criteria are, for instance, the result of regulation and legislation with environmental and safety concerns. The other ones concern the production cost, mechanical and physical properties and weight reduction. Different characteristics are often mentioned as materials selection criteria for automotive industry (Figure I.4) [10-14]. These criteria will vary upon the type of vehicle and component application, as previously mentioned. In many cases, different factors may be conflicting - and therefore a successful design would be only possible through an optimum and balanced solution.

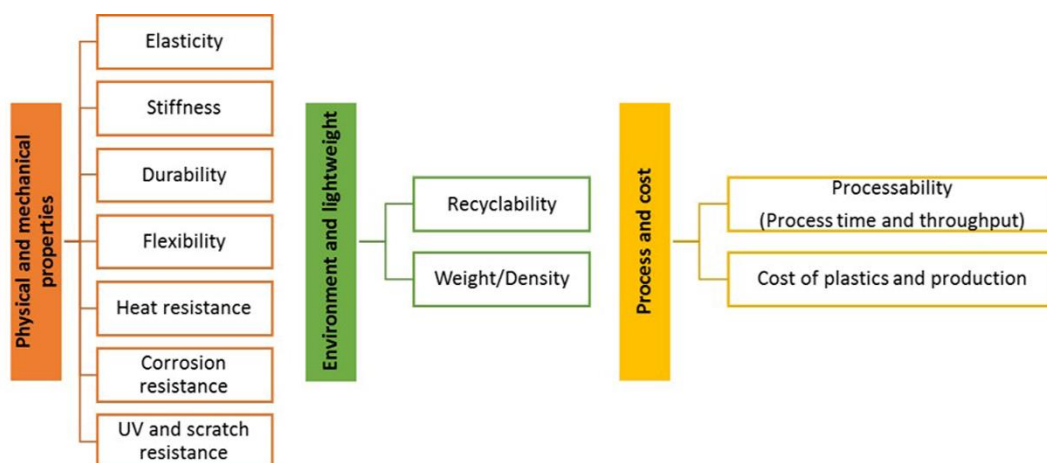


Figure I.4. Criteria used in automotive plastics selection/component design

Many types of petro-based plastics that can provide technical requirements for automotive sector are employed in more than 1000 different parts of all shapes and sizes. The most important polymers in automotive industry are polypropylene (PP), used for instance in body panel bumpers and fuel systems; polyamide (PA), used in seats and electrical components, poly(methyl) methacrylate (PMMA) and polyurethane (PU) used in lighting; polycarbonate (PC) used also in bumpers, dashboards, interior and exterior trim and usually associated with acrylate-butadiene-styrene (ABS)[15].

1.1.2. Why PLA is being viewed as key-material for cars?

Together with other bioplastic polymers such as polyhydroxyalkanoate (PHA), polycaprolactone (PCL), polytrimethylene terephthalate (PTT), biopolyamide (BioPA) and biopolyethylene(BioPE)[16], for instance, poly(lactic acid) (PLA), a plastic currently derived from starch, is becoming one of the most popular alternatives to traditional petroleum-based plastics in automotive applications. Ring-opening polymerization (ROP) of lactide is the preferred commercial route to prepare PLA because of the higher controllability of the polymerization and the possibility to readily get high molecular weight PLA [17]. Three stereoisomers of lactide can be generated *i.e.* L,L-LA, D,D-LA, and D,L-LA (meso lactide) as well as a 50/50 mixture of L,L-LA and D,D-LA referred to as racemic lactide (Figure II.2). Modulation of the polymer stereochemistry leads to PLA with dramatically different properties. For example, PLLA is a semicrystalline polymer (T_g at 60°C , melting transition at 180°C), while poly(rac-lactide) is an amorphous material (T_g at 58°C)[18]. Commercial PLA are

copolymers of poly(L-lactic acid) (PLLA) and poly(D,L-lactic acid) (PDLLA), which are produced from L-lactides and D,L-lactides, respectively[19].

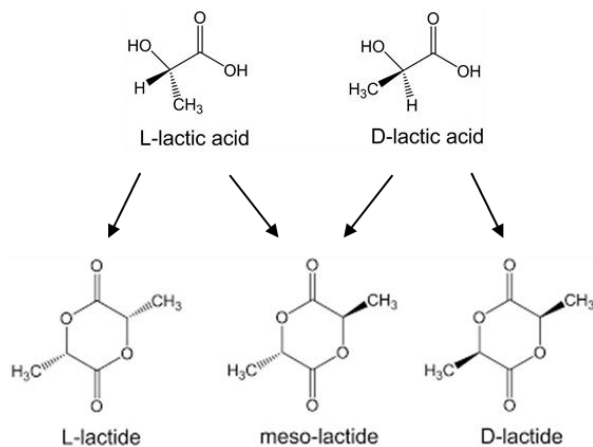


Figure I.5. Stereoisomers of lactide.[18]

Despite the intensive work on R&D about PLA science and technology enables a large-scale production, the industrial application of unmodified PLA is currently limited to short-term goods such as packaging, cold drink cups, bottles, textiles, etc. [20-22]. Nevertheless, a number of factors can contribute to the success of PLA in durable goods, including automotive applications, namely its high strength and rigidity as well as compostability and recyclability[23]. To assess about both strengths and weaknesses of PLA, its physical and mechanical properties can be compared to those of the most commonly used plastics in automotive applications in Table I.1. Mechanical properties of PLA appear very attractive, particularly its Young's modulus (> 3.5 GPa), making it an excellent substitute to commonly used polymers.

Table I.1 Some mechanical and physical properties of common plastics and PLA [24-28]

	PP	PA	PMMA	ABS	PC	PU	PVC	PLA
Young Modulus(GPa)	0.896-1.55	2.62-3.2	2.24-2.8	1.1-2.9	2-2.44	1.31-2.07	2.14-4.14	3.55-3.75
Tensile strength(MPa)	27.6-41.4	90-165	48.3-79.6	28-55	60-72.4	31-62	40.7-65.1	65-70
Impact Strength (J/m) at 24°C	26.7-106.8	53.4-160.2	21.4-26.7	53.4-534	640.8-961.2	800	21.4-160.2	19-26
HDT(°C) load at 1.8 MPa	67	75	97	100	143	46-96	64	50-57
Density(g/cm3)	0.89 - 0.91	1.12-1.14	1.16-1.22	1.1-1.2	1.14-1.21	1.12-1.24	1.3-1.58	1.25

	PP	PA	PMMA	ABS	PC	PU	PVC	PLA
(CO₂)Foot Print (kg/kg)	2.6-2.8	5.5-5.6	3.4-3.8	3.3-3.6	5.4-5.9	4.6-5.3	2.2-2.6	<1
Cost (USD/kg)	1.2-1.3	3.3-3.6	2.6-2.8	2.1-2.5	3.7-4	4.1-5.6	0.93-1	~2

In a context of designing eco-friendly products, both to satisfy customer's demand and more and more strict legislation[29], PLA possesses other undeniable assets compared to petro-based polymers. First, it is derived from cheap bio-resources (starch), which are abundant and renewable. Moreover, one of the most positive points of PLA production in comparison with the other hydrocarbon-based polymers is its low CO₂-emission. Carbon dioxide is proven to be the most important contributor to global climate change. Because carbon dioxide is absorbed from air when plant grows, the use of PLA has the potential to reduce the emission of greenhouse gases compared to petroleum-based polymers. In addition, development of new technologies allows a decrease of greenhouse gases-emissions during PLA process: Vink et al.[30] showed that the net greenhouse gas emission of NatureWorks PLA decreased from 2 kg CO₂ eq./kg polymer in 2003 to 0.3 kg in 2006. Furthermore, Jamshidian et al.[31] estimated that the net greenhouse gas emissions for next PLA generation using wind energy can reach a negative value of -0.7 kg of CO₂ eq./kg polymer (Figure I.5).

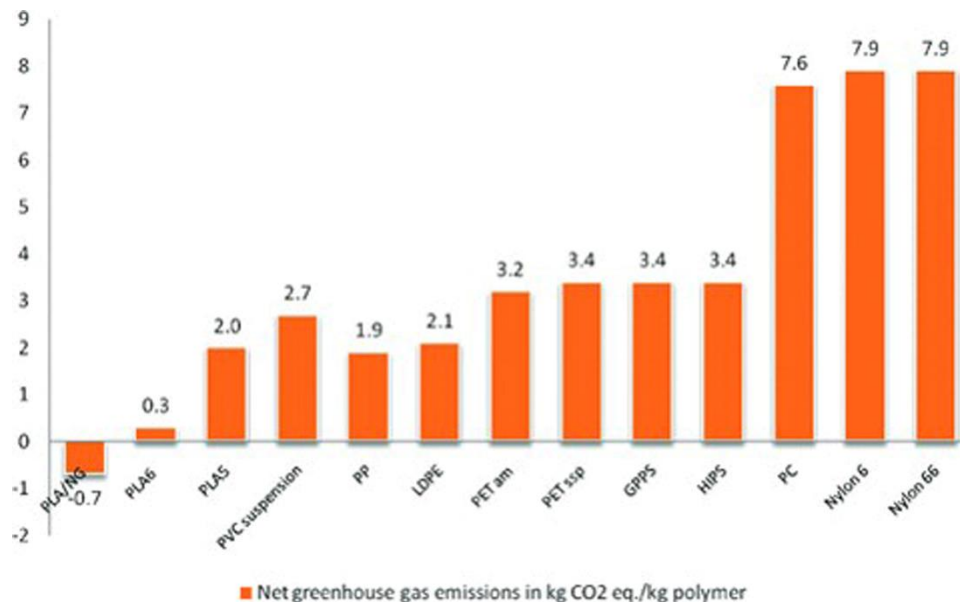


Figure I.5. Net greenhouse gas emission of commercial PLAs and other polymers. PLA/NG= NatureWorks® PLA next generation, PLA5 =NatureWorks® PLA in 2005, PLA6= NatureWorks® in 2006, HIPS= high impact poly(styrene), PC = poly(carbonate), GPPS = general purpose poly(styrene), PET am= PET amorph, PET ssp= PET solid satepolycondensed.[31]

In addition, PLA has received some interest from industrial sectors because of its relatively low price and commercial availability compared to other bioplastics. This is the key-point for any successful polymer application. In fact, the average price of commercial PLA in 2009 reached almost 2 USD/kg, which is sufficiently close to other polymers like PET and considered as the cheapest cost for a biodegradable polymer [32]. Clearly, the PLA market is still in its infancy, but it is expected that the decrease in the production cost and the improvement in product performance will result in a clear acceleration in PLA industrial use. Many researchers developed a more efficient and economical route for cheaper and greener PLA [33-35]. It is estimated that PLA production capacity that currently stands at around 180,000 tons per year should exceed more than one million tons in 2020 [36]. In addition to lower gas emission, more and more affordable cost, and already mentioned appealing mechanical properties, PLA possesses other assets compared to petroleum-based plastics. Among those assets, PLA shows excellent biocompatibility, (bio)degradability and recyclability and easy-processability[37,38]. Thus, PLA can be processed by injection molding, sheet extrusion, blow molding, thermoforming and film forming and is one of the few plastics suitable for 3D printing[39]. This new technology process for plastics is very important for future automotive industry and aftermarket since it allows the realization of automotive parts of incredible complex geometry and it enables to elaborate spare parts on-demand [40,41]. Recently, an electric Street Scooter C16 short distance vehicle was built by a team at Aachen University[42]. 3D printing was used for all of vehicle's exterior plastic parts, including the large front and back panels, door panels, bumper systems, side skirts, wheel arches, lamp masks and a couple of interior components such as the retainer instrument board and a host of smaller components[43]. Local Motors made a car called "the Strati" by building the chassis and body of its cars using giant 3D printers and raw materials[44].

Finally, referring to Table I.1 and comparing to traditional plastics used in automotive applications, neat PLA has many appealing properties such as high rigidity but cannot meet all criteria of automotive sector. In summary, several strategies have thereby been carried out to overcome those drawbacks, among which the most important are brittleness and low heat resistance.

I.2 Aim of the work

The interest to use polymeric materials derived from renewable resources continuously increases because of the considerably improved environmental awareness of society and the fear from the depletion of petrochemical based plastics. In this regard, Poly(lactic acid), PLA, represents the biopolymer that responds the most successfully to the surge of demand for such materials and can satisfy the requirements of large scale processing and application at the same time. The reason for its development mainly relies on a number of interesting properties, including its good processability, good mechanical properties (strength and rigidity), biodegradability, biocompatibility and relatively low-cost. However, in many cases, durable applications of PLA have been significantly limited by its inherent brittleness and limited thermal stability. These points therefore represent the main key-parameters to be improved for its industrial implementation, especially for automotive parts possibly subjected to severe loading and environmental conditions.

Accordingly, the main objective of this thesis concerns the design of new bio-based PLA materials for automotive application. For that reason, it was crucial to develop a new PLA-based materials with both improved thermal and mechanical properties while respecting the biobased character.

I.3 References

1. Reynolds N, Balan Ramamohan A (2013) High-Volume Thermoplastic Composite Technology for Automotive Structures. In: *Advanced Composite Materials for Automotive Applications*. John Wiley & Sons Ltd, pp 29-50. doi:10.1002/9781118535288.ch2
2. Rowe J (2012) *Advanced materials in automotive engineering*. Elsevier,
3. Götz Klink GR, Bartek Znojek, Ojas Wadivkar (2012) *Plastics. The Future for Automakers and Chemical Companies*. A.T.Kearney, Korea
4. Thomas Kevin Swift MGM, Emily Sanchez (2015) *Plastics and Polymer Composites in Light Vehicles*. Economics and Statistics Department/American Chemistry Council,
5. Philp JC et al. (2013) Biobased plastics in a bioeconomy. *Trends in Biotechnology* 31 (2):65-67.
6. Thielen M (2012) *Bioplastics: Basics, Applications, Markets*. Polymedia Publ.,
7. Pilla S (2011) *Handbook of bioplastics and biocomposites engineering applications*, vol 81. John Wiley & Sons,
8. Siracusa V et al. (2008) Biodegradable polymers for food packaging: a review. *Trends in Food Science & Technology* 19 (12):634-643.
9. Bioplastics E (2013) *Applications for bioplastics*. European Bioplastics, Institute for bioplastics and biocomposites. <http://www.european-bioplastics.org/market/applications-sectors/>. 2015
10. Lee E, Flanigan C (2012) *Automotive Plastics and Composites*. In: *Encyclopedia of Polymer Science and Technology*. John Wiley & Sons, Inc. doi:10.1002/0471440264.pst023
11. Szeteiová K (2010) *Automotive materials: plastics in automotive markets today*. Institute of Production Technologies, Machine Technologies and Materials, Faculty of Material Science and Technology in Trnava, Slovak University of Technology Bratislava
12. Andrea DJ, Brown WR (1993) *Material selection processes in the automotive industry*.
13. Ghassemieh E (2011) *Materials in automotive application, state of the art and prospects*. INTECH Open Access Publisher,
14. Weber M, Weisbrod J *Requirements engineering in automotive development-experiences and challenges*. In: *Requirements Engineering, 2002. Proceedings. IEEE Joint International Conference on, 2002*. IEEE, pp 331-340
15. Biron M (2012) *Thermoplastics and thermoplastic composites*. William Andrew,
16. Babu RP et al. (2013) Current progress on bio-based polymers and their future trends. *Progress in Biomaterials* 2 (1):1-16. doi:10.1186/2194-0517-2-8
17. Auras R et al. (2004) An Overview of Polylactides as Packaging Materials. *Macromolecular Bioscience* 4 (9):835-864. doi:10.1002/mabi.200400043
18. Pang X et al. (2010) Poly(lactic acid (PLA): research, development and industrialization. *Biotechnology journal* 5 (11):1125-1136

19. Lim LT et al. (2008) Processing technologies for poly(lactic acid). *Progress in Polymer Science* 33 (8):820-852.
20. FIORI S (2014) Industrial Uses of PLA. *Poly (lactic acid) Science and Technology: Processing, Properties, Additives and Applications* (12):317
21. Lunt J (1998) Large-scale production, properties and commercial applications of polylactic acid polymers. *Polymer Degradation and Stability* 59 (1–3):145-152.
22. Signori F et al. (2009) Thermal degradation of poly(lactic acid) (PLA) and poly(butylene adipate-co-terephthalate) (PBAT) and their blends upon melt processing. *Polymer Degradation and Stability* 94 (1):74-82.
23. Song J et al. (2009) Biodegradable and compostable alternatives to conventional plastics. *Philosophical Transactions of the Royal Society of London B: Biological Sciences* 364 (1526):2127-2139
24. Perego G et al. (1996) Effect of molecular weight and crystallinity on poly(lactic acid) mechanical properties. *Journal of Applied Polymer Science* 59 (1):37-43.
25. Appendix A - Data for Engineering Materials A2 - Ashby, Michael F (2011). In: *Materials Selection in Mechanical Design* (Fourth Edition). Butterworth-Heinemann, Oxford, pp 495-523.
26. Gerdeen JC, Rorrer RA (2011) *Engineering design with polymers and composites*, vol 30. CRC Press.
27. Whelan T (1994) H. In: *Polymer Technology Dictionary*. Springer Netherlands, Dordrecht, pp 177-195. doi:10.1007/978-94-011-1292-5_10
28. Brydson JA (1999) 8 - Principles of the Processing of Plastics. In: *Plastics Materials* (Seventh Edition). Butterworth-Heinemann, Oxford, pp 158-183.
29. Gerrard J, Kandlikar M (2007) Is European end-of-life vehicle legislation living up to expectations? Assessing the impact of the ELV Directive on 'green' innovation and vehicle recovery. *Journal of Cleaner Production* 15 (1):17-27.
30. Vink ET et al. (2007) Original research: the eco-profiles for current and near-future NatureWorks® polylactide (PLA) production. *Industrial Biotechnology* 3 (1):58-81
31. Jamshidian M et al. (2010) Poly-Lactic Acid: Production, Applications, Nanocomposites, and Release Studies. *Comprehensive Reviews in Food Science and Food Safety* 9 (5):552-571. doi:10.1111/j.1541-4337.2010.00126.x
32. Sin LT et al. (2012) Polylactic acid: PLA biopolymer technology and applications. William Andrew,
33. Dusselier M et al. (2015) Shape-selective zeolite catalysis for bioplastics production. *Science* 349 (6243):78-80. doi:10.1126/science.aaa7169
34. Achmad F et al. (2009) Synthesis of polylactic acid by direct polycondensation under vacuum without catalysts, solvents and initiators. *Chemical Engineering Journal* 151 (1–3):342-350.
35. Madhavan Nampoothiri K et al. (2010) An overview of the recent developments in polylactide (PLA) research. *Bioresource Technology* 101 (22):8493-8501.
36. Growth in PLA bioplastics: a production capacity of over 800,000 tonnes expected by 2020 (2012). nova-Institute, Bio-based news

37. Nair LS, Laurencin CT (2007) Biodegradable polymers as biomaterials. *Progress in Polymer Science* 32 (8–9):762-798.
38. Bhardwaj R, Mohanty AK (2007) Advances in the Properties of Polylactides Based Materials: A Review. *Journal of Biobased Materials and Bioenergy* 1 (2):191-209. doi:10.1166/jbmb.2007.023
39. Canessa E et al. (2013) Low--cost 3D Printing for Science, Education and Sustainable Development. *LOW-COST 3D PRINTING*:11
40. Campbell T et al. (2011) Could 3D printing change the world. *Technologies, Potential, and Implications of Additive Manufacturing*, Atlantic Council, Washington, DC
41. Reeves P, Mendis D (2015) The Current Status and Impact of 3D Printing Within the Industrial Sector: An Analysis of Six Case Studies.
42. Staff S (2014) Revolutionary New Electric Car Built and Tested in One Year with Objet1000 Multi-material 3D Production System. *Stratasys*. <http://blog.stratasys.com/2014/11/18/streetscooter-3d-printing/>. 2016
43. Staff S (2014) Revolutionary New Electric Car Built and Tested in One Year with Objet1000 Multi-material 3D Production System. *stratasys*. <http://blog.stratasys.com/2014/11/18/streetscooter-3d-printing/>. Accessed 14-01-2016
44. Bunkley N (2014) "World's first" 3D printed car created and driven by Local Motors. *Automotive News*. <http://www.autonews.com/article/20141027/OEM06/310279987/auto-industry-uses-3-d-printing-heavily-in-product-development>. Accessed 14-01-2016

CHAPTER II

STATE OF ART

State of art

Development of high-performance PLA-based materials

Light weighting is an important issue for the automotive industry, making plastics attractive materials to address this challenge. Beyond the benefits linked to vehicle's weight-reduction, the future lies on selecting more environmentally friendly plastics, particularly bioplastics. Due to their renewable origin, bioplastics help minimizing the environmental impact of car-production by further reducing CO₂-emissions and energy consumption[1,2]. Besides, it is very crucial for the industrial actors to develop sustainable alternatives to products derived from petroleum oil, since the price of petroleum oil is unstable and its feedstock will end up in a near future.

Within the bioplastics existing today on the market, some of them are already suitable for the automotive sector, more particularly poly(lactic acid) (PLA)-based materials and its composites[3]. Several key-points contribute to the success of PLA, especially its excellent (bio)degradability/recyclability as well as its attractive physical and mechanical properties such as high rigidity, strength and easy processability[4,5]. However, although PLA can fulfill the environmental regulations of automotive sector, the development of technical PLA-based materials for automotive applications must still encompass some key-characteristics, not achieved yet, such as high toughness, durability, processability at high temperature and high production rate at affordable cost[6]. Several strategies such as blending with other petropolymers, plasticizers, impact-modifiers, micro-sized and/or nano-sized fillers have thereby been proposed to overcome those drawbacks and can make PLA suitable for automotive application[7,8]. Research works have also aimed at improving the crystallinity and processability via blending, plasticizing, stereo-complexing and other modifications depending on the properties to be improved upon a given application. However, antagonist effects may appear in few cases. Those are described in details in the next sections with an emphasis on PLA-based materials fitting to the automotive requirements in terms of processing (e.g. injection molding), properties (e.g. stiffness) and durability.

II.1 Highly tough and/or ductile PLA-based blends

In the cases that require a high level of impact strength and ductility, especially for vehicle's exterior parts, impact toughness and ductility of PLA in its pristine state are insufficient.

Therefore, there have been tremendous efforts in developing ways to improve these mechanical properties. In this part, these approaches are summarized, with a focus on how the protocols also influence other mechanical properties of resultant materials.

II.1.1. Plasticized PLA blends

Plasticization is a widely used technique to improve processability and ductility of thermoplastics. The main role of plasticizers is to decrease glass transition temperature of polymer. In addition, plasticization frequently opens new possibilities for material processing by lowering degradation rate, allowing the process of materials in different equipments with reduced pressure and mixing time during extrusion [9]. Furthermore, it can also increase polymer's ductility and flexibility related to the decrease of glass transition temperature. The choice of plasticizers for PLA is dictated by intended applications, for instance non-toxicity of plasticizer for food and medical applications, as well as by general criteria such as non-volatility, to avoid evaporation during processing, miscibility for creating a homogenous blend with PLA, etc. Another point is that plasticizer must not migrate as much as possible from the material bulk, otherwise the PLA blend can rapidly regain the inherent brittle properties of neat PLA [10].

Many different molecules and classes of plasticizers have been tested for PLA [11,12] and will be discussed in the forthcoming part as follows: monomeric plasticizers, oligomeric and polymeric plasticizers and mixed plasticizers. Only plasticizers designed for injection molded parts were selected here. Examples of thermal and mechanical properties of PLA plasticized with those classes of plasticizers are given in Table II.1 and presented in more details afterwards.

Table II.1. Thermal and mechanical properties of plasticized PLA blends

Plasticized PLA blends	Molecular weight(g/mol)	Content (wt%)	T _g (°C)	σ (MPa)	E(GPa)	ε(%)	Ref.
Monomeric Plasticizers							
PLA	74000	100	54	57	3.75	5	
Loxiol GMS95	-	2.5	-	52	3.4	14	[13]
		5	-	48	3.2	7	
		10	45	45	3	8	
Dehydat VPA 1726	-	2.5	-	53	3.3	5	[13]
		5	-	47	3	6	
		10	40	38	2.5	13	
PLA	74500	100	62	66	1.02	11	
ATBC	402.5	10	44	51	0.97	11	[14]
		20	38	30	0.27	317	

Plasticized PLA blends	Molecular weight(g/mol)	Content (wt%)	T _g (°C)	σ (MPa)	E(GPa)	ε(%)	Ref.
DOA	370.6	10	45	29	0.72	36	
		20	45	21	0.67	78	
GTA	218.2	10	48	38	0.76	8	
		20	29	24	0.01	443	
Polymeric Plasticizers							
PEG	1500	2.5	-	50	3.2	5	[13]
		5	-	44	2.5	7	
		10	28	38	1.3	180	
PLA	121400	100	58.6	69.8	1.77	6	
PPA	1900	5	49.3	63.2	1.39	6	[15]
		10	40.6	49.6	1.3	157	
		15	33.3	39.8	0.882	315	
		20	27	25.7	0.554	362	
		25	24.3	14.4	0.374	410	
Mixed Plasticizers							
PLA	207400	100	-	58	-	4	
TAC/PBGA	-	5	-	48	-	4	[16]
		9	-	36	-	180	
		13	-	24	-	349	
		29	-	17	-	327	

Where T_g is the glass transition temperature; σ, E and ε refer respectively to the tensile strength, elastic modulus and tensile elongation at break.

Jacobsen and Fritz[13] used glucose monoester (DehydVPA 1726), partially fatty esters (LoxiolVR GMS95) and polyethylene glycol with a molecular weight of 1500 g/mol (PEG1500), to plasticize PLA and examined the influence of these plasticizers over tensile and unnotched Charpy impact strength of injection-molded PLA specimens. A significant improvement in both elongation (180%) and impact resistance (unbroken specimens under unnotched Charpy impact tests) was reported with the addition of 10 wt % PEG1500. In the case of glucose monoester and partial fatty acid ester, elongation of PLA was improved but impact strength was slightly decreased at all concentrations examined (i.e., 2.5–10wt %). Murariu et al.[14] studied the plasticization of PLA using three low-molecular weight ester-type plasticizers, *bis*-(2-ethylhexyl) adipate (DOA), glycerol triacetate (GTA), and acetyl tributyl citrate (ATBC). Addition of up to 20 wt % plasticizer led to a gradual decrease of Young's modulus and increase of ductility in the following order of efficiency: GTA > ATBC > DOA. The best notched impact performance was seen in PLA plasticized with 20 wt % GTA, with unbroken specimens. By comparison, addition of ATBC led to the lowest improvement in

the impact strength among the three plasticizers, with “only” an increase of 77% at 20 wt % ATBC.

The main drawback of monomeric plasticizers is their tendency to migrate out from the polymer bulk[17]. This drawback may be overcome by using polymeric plasticizers [13,15]. Recently, it has been shown that PLA can be efficiently plasticized and toughened by melt-blending with poly(1,2-propylene glycol adipate) (PPA) [15]. Thermal and dynamic mechanical analysis revealed that PPA was partially miscible with PLA and morphological investigation of the blends showed that PPA was compatible with PLA. The elongation at break and the impact strength dramatically increased due to the plastic deformation (Table II.1). However, as a side effect, the blends showed a decrease in the tensile strength and Young's modulus with the increase of PPA content (5–25 wt%). The notched Izod impact strength reached 100 J/m with 25wt% of PPA. It shows that polymeric plasticizers can bring additional increase in impact strength. Nevertheless, increasing the molecular mass of plasticizers can lead to their lower miscibility with the polymer, causing a phase-separation, *i.e.* formation of a two-phase system [18].

Mixed plasticizers combine an oligomeric or polymeric plasticizer with a small molecule plasticizer. Therefore, they can lead to a medium level of drop in T_g and more balanced mechanical properties (in terms of elongation, tensile modulus and strength) than the individual plasticizers. Mixed plasticizers combining low-molecular-weight triacetin (TAC) and oligomeric poly(1,3-butylene glycol adipate) (PBGA) have been employed to improve ductility of PLA, as reported by Ren *et al.*[16]. They found that this combination led to a significant improvement in the elastic properties (for plasticizer content higher than 5 wt%) with a dramatic decrease of tensile strength as the content of plasticizer increased (Table II.1). For enhancing mechanical properties without altering too much rigidity of PLA and improving flexibility and toughness, Notta-cuvier *et al.*[8] had the idea to combine plasticizers with Halloysite Nanotubes (HNT) as reinforcing nanofillers, leading to more attractive properties for automotive applications. In particular, this composition enabled the combination of the good rigidity and tensile flexural strength imparted by HNT with better ductility and toughness provided by TBC plasticizer. Tensile behavior and impact results are represented in Figure II.1 and show that ductility and impact resistance of PLA-HNT-TBC ternary blend were improved in an extent that depends on the amount of plasticizer. Moreover, a high content of TBC (12.5-15%wt) enhanced the impact resistance of blend, but led to a drop in rigidity and flexural strength. For a good balance of properties, an optimized PLA-HNT-TBC composition

containing 10 wt% of plasticizer was proposed as a biosourced alternative blend for automotive application.

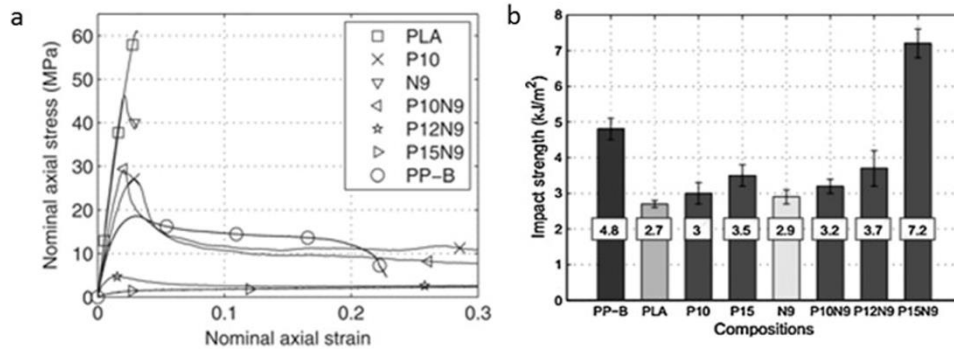


Figure II.1. (a) Nominal behaviors of (PLA/TBC/HNT) compositions and PP-B–Tensile tests at 1 mm min^{-1} ; (b) Izod impact resistance (notched specimens) of (PLA/TBC/HNT) compositions and PP-B. Sample codes refers to following weight contents (PLA/TBC/HNT): N9 (91/0/9); P10 (90/10/0); P15 (85/15/0); P10N9(81/10/9); P12N9 (78.5/12.5/9); P15N9 (76/15/9) [8]

In summary, several studies have demonstrated that plasticizers can play a significant role to tune properties of PLA-based blends, mainly to improve their flexibility and ductility and may also pave the way to novel applications. However, there are still some limitations associated with plasticization including leaching during use, lack of thermal stability and substantial reduction in strength and modulus. This illustrates the need to carefully estimate plasticizer content to reach the better compromise between ductility and strength, in particular, especially for automotive applications.

II.1.2. Rubber-toughened PLA blends

Other strategies than plasticization can be successful to improve the ductility of PLA, together with other maintained properties such as toughness. Among them, melt-blending with rubbers was proved to be an efficient technology, thanks to the remarkable toughening effect of rubbers and the fact that this method is based on easy-to-perform and cost-effective techniques. A variety of biodegradable and non-biodegradable flexible polymers have been used as toughness modifiers for PLA in order to improve stiffness-toughness balance. Different reviews report the most commonly used polymeric additives as effective PLA impact modifiers[11,19-24]. However, this section will be strictly limited to recent and noteworthy works developing rubber-toughened PLA-blends for engineering applications requiring high ductility and impact toughness.

When aiming to improve PLA ductility and impact toughness, the use of impact modifier can be of high interest, as it allows increasing the energy dissipation through the material during deformation, without affecting its stiffness and thermal stability[25]. Several commercial impact modifiers are specifically designed in order to toughen PLA. When dispersed in the form of rubbery microdomains (with an average size around 0.1-1.0 μm) within PLA matrix, they enable a significant increase of energy absorption during impact test[26,27]. However, it is well-known that their toughening effect is of varying amplitude, depending on their miscibility extent with the PLA matrix, their thermal stability under PLA processing temperature, the interfacial adhesion between the dispersed rubbery phase and the continuous PLA matrix within the blend, etc. Among impact modifiers compatible with PLA, Biomax[®] Strong from Dupont Company is probably the most investigated one, as specifically designed to improve PLA toughness. In this regard, Biomax[®] Strong was used by Taib *et al.*[28], who have highlighted a significant improvement in notched Izod impact strength of the brittle PLA from 3.6 kJ/m² to 14 kJ/m² and 28 kJ/m² at 10 and 20 wt% Biomax[®] Strong. Using Biomax[®]Strong 100 (BS) impact modifier, Notta-cuvier *et al.*[29] performed PLA-plasticizer-impact modifier-nanoclay quaternary compositions designed for automotive applications. Good ductility and toughness were achieved with the binary blend (PLA-BS) with a resiliency of 16.5 kJ/m². A synergistic effect of BS (10 wt%), plasticizer TBC (10wt%) and nanoclay Cloisite[®]25A (1wt%) was surprisingly evidenced with an optimal toughness of 42.8 kJ/m². Analysis also revealed that a compromise has to be found between high tensile rigidity and strength in one hand, and high ductility on the other hand, as illustrated in Figure II.3. In that Figure, mechanical properties of a mineral (talc)-filled polypropylene (PP-talc), commonly used in automotive applications, were taken as a reference. The composition PLA +10 wt% BS +10 wt% TBC +3 wt % CL25A (composition 8 in Figure II.3) is the one that globally led to the most interesting properties compared to PP-talc. In particular, this composition was characterized by an interesting level of ductility while its rigidity and strength were maintained higher than those of the mineral-filled polypropylene (10 kJ/m² compared to 4.8 kJ/m² for PP-talc).

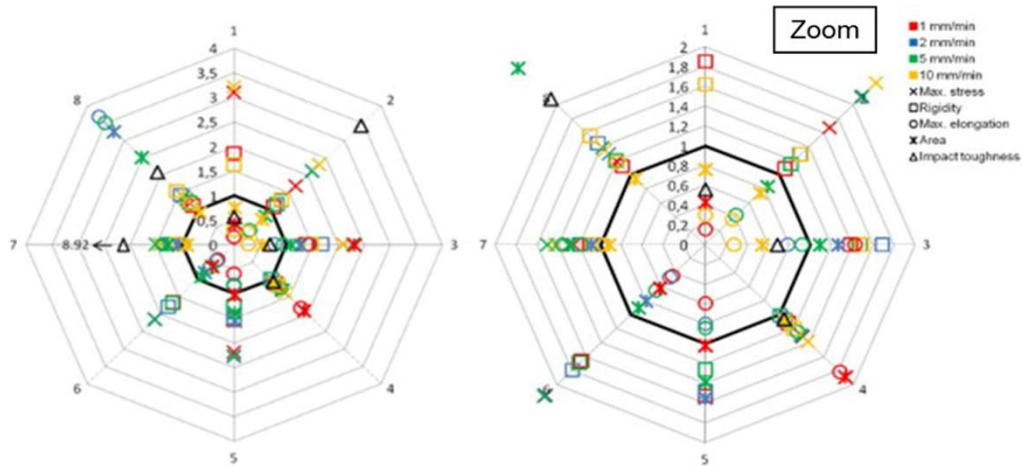


Figure II.3. Summary of all mechanical properties compared to those of PP-B. (numbers refer to (PLA/TBC/BS/CL25A) composition codifications: 1 (100/0/0/0); 2 (90/0/10/0); 3 (90/10/0/0); 4 (80/10/10/0); 5 (90/0/10/1); 6 (90/0/10/3); 7 (80/10/10/1); 8 (80/10/10/3), in weight percentages. Values presented are ratios of properties of compositions 1 to 8 divided by those of PP-talc, so that qualitative comparisons are immediate (a value higher than 1 stands for a mechanical property higher than that of PP-talc, e.g.)[29]

It can be noted that Ethylene Acrylate Biomax[®] Strong (BS) impact modifier was also used in the present work in order to develop a PLA/PMMA/BS ternary blend capable of competing with commercial ABS/PC blend for the manufacture of injection-molded automotive parts, as described in details latter in this manuscript (see especially Chapter III).

Zhang *et al.*[30] developed super-toughened PLA multiphase reactive blends using a commercial class of renewable elastomeric copolymerspolyether block amide PEBA (Pebax[®]) offering high impact resistance and excellent elasticity and an ethylene-methyl acrylate-glycidyl methacrylate (EMA-GMA) terpolymer impact modifier (commercialized under the name of Lotader[®] AX8900) to improve the interfacial adhesion of PLA/PEBA blends and enhance toughness. As shown in Figure II.4b, only a limited improvement of impact strength was achieved for binary PLA/PEBA blend while a significant enhancement of the PLA impact toughness was achieved thanks to addition of the impact modifier, together with a higher elongation at break. This latter increased with the EMA-GMA content reaching almost 73% with 20 wt% of impact modifier (20 times higher than that of the neat PLA). Nevertheless, a decrease of tensile strength and modulus for ternary blends was noticed when increasing EMA-

GMA content (Figure II.4a). It can be attributed to the presence of soft PEBA and EMA-GMA elastomers.

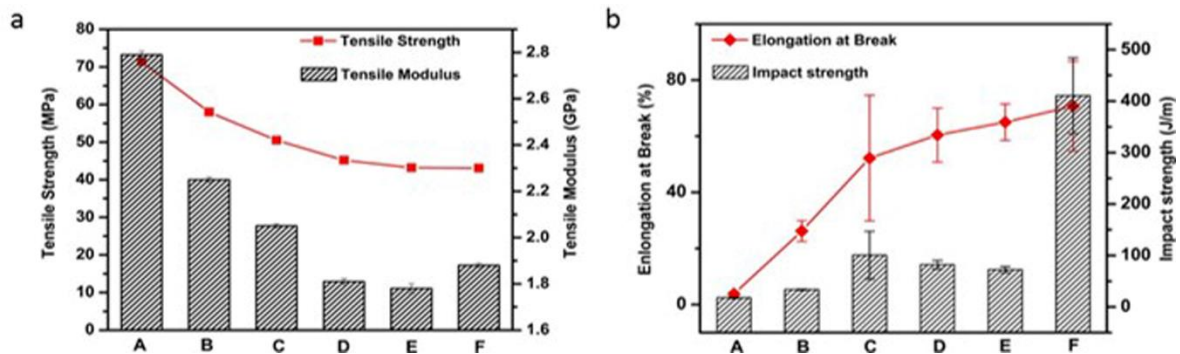


Figure II.4. (a) Tensile properties of PLA/EMA-GMA/PEBA ternary blends as a function of the weight fraction (b) Notched Izod impact strength and percent elongation at break of PLA/EMA-GMA/PEBA ternary blends as a function of the weight fraction/ (A) Neat PLA; (B) PLA/PEBA(80/20); (C) PLA/EMA-GMA(80/20);(D)PLA/EMA-GMA/PEBA(70/10/20);(E)PLA/EMA-GMA/PEBA(70/15/15); (F) PLA/EMA-GMA/PEBA(70/20/10). [30]

Good interfacial adhesion was achieved by addition of Lotader AX8900. A super-tough PLA ternary blend was thus developed, exhibiting an impact strength of 500 J/m with only partial break of impact specimens, therefore allowing this blend to be used in automotive interior parts.

Although many investigated solutions to decrease PLA brittleness and/or improve PLA impact strength are not fully eco-friendly, blending PLA with eco-friendly rubber modifiers [31-36], elastomers [37,38] and biodegradable polymers [39,40] has gained momentum in recent years. Zhang *et al.*[31] reported an improvement in the impact strength of PLA with the incorporation of 20 wt% of epoxidized natural rubber containing 20 mol% (ENR20) and 50 mol% (ENR50) of epoxidation content. ENR-20 was found to impart higher impact strength to PLA matrix as compared with ENR-50 (Figure II.5). Moreover, the higher content of epoxy groups in ENR-50 led to an increase of viscosity and therefore a decreased deformability of the blends. Inter chain cross-linking reactions and molecular entanglements were more pronounced in PLA/ENR-50 blends, which in turn increased the tensile strength.

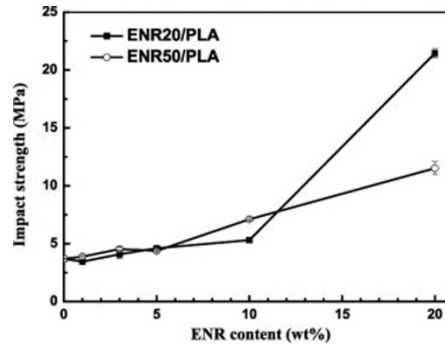


Figure II.5. Impact strength of pure PLA, ENR20/PLA and ENR50/PLA blends [31]

II.1.3. Annealing process

In addition to plasticization or use of an impact modifier, process modifications may also lead to an enhancement of mechanical properties, especially strength and rigidity. Among additional approaches related to process modification, annealing was revealed in literature as a good solution to improve the mechanical properties of PLA blends (in terms of rigidity and impact strength), in particular for injection-molded parts, by modifying its inherent crystalline structure.[41-47] In this regard, Perego *et al.*[47] have studied the effect of crystallinity on mechanical properties of poly(L-lactic acid) (PLLA) with different molecular weight. To promote crystallization, PLLA injection-molded specimens were annealed at 105°C for 90 min under nitrogen. They demonstrated by DSC analyses that the degree of crystallinity of PLA reached 42-65 J/g instead of 3-13 J/g for non-annealed PLLA depending on the molecular weight (\bar{M}_v). Annealing of PLLA samples also led to some increase of impact strength with values of notched impact strength ranging from 66 to 70 J/m, depending on molecular weight of PLLA. The highest tensile elastic modulus was of 4.2 GPa, due to higher crystallinity degree of annealed materials (Table II.3).

Table II. 3 Mechanical properties of non-annealed and annealed PLLA[47].

Property Specimens	Molecular weight (\bar{M}_v)	Notched Impact Strength (J/m)	Modulus of elasticity (GPa)
PLLA-I	23,000	19	3.65
Annealed PLLA-I	20,000	32	4.2
PLLA-II	31,000	22	3.6
Annealed PLLA-II	33,500	55	4.0
PLLA-III	58,000	25	3.6
Annealed PLLA-III	47,000	70	4.15
PLLA-IV	67,000	26	3.65
Annealed PLLA-IV	71,000	66	4.15

From a general viewpoint, in automotive industry, annealing process is mainly used for semi-finished components after forging or cold-forming in the aim of producing uniform material structure, offering softness and removing residual stresses for both alloy and plastic component [48,49]. Annealing is done by heating the material at a specific temperature for a definite period of time then cooling it slowly to room temperature. This process is used to control the degree of crystallinity and/or orientation of the material or to remove internal stresses in the product that can be created by the primary processing. Annealing can also improve impact resistance and reduce tendency to crazing and cracking in service and offer additional value to final alloy, such as improved welding properties, improved corrosion resistance and good dimensional and shape accuracy. Unfortunately, this post-process is expensive and involves longer production time. Therefore, it cannot be seen as a promising solution for mass production characterizing the automotive industry.

II.2 Heat resistance PLA-based blends

In some applications like automotive sector, heat resistance over extended periods of time is required. Yet, heat resistance has been an important issue for plastics used in engineering applications. Indeed, all polymers exhibit a wide variation of mechanical and physical properties in function of temperature (Figure II.6).

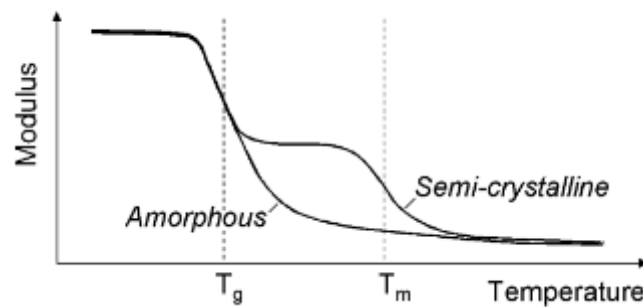


Figure II.6. Modulus versus temperature behavior for an amorphous and semi-crystalline polymer[50]

Not to mention extreme temperature attained into combustion chambers, automotive parts may be facing service temperature ranging from -40°C for a car parked outdoors in a cold country to 85°C for driver interior and even 125°C under bonnet [51]. When increasing temperature, polymer strength and rigidity, in particular, tend to decrease. Above the glass transition temperature (T_g), rigidity drops in a more pronounced way and becomes too low to enable the use of the material in these technical parts. In this regard, Heat Deflection Temperature (HDT) is defined as the temperature at which a standardized test bar deflects of a

specified distance under an imposed load value (see ASTM D648 procedure). HDT therefore constitutes an effective way to evaluate the thermal stability, or the heat resistance, of plastics [52]. In this regard, many researchers have studied the improvement of the heat resistance of PLA by manufacturing PLA-based green composites with reinforcing fibers. Thus, wood fibers [53], banana fibers [54], kenaf fibers [55], bamboo fibers [56] and cellulose fibers [57] were all noted to increase HDT but the resulting composites proved being brittle.

On the contrary, nanofilled PLA/petroleum-based thermoplastic blends can offer a good balance between thermal stability and ductility allowing their use in automotive sector, as described in the next paragraphs.

II.2.1. Highly thermal PLA-based nanocomposites

Polymer nanocomposites are commonly defined as the combination of polymer matrix and nanofillers that have at least one dimension in the nanometer range. The nanofillers can be one-dimensional (1D - platelet-like nanofillers), two dimensional (2D- nanofibers or whiskers) or three dimensional (3D - nanospheres). The use of nanocomposites in vehicle parts and systems is expected to improve manufacturing speed, enhance thermal stability and reduce weight. Applying this technology only to structurally noncritical parts such as front and rear panels, cowl ventilator grids and valve/timing covers could already allow to reduce weight. Indeed, nanocomposite plastic parts offer a 25% weight savings on average compared to highly (micro)filled plastics and as much as 80% compared to steel [58,59]. As important as the process advantages and weight and energy savings are nanocomposites can offer enhanced physical properties. Depending on the compositions, nanocomposites can show stiffness and strength comparable to or even better than metals [60-66]. Nanofillers can also improve corrosion resistance, noise dampening, thermal stability and dimensional stability of a material. However, as a relatively new approach, it is still unknown if the cost/performance ratio of nanocomposites will be superior to the cost/performance ratio of materials currently used by the automotive industry.

Today, layered silicate (clay) nanocomposites (PLS) are one of most well-known nanocomposites. Their interesting properties at low nanofiller content make them appealing in academic as well as in industrial realms[67]. Mainly three methods have been proposed to prepare nanocomposites: *in situ* intercalative polymerization, solution intercalation, and melt intercalation [68,69]. Clay materials can be dispersed and exfoliated into polymers by conventional melt-compounding or solution method. Toyota Motor Company successfully

pioneered *in situ* intercalation polymerization method to create Nylon-clay hybrid (NCH) to make an automotive timing belt cover[70]. Although the *in situ* intercalative polymerization method is the most efficient technique to obtain an exfoliated structure, it is not the most viable option for the current industry challenges [68,71]. Alternatively, melt-intercalation technique is still more versatile and less environmentally harmful. Main interests in comparison with other approaches are the utilization of shear-force and the absence of solvent during preparation. The applied shear force during mixing promotes the diffusion of the polymer chains from the bulk to the clay gallery spacing, resulting in further nanoplatelet delamination and in improved nanofiller distribution and dispersion[69]. Therefore, it is considered as the most efficient method for the preparation of polymer nanocomposites from an industrial viewpoint.

Due to enhanced barrier properties, high heat deflection temperature, improved rate of biodegradation and optical and antimicrobial properties potentially achieved with the addition of layered silicates, numerous researches focus on the development of PLA-based nanocomposites blends for food packaging and medical applications[60-66]. However, limited studies deal with PLA-based nanocomposites for automotive application, for instance in the form of PLA nanocomposite foams and injection-molded PLA nanocomposites [72,26,73-79]. Liu et al.[26] developed a TPU-toughened PLA/talc/organic modified clay (montmorillonite; OMC) nanocomposite in order to enhance heat resistance and mechanical properties and demonstrated that annealing process is necessary for improving heat resistance of resulting PLA blends. As shown in Table II.4, the difference between all compositions, for injection-molded specimens, were negligible before annealing with values of HDT of about 60°C. Annealing then increased HDT values to more than 120°C due to some interactions between PLA and TPU molecular chains as well as due to the increase of crystallinity resulting from the addition of the inorganic fillers.

Table II.4 Heat deflection temperatures of PLA, the PLA/TPU blends, and the nanocomposites [26]

Specimens	Content wt%				HDT of Injection molded specimens (°C)	HDT of Annealed specimens (°C)
	PLA	TPU	Talc	OMC		
LA	100	0	0	0	59.2	–
LAT4C0	96.0	0	4.0	0	61.1	129.5
LAT4C02	94.0	0	4.0	2.0	63.9	133.3
LAT4C06	90.0	0	4.0	6.0	60.1	133.4
LAT4C10	86.0	0	4.0	10.0	63.1	126.1
LAT4C14	82.0	0	4.0	14.0	61.7	130.6

Specimens	Content wt%				HDT of Injection molded specimens (°C)	HDT of Annealed specimens (°C)
	PLA	TPU	Talc	OMC		
LU	90	10	0	0	60.6	–
LUT4C0	86.4	9.6	4.0	0	60.1	130.3
LUT4C02	84.6	9.4	4.0	2.0	58.9	122.7
LUT4C06	81.0	9.0	4.0	6.0	60.6	115.3
LUT4C10	77.4	8.6	4.0	10.0	59.2	123.1
LUT4C14	73.8	8.2	4.0	14.0	59.1	128.1

Thermal stability, mechanical performances and added values such as flame-retardant property are among the most targeted properties for PLA materials intended for the automotive sector. Sinha Ray *et al.*[74] reported flexural properties of neat PLA and various PLA nanocomposites prepared with organically modified layered silicate (OMLS)(injection-molded samples). The flexural modulus, flexural strength, and distortion at break of neat PLA and various PLA nanocomposites were measured at 25°C and results showed a significant increase of flexural modulus for PLA nanocomposites with 4 wt% of OMLS (PLACN4 - 5.5GPa) when compared to that of neat PLA (4.8GPa). This was followed by a much slower increase with OMLS content, and a maximum at 5.8 GPa (increase of 21%) for 7 wt% OMLS (PLACN7). In addition, the flexural strength and distortion at break remarkably increased for PLACN4, then gradually decreased when increasing OMLS loading. It revealed that a high content of OMLS leads to a brittle material and there is an optimal amount of OMLS in nanocomposites that must be carefully adjusted in order to achieve the most significant improvement of mechanical properties. Murariu *et al.*[73] developed a calcium sulfate-containing PLA-based nanocomposite with flame retardant properties for technical applications requiring rigidity, heat resistance and dimensional stability. Accordingly, PLA- β -anhydrite II (AII) composites characterized by specific end-use flame retardant properties were added with selected OMLS. Co-addition of AII and OMLS led to PLA nanocomposites characterized by a good nanofiller dispersion, thermal stability and adequate mechanical resistance. The flame retardant properties as shown by cone calorimetry (Table II.5) displayed a significant increase in the ignition time (TTI) compared to neat PLA and a substantial decrease, about 40%, of the maximum (peak) rate of heat release (pHRR), whereas the UL94 HB test was successfully passed in terms of non-dripping effect and extensive char formation (Figure II.7).

Table II.5 Comparative flame retardant properties of PLA nanocomposites compared to pristine PLA as determined by calorimeter testing at heating flux of 35 kW/m². [73]

Composition (% by weight),	TTI, s	pHRR, kW/m ²	Decrease of pHRR, %
PLA (reference)	75	374	Reference
PLA-43% AII	98	319	15
PLA-3% B104	75	285	24
PLA-3% C30B	62	244	35
PLA-40% AII-3% C30B	88	230	39
PLA-40% II-3% B104	91	217	42

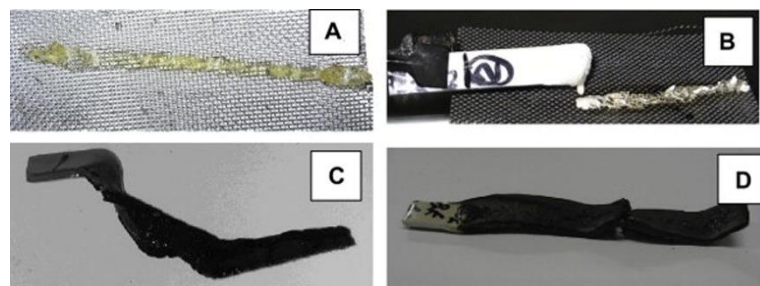


Figure II.7. Illustration of the behavior during UL94 HB testing: specimens burned with drips (PLA (A) and PLA-43% AII (B)) and without drips (PLA-40% AII-3% C30B (C) and PLA-40% AII-3% B104 (D)) [73].

In summary, PLA-based nanocomposites show very interesting properties that should enable a more widespread use in automotive applications in the next future, in particular for energy consumption reduction purposes thanks to weight reduction. High strength and rigidity of those materials are also undeniable assets. However, nanofilled PLA blends still exhibit low heat resistance without additional thermal process such as annealing.

In that context, another strategy can be suitable to achieve thermal properties unattainable for neat PLA. Melt blending PLA with petroleum-based thermoplastic polymers will be discussed next section.

II.2.2. PLA/petro-sourced polymer blends of high thermal stability

Thanks to the high thermal stability of commonly used petroleum-based thermoplastics compared to that of PLA, indicated by their value of HDT (see Chapter I ,Table I.1), lots of researches are interested in compounding PLA with (petro/bio)-sourced polymers in order to improve PLA HDT[80,81]. In some cases, compounding in association with toughening modifiers also allows achieving high impact property, leading to a competitive partially

biobased material with enhanced thermal stability and mechanical performances, suitable for use in vehicle parts. Among them, PLA/PC blends have been widely reported [82-87] as a simple binary blends or with addition of some additives like chain-extenders and compatibilizers in order to significantly enhance toughness and heat resistance while minimizing the drop in stiffness. Recently, Srithep *et al.*[86] developed a PLA/PC blend with the addition of epoxy-based chain extender (CE) in order to improve compatibility of the blend by reaction between the epoxide groups in CE and hydroxyl/carboxylic end-groups of PLA and PC. HDT value of PLA/PC blend without and with addition of CE was improved from 62°C for PLA+50%PC to 106°C after mixing with CE (Table II.6).

Table II.6 Heat deflection temperatures of PLA/polycarbonate (PLA/PC) and/or chain extender (CE) blends (HDT normalized measurement test)[86]

Compounds	HDT (°C)
PLA	55
PLA+30% PC	57
PLA+50% PC	62
PLA+50% PC+1.1%CE	106
PC	136

PMMA is often viewed as an excellent polymer partner for PLA, resulting in blends of high miscibility, excellent thermal stability with increased heat deflection temperature, high sustainability and good ageing behavior[88-91]. Recently, Samuel *et al.*[90] have dealt with miscible PLA/PMMA blends of enhanced thermo-mechanical properties and have confirmed that the addition of even a moderate amount of PMMA can deeply modify the thermal properties of PLA (in terms of T_g and HDT values), which were adjusted between those of neat PLA and neat PMMA. More precisely, HDT value progressively increased from 51.5 °C to 54.8°C with 20 wt% PMMA and up to 61.9°C with 50 wt% PMMA. Note that these results have motivated the design of PLA/PMMA blends in the present PhD research work.

II.2.3. Heat-resistance PLA-based stereocomplexes

Together with the development of PLA/petro-sourced polymer associations, other studies focus on making PLA stereocomplexes (sc-PLA) [92] for the key-fact that stereocomplexing is generally judged as an effective method to increase material crystallinity. Poly(L-lactic acid)

(PLLA) and poly(D-lactic acid) (PDLA) readily form stereocomplex crystallites with a distinct crystal structure that has a high melting point in the range of 220–230 °C, *i.e.* at a value that is significantly higher than those of PLA homocrystallites (approximately 170 °C) [93,94]. Stereocomplexing can therefore enhance PLA properties in terms of thermal resistance and hydrolysis resistance, in particular. A drawback of stereocomplexing is that it can lead to brittle PLA-based materials, which could reduce industrial implementations, as proven by Torres *et al.*[95]. Other researches [96-98] aimed at improving the heat deflection temperature and toughness of PLA using stereocomplexing simultaneously. In the same way, Nam *et al.*[99] performed sc-PLA by extruding poly(L-lactic acid) (PLLA) with various amounts of poly(D-lactic acid) (PDLA) and 10-20 wt% of two types of commercial impact modifiers (BioStrong 120, Elvaloy) in order to enhance both thermal (Table II.7) and mechanical properties.

Table II.7 Heat deflection temperatures of sc-PLA blends with or without impact modifiers[99]

Compounds	HDT(°C)
PLLA	56
PLLA/PDLA (92/8)	110
PLLA/PDLA (85/15)	110
PLLA/PDLA (75/25)	110
PDLA	53
PLLA/PDLA (92/8)+ 10 wt% Strong 120	70
PLLA/PDLA (92/8)+ 20 wt% Strong 120	65
PLLA/PDLA (85/15) + 10 wt% Strong 120	87
PLLA/PDLA (85/15) + 20 wt% Strong 120	79
PLLA/PDLA (92/8) + 10 wt% Elvaloy	90
PLLA/PDLA (92/8) + 20 wt% Elvaloy	81
PLLA/PDLA (85/15) + 10 wt% Elvaloy	101
PLLA/PDLA (85/15) + 20 wt% Elvaloy	97

As shown in Table II.7, HDT dramatically increased over 100°C thanks to the incorporation of different amounts of PDLA. Nevertheless, impact strength decreased with addition of PDLA

(18 J/m for neat PLLA to 11 J/m with 15 wt% of PDLA). Once impact modifiers were added, HDT decreased with the increase of impact modifier content (Table II.7). Taking into account all results, a well-balanced composition of toughened sc-PLA with 10 wt% of impact modifier was selected that can compete with (petro)polymers. In this context, Corbion Purac[100] have created a developmental grade of high heat resistance PLA (not commercialized yet) that in a stereocomplex form could replace PS, PP and ABS type materials in applications where heat performance (HDT) is a key requirement.

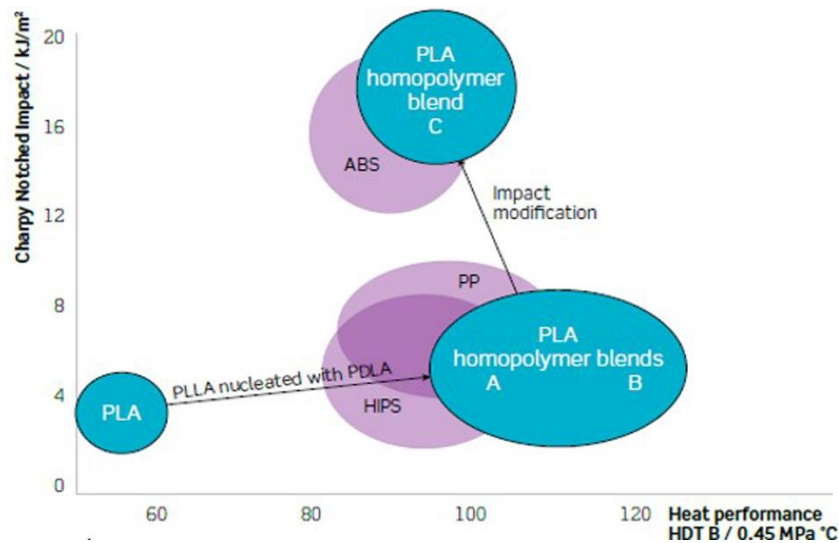


Figure II.8. Typical results of using PLA homopolymer blends: a heat performance similar to PS, PP and ABS (*Blend A*: PLLA + PDLA + nucleating agent; *Blend B*: *Blend A* + talc; *Blend C*: *Blend A* + talc + impact modifier). [100]

As shown in Figure II.8, the key-driver behind the improvement of HDT in *Blend A* is PLLA homopolymers that are nucleated with a small amount of PDLA homopolymers and a traditional nucleating agent. The improved heat performance of blend A was obtained without adding a significant amount of filler. To achieve a higher modulus, and an even higher temperature resistance, talc was added to *blend A* to form *Blend B* (respectively 4 GPa and 120°C instead of 3GPa and 105°C for *Blend A*), leading to better performances than those of PP and PS blends. To achieve an impact resistance comparable to that of ABS, *blend A* was impact modified and in order to minimize the drop in modulus, talc was added to this blend to obtain the *blend C*, characterized by a good balance of properties (33kJ/m² for impact resistance, 3.5 GPa for tensile modulus and 95°C for HDT).

Sections II.1 and II.2 have presented the most efficient way to improve PLA impact strength, ductility and thermal stability in order to make properties of PLA-based materials

compatible with their implementation as automotive components. Another key-point when developing materials for use in automotive industry is to ensure their good processability by mass production methods, typically by injection-molding. This subject is discussed in the next section.

II.3 Mold-injected PLA-materials for automotive applications

In automotive industry, PLA components are generally produced by injection-molding, similarly to other thermoplastics. Assets of injection molding are in particular a continuous production capacity with minimal maintenance and labor, allowing significant economies on large-scale. Several factors are involved in the injection molding process and have a great influence on the injected part, such as material formability, characteristics of molding machine, mold-design and process conditions (melt and mold temperature, pressure, etc.) [101,102].

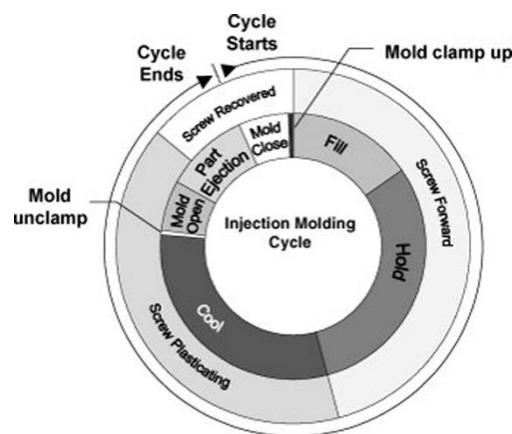


Figure II.9. Typical cycle for an injection molding process [103]

The typical cycle for an injection-molding process was detailed by Lim *et al.*[103] (Figure II.9). They described the different steps of the cycle and gave some advices to avoid defects in injection-molded products. While the cooling time must be sufficient to ensure a dimensionally stable injected part, cycle time has to be minimized to maximize the production throughput.

The slow crystallization rate of PLA compared to that of commonly injection-molded thermoplastics is a major obstacle for use in automotive industry, *i.e.* at high production rate. Indeed, an injection-molding cycle time in automotive industry typically ranges from 20 to 60 s [104], that implies in particular high cooling rate. However the crystallization half-time, $t_{1/2}$, of a pure sample of PLA was reported in the literature in the range of 17-45 min depending on

crystallization temperature, stereochemistry and molecular weight[105]. Therefore, injection-molding PLA for automotive parts is limited to the manufacturing of parts for which high crystallinity degree is not required. Indeed, using a post annealing step or longer cycle time to obtain sufficient crystallinity for PLA component would be impractical for a high volume automotive production. In addition, slow crystallization rate of PLA also causes difficulties during part ejection, therefore increasing again molding cycle duration.

An efficient way to accelerate crystallization of PLA is the incorporation of nucleating agents. In polymers, nucleating agents provide additional sites for crystallization initiation and also influence the crystalline morphology and crystallization kinetics [106-108]. For example, blending PLA with 5 wt% of talc can fundamentally change the crystalline morphology of the blend (Figure II.10). Judging from those polarized optical micrographs of PLA formulations, after non-isothermal crystallization from the melt, spherulite concentration increases and spherulite size decreases in PLA/talc compared to neat PLA. Therefore, talc addition can lead to much more heterogeneous nuclei and can reduce the size of spherulites[109]. Nucleating agents can therefore present a remarkable effect on the kinetics of crystallization by reducing the crystallization half-time, leading to a better processability of PLA. In some cases, they may also lead to enhanced mechanical properties.

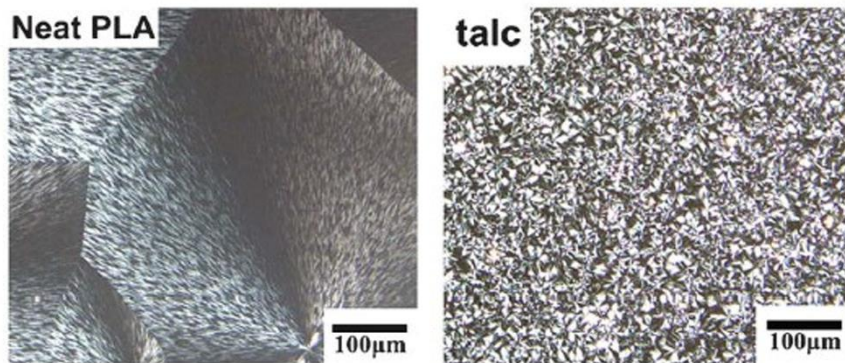


Figure II.10. Polarized optical micrographs of neat PLA (left) and PLA containing 5 wt% talc (right) at 122 °C after quenched from 180 °C [109].

Kolstad [110] showed that talc can be added to PLLA to effectively modify the crystallization rate of the polymer. The crystallization half-time of the polymer reduced from 3 min at 110 °C to approximately 25 s with the addition of 6 wt% talc to PLLA. At the same content of talc, for 3% mesolactide copolymerized with the L-lactide, the crystallization half-time is reduced from 7 min to 1 min, showing that the stereocomplex of PLLA and PDLA can also be regarded as a potential tool for self-nucleation of PLLA. Schmidt and Hillmyer [111] investigated self-

nucleation of PLLA, in which small crystallites of the stereocomplex were formed by blending up to 15% PDLA into PLLA. They compared the effectiveness of self-nucleation with the heterogeneous nucleation obtained from the addition of talc, finding self-nucleation more efficient. Self-nucleation reduced the crystallization half-time by nearly 40-fold, in the best case, while a similar loading of talc only decreased the half-time by just over 2-fold under the same conditions. While the majority of works dealing with nucleation of PLA are focused on the study of crystallization kinetics, morphology and some mechanical properties, Harris and Lee [105] pushed forward the study of nucleated PLA using talc and ethylene bis-stearamide (EBS) by optimizing the injection molding process parameters and post processing in order to increase crystallinity in the finished injected part. Furthermore, heat deflection temperature and flexural strength were analyzed. The authors showed that the addition of 2% of nucleating agent (talc or EBS) improved the crystallization rate by over 20-times and 65-times for EBS and talc, respectively, compared to neat PLA. The authors then worked on the optimization of processing conditions, especially for the nucleated samples, ever aiming at increasing PLA crystallinity and mechanical performances. Post-annealing processing of both nucleated and neat PLA materials was found to increase the crystallinity of PLA to a maximum level of 42% (Figure II.11a). Interestingly, annealing process is significantly faster in presence of nucleating agent. Injection molding the PLA materials into a preheated mold (110°C) was found to significantly increase the crystalline content of the molded specimens to their maximum level (41-43%) in both neat and nucleated PLA materials (Figure II.11b). Furthermore, the same crystallinity was reached at a lower temperature in the nucleated samples than for neat PLA (for instance a crystallinity ratio of 35% was reached at a mold temperature of about 80°C for nucleated samples, compared to about 100°C for neat PLA). The combination of nucleating agents and process optimization therefore allowed increasing crystallinity level in final injection molded part, together with a decrease in processing time. Moreover, an increase of 30°C in the heat deflection temperature (Figure II.11c) and an improvement of flexural modulus by upwards of 25% were achieved thanks to material nucleation and process optimization.

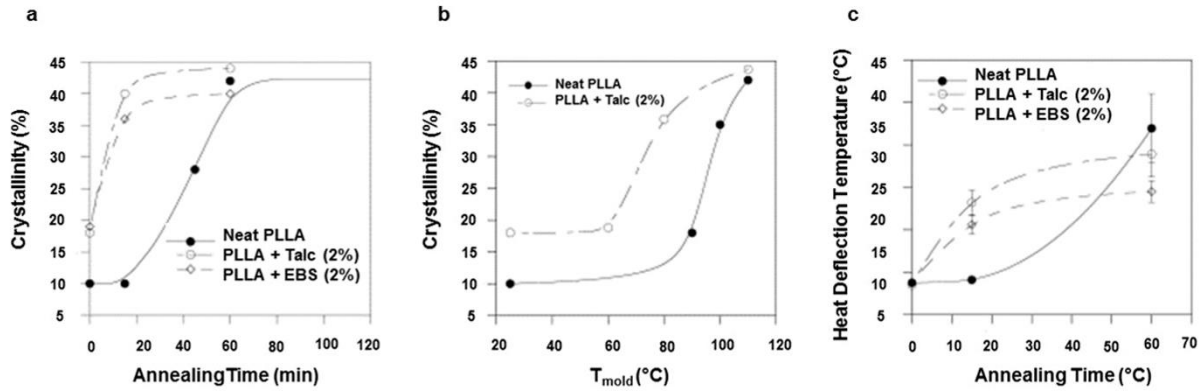


Figure II.11. (a) Crystallinity *versus* annealing time at 80 °C for neat PLA, PLA + talc, and PLA + EBS samples; (b) Crystallinity as a function of injection molding mold temperature for neat PLA and PLA + talc samples; (C) Dependence of heat deflection temperature (HDT) on annealing time at 80 °C for neat PLA, PLA + talc, and PLA + EBS samples. [105]

Previously exposed researches demonstrate that PLA crystallization kinetics can be improved in order to make PLA-based materials suitable for high-rate production process by injection molding, typical of automotive industry. More precisely, the increase of crystallization rates achieved in these works and discussed in this section can result in reduction of both cycle time and energy consumption during injection molding process. Moreover, materials with higher crystallinity degree show increased mechanical properties, especially in terms of rigidity and strength and sometimes thermal resistance, and are thought to have better durability. The issue of durability of PLA blends constitutes the subject of the next section.

II.4. Durable PLA/polymer blends

Plastics and polymer composites recently developed can have mechanical performances that withstand the related stresses of many applications, including highly-loaded parts. However, some operating conditions, such as high temperature, corrosive chemicals in fluids and lubricants, electric currents, weather variations, or minerals from roadways, may be too harsh to be endured by some plastics and polymer composites over a whole vehicle's lifetime. Hence, both interior and exterior parts are exposed to a large range of temperature (-40 to 80°C) together with high humidity level, throughout the vehicle lifetime (possibly higher than 10 years). Obviously, these conditions can have long term detrimental effects on the durability, performance and aesthetics of the materials in automotive components. Suitability of a material for automotive application must therefore be evaluated regarding long-term performances.

Under specific conditions, PLA presents a fast degradation rate, which makes it appealing for disposable applications, but inadequate for applications requiring long-term

durability. It explains why the majority of current commercial applications for PLA blends are oriented to clothing and linens, disposable packaging and objects (*e.g.*, water cups). Unfortunately, very few researches and applications concern the use of PLA in durable goods[112,113], and even less in case of severe environmental conditions such as in automotive applications. Among the few available works, Harris *et al.*[114] have investigated the durability of a commercial injection-molding grade of PLA through its crystallization behavior. Commercially available injection-molding grade of PLA and annealed PLA were conditioned at a temperature of 50°C and 90% relative humidity (RH) for 12 weeks, which corresponds to a simulated environment for automotive interiors. Moisture absorption, molecular weight and mechanical performances were investigated. Both amorphous and crystalline PLA showed significant moisture absorption, allowing hydrolysis to occur with a linear regression of average molecular weight more accentuated for amorphous PLA (Figure II.12a,b). The effect of moisture and heat-conditioning on mechanical performances was examined through the evolution of flexural strength (Figure II.12c). This one decreased significantly for both amorphous and annealed PLA. As a conclusion, properties of the conditioned samples were not maintained, even for crystalline PLA, and commercial PLA grades remain inadequate for durable use in automotive parts.

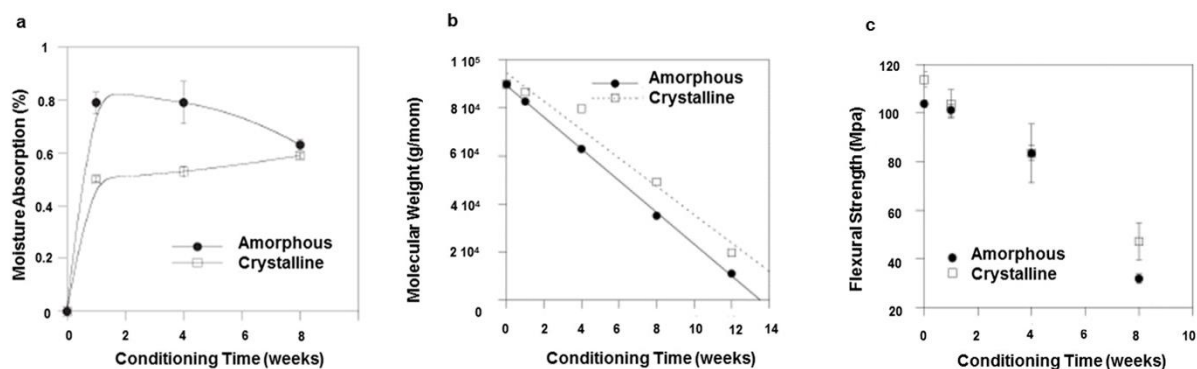


Figure II.12. (a) Moisture absorption as a function of conditioning time for amorphous and crystalline PLA; (b) Dependence of molecular weight on conditioning time for amorphous and crystalline PLA; (c) Dependence of flexural strength on conditioning time for amorphous and crystalline PLA. [114]

However, different approaches have proven to improve the durability of PLA-based materials. A possible approach is to blend PLA with resins that are not susceptible to hydrolysis and could prevent contact between PLA and water by acting as moisture barrier.[115,116] In this regard,

Harris *et al.* [116] have studied the durability of PLA/PC blends (PLA content equal to 100 wt%; 45 wt%; 30 wt% and 25 wt%, with corresponding codifications PLA-100; PLA-45; PLA-30 and PLA-25) for use in injection-molded automotive interior parts. Harsh conditions were imposed to study the durability of PLA/PC blends, namely 70°C and 90% RH for 62 days corresponding to 10 years of in-field exposure for an automotive interior component in a southern Florida climate. Durability of ABS/PC was used as a basis of comparison. Results demonstrated that the presence of PC can improve the long-term performance of the blends compared to neat PLA (durability increase for 1 in-field exposure year). Nevertheless, all samples containing PLA exhibited extreme degradation after 14 conditioning days, resulting to a drop in mechanical performances (here in terms of flexural strength, Figure II.13a) together with the formation of a large amount of brown liquid residue at the sample surfaces due to the hydrolysis of the PC phase (accompanied by the apparition of potentially health-harmful Bisphenol-A (BPA) – Figure II.13b,c). Although PC was initially blended to stabilize PLA and improve the overall durability, final durability of the blend was marginally improved due to the hydrolytic degradation of PC. It can be noted that PC suffered more from hydrolysis when blended with PLA than with ABS.

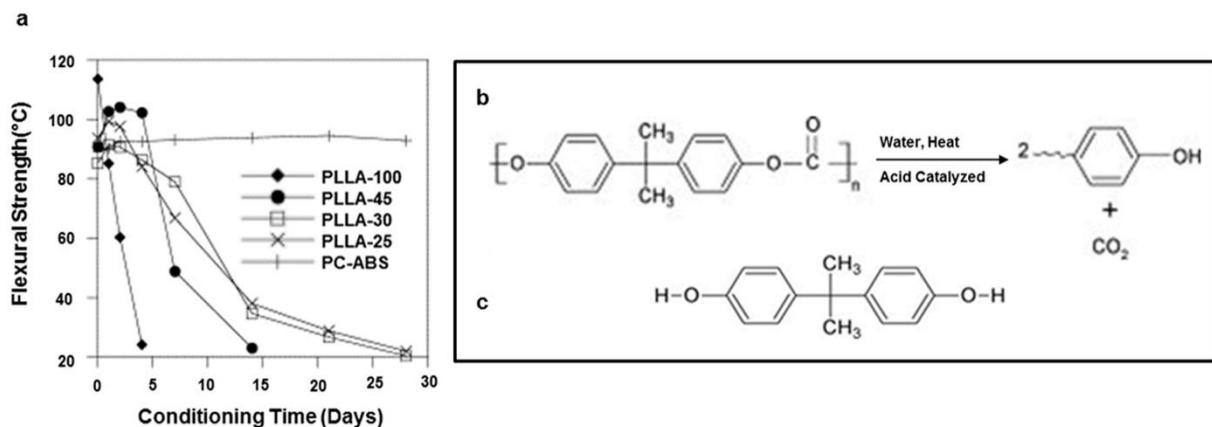


Figure II.13. (a) Flexural strength as a function of conditioning time of PLA/PC blends; (b) Hydrolysis reaction of polycarbonate; (c) Chemical structure of bisphenol-A (BPA) [116]

As a conclusion, the formation of PC/PLA blends has not achieved yet a durability level high enough for automotive applications, regardless of PC content. However, blending PLA with more durable polymer resins in order to enhance durability of blends constitutes a promising research field.

CONCLUSIONS

Automotive industry is one of the mainsprings of development of bioplastics and biocomposites for durable applications, due to its well-structured network of car manufacturers, original equipment manufacturers (OEMs), and material suppliers. All have indeed considerable needs in bioplastics and biocomposites in order to meet the increasingly binding objectives in terms of reduction of vehicle weight combined with increasing demand in more environmentally friendly materials.

In this chapter, a special attention is paid on the development of PLA based blends and on the different modifications that may enhance PLA performances in terms of mechanical properties (ductility combined with high rigidity and strength), high heat-resistance, durability and good processability, even under high-rate production. Some of these modifications lead to relevant materials for use in the automotive sector, allowing carmakers to invest into ecofriendly vehicles using developed PLA-based bioplastics and biocomposites. However, up to now, automotive applications of tailored PLA compounds are limited to interior parts, particularly due to the long term durability under the severe environmental conditions that exterior parts have to undergo. However, research is on a right path to offer in the next future PLA-based blends suitable for exterior parts of vehicle, spare parts for a less storage facilities.

REFERENCES

-
1. Brostow W, Datashvili T (2016) *Environmental Impact of Natural Polymers*. In: *Natural Polymers*. Springer, pp 315-338
 2. Akampumuza O et al. (2016) *Review of the applications of biocomposites in the automotive industry*. *Polymer Composites*:n/a-n/a. doi:10.1002/pc.23847
 3. Niaounakis M (2015) *6 - Automotive Applications*. In: *Biopolymers: Applications and Trends*. William Andrew Publishing, Oxford, pp 257-289.
 4. Garlotta D *A Literature Review of Poly(Lactic Acid)*. *Journal of Polymers and the Environment* 9 (2):63-84. doi:10.1023/a:1020200822435
 5. Avérous L (2008) *Chapter 21 - Polylactic Acid: Synthesis, Properties and Applications*. In: Gandini MNB (ed) *Monomers, Polymers and Composites from Renewable Resources*. Elsevier, Amsterdam, pp 433-450.
 6. Maxwell J (1994) *Plastics in the automotive industry*. Elsevier,
 7. Auras RA et al. (2011) *Poly (lactic acid): synthesis, structures, properties, processing, and applications*, vol 10. John Wiley & Sons,
 8. Notta-Cuvier D et al. (2015) *Tailoring Polylactide Properties for Automotive Applications: Effects of Co-Addition of Halloysite Nanotubes and Selected Plasticizer*. *Macromolecular Materials and Engineering*:n/a-n/a. doi:10.1002/mame.201500032
 9. 1 - INTRODUCTION A2 - Wypych, George (2012). In: *Handbook of Plasticizers (Second Edition)*. William Andrew Publishing, Boston, pp 1-6.
 10. Ljungberg N, Wesslén B (2005) *Preparation and Properties of Plasticized Poly(lactic acid) Films*. *Biomacromolecules* 6 (3):1789-1796. doi:10.1021/bm050098f
 11. Liu H, Zhang J (2011) *Research progress in toughening modification of poly(lactic acid)*. *Journal of Polymer Science Part B: Polymer Physics* 49 (15):1051-1083. doi:10.1002/polb.22283
 12. Ruellan A et al. (2015) *CHAPTER 5 Plasticization of Poly(lactide)*. In: *Poly(lactic acid) Science and Technology: Processing, Properties, Additives and Applications*. The Royal Society of Chemistry, pp 124-170. doi:10.1039/9781782624806-00124
 13. Jacobsen S, Fritz HG (1999) *Plasticizing polylactide—the effect of different plasticizers on the mechanical properties*. *Polymer Engineering & Science* 39 (7):1303-1310. doi:10.1002/pen.11517

14. Murariu M et al. (2008) *Poly(lactide) (PLA) designed with desired end-use properties: I. PLA compositions with low molecular weight ester-like plasticizers and related performances. Polymers for Advanced Technologies 19 (6):636-646. doi:10.1002/pat.1131*
15. Zhang H et al. (2013) *Thermal, mechanical, and rheological properties of poly(lactide)/poly(1,2-propylene glycol adipate). Polymer Engineering & Science 53 (1):112-118. doi:10.1002/pen.23238*
16. Ren Z et al. (2006) *Dynamic mechanical and thermal properties of plasticized poly(lactic acid). Journal of Applied Polymer Science 101 (3):1583-1590. doi:10.1002/app.23549*
17. Wojciechowska P (2012) *The Effect of concentration and type of plasticizer on the mechanical properties of cellulose acetate butyrate organic-inorganic hybrids. INTECH Open Access Publisher,*
18. Suvorova AI et al. (1993) *Chemical structure of plasticizers, compatibility of components and phase equilibrium in plasticized cellulose diacetate. Die Makromolekulare Chemie 194 (5):1315-1321. doi:10.1002/macp.1993.021940506*
19. Kfoury G et al. (2013) *Recent advances in high performance poly (lactide): from “green” plasticization to super-tough materials via (reactive) compounding. Frontiers in chemistry 1*
20. Sangeetha VH et al. (2016) *State of the art and future perspectives of poly(lactic acid) based blends and composites. Polymer Composites:n/a-n/a. doi:10.1002/pc.23906*
21. Odent J et al. (2015) *Highly Toughened Poly(lactide)-Based Materials through Melt-Blending Techniques. In: Biodegradable Polyesters. Wiley-VCH Verlag GmbH & Co. KGaA, pp 235-274. doi:10.1002/9783527656950.ch10*
22. Anderson KS et al. (2008) *Toughening Poly(lactide). Polymer Reviews 48 (1):85-108. doi:10.1080/15583720701834216*
23. Hongzhi L, Jinwen Z (2012) *Toughening Modification of Poly(lactic acid) via Melt Blending. In: Biobased Monomers, Polymers, and Materials, vol 1105. ACS Symposium Series, vol 1105. American Chemical Society, pp 27-46. doi:doi:10.1021/bk-2012-1105.ch003*
10.1021/bk-2012-1105.ch003
24. Detyothin S et al. (2010) *Poly(Lactic Acid) Blends. In: Poly(Lactic Acid). John Wiley & Sons, Inc., pp 227-271. doi:10.1002/9780470649848.ch16*
25. Perkins WG (1999) *Polymer toughness and impact resistance. Polymer Engineering & Science 39 (12):2445-2460. doi:10.1002/pen.11632*

26. Liu Z-W et al. (2014) *Mechanical and thermal properties of thermoplastic polyurethane-toughened polylactide-based nanocomposites*. *Polymer Composites* 35 (9):1744-1757. doi:10.1002/pc.22828
27. Natureworks (2007) *Technology Focus Report: Toughened PLA*.
28. Taib RM et al. (2012) *Thermal, mechanical, and morphological properties of polylactic acid toughened with an impact modifier*. *Journal of Applied Polymer Science* 123 (5):2715-2725. doi:10.1002/app.34884
29. Notta-Cuvier D et al. (2014) *Tailoring polylactide (PLA) properties for automotive applications: Effect of addition of designed additives on main mechanical properties*. *Polymer Testing* 36 (0):1-9.
30. Zhang K et al. (2014) *Supertoughened Renewable PLA Reactive Multiphase Blends System: Phase Morphology and Performance*. *ACS Applied Materials & Interfaces* 6 (15):12436-12448. doi:10.1021/am502337u
31. Zhang C et al. (2013) *Thermal, mechanical and rheological properties of polylactide toughened by epoxidized natural rubber*. *Materials & Design* 45:198-205.
32. Pattamaprom C et al. (2016) *Improvement in impact resistance of polylactic acid by masticated and compatibilized natural rubber*. *Iranian Polymer Journal* 25 (2):169-178. doi:10.1007/s13726-015-0411-7
33. Pongtanayut K et al. (2013) *The Effect of Rubber on Morphology, Thermal Properties and Mechanical Properties of PLA/NR and PLA/ENR Blends*. *Energy Procedia* 34:888-897.
34. Desa M et al. *Mechanical and Thermal Properties of Rubber Toughened Poly (Lactic Acid)*. In: *Advanced Materials Research*, 2015. Trans Tech Publ, pp 222-226
35. Sun Y, He C (2013) *Biodegradable "Core-Shell" Rubber Nanoparticles and Their Toughening of Poly(lactides)*. *Macromolecules* 46 (24):9625-9633. doi:10.1021/ma4020615
36. Odent J et al. (2013) *Toughening of polylactide by tailoring phase-morphology with P[CL-co-LA] random copolyesters as biodegradable impact modifiers*. *European Polymer Journal* 49 (4):914-922.
37. Meyva Y, Kaynak C (2015) *Toughening of Polylactide by Bio-Based and Petroleum-Based Thermoplastic Elastomers*. *International Polymer Processing* 30 (5):593-602. doi:10.3139/217.3113
38. Li Y, Shimizu H (2007) *Toughening of polylactide by melt blending with a biodegradable poly (ether) urethane elastomer*. *Macromolecular Bioscience* 7 (7):921-928
39. Todo M, Takayama T *Fracture Mechanisms of Biodegradable PLA and PLA/PCL Blends*.

40. Todo M, Takayama T (2007) Toughening of bioabsorbable polymer blend by microstructural modification. In: Watanabe M, Okuno O, Sasaki K, Takahashi N, Suzuki O, Takada H (eds) *Interface Oral Health Science 2007: Proceedings of the 2nd International Symposium for Interface Oral Health Science, Held in Sendai, Japan, Between 18 and 19 February, 2007*. Springer Japan, Tokyo, pp 95-104. doi:10.1007/978-4-431-76690-2_9
41. Turng L-S, Sriเทพ Y Annealing conditions for injection molded poly (lactic acid). *Society of Plastics Engineers (SPE)*
42. Grijpma DW et al. (2002) Improvement of the mechanical properties of poly(D,L-lactide) by orientation. *Polymer International* 51 (10):845-851. doi:10.1002/pi.988
43. Carrasco F et al. (2010) Processing of poly(lactic acid): Characterization of chemical structure, thermal stability and mechanical properties. *Polymer Degradation and Stability* 95 (2):116-125.
44. Nascimento L et al. (2010) Effect of the Recycling and Annealing on the Mechanical and Fracture Properties of Poly(Lactic Acid). *Journal of Polymers and the Environment* 18 (4):654-660. doi:10.1007/s10924-010-0229-5
45. Gámez-Pérez J et al. (2011) Fracture behavior of quenched poly (lactic acid). *Express Polym Lett* 5 (1):82-91
46. Yang G et al. (2012) Toughening of poly (L-lactic acid) by annealing: the effect of crystal morphologies and modifications. *Journal of Macromolecular Science, Part B* 51 (1):184-196
47. Perego G et al. (1996) Effect of molecular weight and crystallinity on poly(lactic acid) mechanical properties. *Journal of Applied Polymer Science* 59 (1):37-43. doi:10.1002/(sici)1097-4628(19960103)59:1<37::aid-app6>3.0.co;2-n
48. Edenhofer B et al. (2013) The flexible heat treatment of automotive components in a novel type of pusher furnace. *La Metallurgia Italiana* (2)
49. Funatani K (2004) Heat treatment of automotive components: current status and future trends. *Trans Indian Inst Met* 57 (4):381-396
50. Tucker N, Lindsey K (2002) *An introduction to automotive composites*. iSmithers Rapra Publishing,
51. Johnson RW et al. (2004) The changing automotive environment: high-temperature electronics. *Electronics Packaging Manufacturing, IEEE Transactions on* 27 (3):164-176
52. ASTM Standard Test Method for Deflection Temperature of Plastics Under Flexural Load in the Edgewise Position. ASTM. <http://www.astm.org/Standards/D648.htm>. 2016

53. Huda MS et al. (2006) *Wood-fiber-reinforced poly(lactic acid) composites: Evaluation of the physicomechanical and morphological properties. Journal of Applied Polymer Science* 102 (5):4856-4869. doi:10.1002/app.24829
54. Shih Y-F, Huang C-C (2011) *Poly(lactic acid) (PLA)/banana fiber (BF) biodegradable green composites. Journal of Polymer Research* 18 (6):2335-2340. doi:10.1007/s10965-011-9646-y
55. Lee B-H et al. (2009) *Bio-composites of kenaf fibers in polylactide: Role of improved interfacial adhesion in the carding process. Composites Science and Technology* 69 (15–16):2573-2579.
56. Shi QF et al. (2012) *Influence of heat treatment on the heat distortion temperature of poly(lactic acid)/bamboo fiber/talc hybrid biocomposites. Journal of Applied Polymer Science* 123 (5):2828-2836. doi:10.1002/app.34807
57. Ganster J, Fink H-P (2006) *Novel cellulose fibre reinforced thermoplastic materials. Cellulose* 13 (3):271-280. doi:10.1007/s10570-005-9045-9
58. Chanda M, Roy SK (2008) *Industrial polymers, specialty polymers, and their applications, vol 74. CRC press,*
59. Coelho MC et al. (2012) *Nanotechnology in automotive industry: research strategy and trends for the future—small objects, big impacts. Journal of nanoscience and nanotechnology* 12 (8):6621-6630
60. Mai Y-W, Yu Z-Z (2006) *Polymer nanocomposites. Woodhead publishing,*
61. Huang J-W et al. (2009) *Poly(lactide)/nano and microscale silica composite films. I. Preparation and characterization. Journal of Applied Polymer Science* 112 (3):1688-1694. doi:10.1002/app.29616
62. Frone AN et al. (2011) *Cellulose fiber-reinforced poly(lactic acid). Polymer Composites* 32 (6):976-985. doi:10.1002/pc.21116
63. Li ZQ et al. (2010) *Preparation and Characterization of Bacterial Cellulose/Poly(lactide) Nanocomposites. Polymer-Plastics Technology and Engineering* 49 (2):141-146. doi:10.1080/03602550903284198
64. Shameli K et al. (2010) *Silver/poly(lactic acid) nanocomposites: preparation, characterization, and antibacterial activity. International journal of nanomedicine* 5:573-579
65. Xu X et al. (2006) *Biodegradable electrospun poly(l-lactide) fibers containing antibacterial silver nanoparticles. European Polymer Journal* 42 (9):2081-2087.
66. González A et al. (2012) *Fire retardancy behavior of PLA based nanocomposites. Polymer Degradation and Stability* 97 (3):248-256.

67. Sinha Ray S, Okamoto M (2003) *Polymer/layered silicate nanocomposites: a review from preparation to processing*. *Progress in Polymer Science* 28 (11):1539-1641.
68. Alexandre M, Dubois P (2000) *Polymer-layered silicate nanocomposites: preparation, properties and uses of a new class of materials*. *Materials Science and Engineering: R: Reports* 28 (1–2):1-63.
69. Sinha Ray S, Bousmina M (2005) *Biodegradable polymers and their layered silicate nanocomposites: In greening the 21st century materials world*. *Progress in Materials Science* 50 (8):962-1079.
70. Kurauchi T et al. (1991) *Nylon 6-clay hybrid-synthesis, properties and application to automotive timing belt cover*. *SAE Technical Paper*,
71. Paul M-A et al. (2003) *Exfoliated Polylactide/Clay Nanocomposites by In-Situ Coordination–Insertion Polymerization*. *Macromolecular Rapid Communications* 24 (9):561-566. doi:10.1002/marc.200390082
72. Khankrua R et al. (2013) *Thermal and Mechanical Properties of Biodegradable Polyester/Silica Nanocomposites*. *Energy Procedia* 34:705-713.
73. Murariu M et al. (2010) *New trends in polylactide (PLA)-based materials: “Green” PLA–Calcium sulfate (nano)composites tailored with flame retardant properties*. *Polymer Degradation and Stability* 95 (3):374-381.
74. Sinha Ray S et al. (2003) *New polylactide-layered silicate nanocomposites. 2. Concurrent improvements of material properties, biodegradability and melt rheology*. *Polymer* 44 (3):857-866.
75. Pilla S et al. (2010) *Microcellular processing of polylactide–hyperbranched polyester–nanoclay composites*. *Journal of Materials Science* 45 (10):2732-2746. doi:10.1007/s10853-010-4261-6
76. Ameli A et al. (2014) *Development of high void fraction polylactide composite foams using injection molding: Mechanical and thermal insulation properties*. *Composites Science and Technology* 90:88-95
77. Pilla S et al. (2007) *Solid and Microcellular Polylactide-Carbon Nanotube Nanocomposites*. *International Polymer Processing* 22 (5):418-428. doi:10.3139/217.2071
78. Kramschuster A et al. (2007) *Injection Molded Solid and Microcellular Polylactide Compounded with Recycled Paper Shopping Bag Fibers*. *International Polymer Processing* 22 (5):436-445. doi:10.3139/217.2063

79. Seo J-H et al. (2012) *Combined Effects of Chemical and Microcellular Foaming on Foaming Characteristics of PLA (Poly Lactic Acid) in Injection Molding Process*. *Polymer-Plastics Technology and Engineering* 51 (5):455-460. doi:10.1080/03602559.2011.651239
80. NatureWorks (2007) *Technology Focus Report: Blends of PLA with Other Thermoplastics*. NatureWorks LLC,
81. Guo X et al. (2015) *Poly(lactic acid)/polyoxymethylene blends: Morphology, crystallization, rheology, and thermal mechanical properties*. *Polymer* 69:103-109.
82. Hashima K et al. (2010) *Structure-properties of super-tough PLA alloy with excellent heat resistance*. *Polymer* 51 (17):3934-3939.
83. Wang Y et al. (2012) *Improvement in toughness and heat resistance of poly(lactic acid)/polycarbonate blend through twin-screw blending: Influence of compatibilizer type*. *Journal of Applied Polymer Science* 125 (S2):E402-E412. doi:10.1002/app.36920
84. Lin L et al. (2015) *Improving the impact property and heat-resistance of PLA/PC blends through coupling molecular chains at the interface*. *Polymers for Advanced Technologies* 26 (10):1247-1258. doi:10.1002/pat.3560
85. Lin L et al. (2015) *Super Toughened and High Heat-Resistant Poly(Lactic Acid) (PLA)-Based Blends by Enhancing Interfacial Bonding and PLA Phase Crystallization*. *Industrial & Engineering Chemistry Research* 54 (21):5643-5655. doi:10.1021/acs.iecr.5b01177
86. Srithep Y et al. (2014) *Processing and characterization of poly(lactic acid) blended with polycarbonate and chain extender*. *Journal of Polymer Engineering*, vol 34. doi:10.1515/polyeng-2013-0309
87. Liu J (2014) *Heat resistant, flame retardant polylactic acid compounds*. Google Patents,
88. Eguiburu JL et al. (1998) *Blends of amorphous and crystalline polylactides with poly(methyl methacrylate) and poly(methyl acrylate): a miscibility study*. *Polymer* 39 (26):6891-6897.
89. Li S-H, Woo EM (2008) *Immiscibility–miscibility phase transitions in blends of poly(L-lactide) with poly(methyl methacrylate)*. *Polymer International* 57 (11):1242-1251. doi:10.1002/pi.2469
90. Samuel C et al. (2013) *PLLA/PMMA blends: A shear-induced miscibility with tunable morphologies and properties?* *Polymer* 54 (15):3931-3939.
91. Zhang G et al. (2003) *Miscibility and phase structure of binary blends of polylactide and poly(methyl methacrylate)*. *Journal of Polymer Science Part B: Polymer Physics* 41 (1):23-30. doi:10.1002/polb.10353

92. Tsuji H (2007) *Poly(lactide) Stereocomplexes: Formation, Structure, Properties, Degradation, and Applications*. *Macromolecular Bioscience* 7 (12):1299-1299. doi:10.1002/mabi.200700275
93. Ikada Y et al. (1987) *Stereocomplex formation between enantiomeric poly(lactides)*. *Macromolecules* 20 (4):904-906. doi:10.1021/ma00170a034
94. Tsuji H et al. (1991) *Stereocomplex formation between enantiomeric poly(lactic acid)s*. 4. *Differential scanning calorimetric studies on precipitates from mixed solutions of poly(D-lactic acid) and poly(L-lactic acid)*. *Macromolecules* 24 (20):5657-5662. doi:10.1021/ma00020a027
95. Torres L et al. (2016) *Effect of multi-branched PDLA additives on the mechanical and thermomechanical properties of blends with PLLA*. *Journal of Applied Polymer Science* 133 (1):n/a-n/a. doi:10.1002/app.42858
96. Zou J et al. (2012) *Effects of Poly (D-lactide acid) on the Properties of Crystallization and Thermal Behavior of Poly (L-lactide acid)*. *Advances in Information Sciences & Service Sciences* 4 (10)
97. Oyama HT, Abe S (2015) *Stereocomplex Poly(lactic acid) Alloys with Superb Heat Resistance and Toughness*. *ACS Sustainable Chemistry & Engineering* 3 (12):3245-3252. doi:10.1021/acssuschemeng.5b00832
98. Sun B et al. (2016) *Enhanced toughness and strength of poly (d-lactide) by stereocomplexation with 5-arm poly (l-lactide)*. *Journal of Applied Polymer Science* 133 (1):n/a-n/a. doi:10.1002/app.42857
99. Nam B-U, Lee B-S (2012) *Toughening of PLA stereocomplex by Impact modifiers*. *Journal of the Korea Academia-Industrial cooperation Society* 13 (2):919-925
100. Purac C (2015) *High heat PLA*

Unlocking bioplastic potential for durable applications.

101. Min BH (2003) *A study on quality monitoring of injection-molded parts*. *Journal of Materials Processing Technology* 136 (1–3):1-6.
102. Spina R (2004) *Injection moulding of automotive components: comparison between hot runner systems for a case study*. *Journal of Materials Processing Technology* 155–156:1497-1504.
103. Lim LT et al. (2008) *Processing technologies for poly(lactic acid)*. *Progress in Polymer Science* 33 (8):820-852.
104. Mazumdar S (2001) *Composites manufacturing: materials, product, and process engineering*. CrC press,

105. Harris AM, Lee EC (2008) *Improving mechanical performance of injection molded PLA by controlling crystallinity. Journal of Applied Polymer Science* 107 (4):2246-2255. doi:10.1002/app.27261
106. Li M et al. (2010) *Nonisothermal crystallization kinetics of poly(lactic acid) formulations comprising talc with poly(ethylene glycol). Polymer Engineering & Science* 50 (12):2298-2305. doi:10.1002/pen.21755
107. Urayama H et al. (2003) *Controlled crystal nucleation in the melt-crystallization of poly(l-lactide) and poly(l-lactide)/poly(d-lactide) stereocomplex. Polymer* 44 (19):5635-5641.
108. Petchwattana N et al. (2014) *Influence of talc particle size and content on crystallization behavior, mechanical properties and morphology of poly (lactic acid). Polymer bulletin* 71 (8):1947-1959
109. Zhou J et al. (2013) *Synthesis and characterization of triblock copolymer PLA-b-PBT-b-PLA and its effect on the crystallization of PLA. RSC Advances* 3 (40):18464-18473. doi:10.1039/c3ra42096e
110. Kolstad JJ (1996) *Crystallization kinetics of poly(L-lactide-co-meso-lactide). Journal of Applied Polymer Science* 62 (7):1079-1091. doi:10.1002/(sici)1097-4628(19961114)62:7<1079::aid-app14>3.0.co;2-1
111. Schmidt SC, Hillmyer MA (2001) *Poly(lactide) stereocomplex crystallites as nucleating agents for isotactic polylactide. Journal of Polymer Science Part B: Polymer Physics* 39 (3):300-313. doi:10.1002/1099-0488(20010201)39:3<300::aid-polb1002>3.0.co;2-m
112. LTD. NCU (2006) *NEC & UNITIKA Realize Bioplastic Reinforced with Kenaf Fiber for Mobile Phone Use.*
113. Fujitsu Limited FL, Ltd., and Toray Industries, Inc (2005) *Fujitsu and Toray Develop World's First Environmentally-Friendly Large-Size Plastic Housing for Notebook PCs.*
114. Harris AM, Lee EC (2010) *Heat and humidity performance of injection molded PLA for durable applications. Journal of Applied Polymer Science* 115 (3):1380-1389. doi:10.1002/app.30815
115. Finnis A (2014) *Poly(lactic Acid)-Based Polymer Blends for Durable Applications. WEST VIRGINIA UNIVERSITY,*
116. Harris AM, Lee EC (2013) *Durability of polylactide-based polymer blends for injection-molded applications. Journal of Applied Polymer Science* 128 (3):2136-2144. doi:10.1002/app.38407

RESEARCH STRATEGIES

Research strategies

As stated before, the aim of this present research work is to elaborate tough and ductile PLA-based materials with improved thermal properties to be used in technical application such as automotive application, upon the design of PLA-based compounds with the use of different additives and process modification. Several bulk-modification methods are employed to improve mechanical properties (mainly toughness), thermal stability, processibility and crystallinity of PLA. Blending are chosen as effective alternative way to develop new PLA-based materials with desired properties in this thesis. New PLA-based compounds are developed with addition of commercial rubber impact modifier to improve impact resistance and ductility, petro-sourced polymer for enhanced thermal stability, and other strategies to improve crystallinity of PLA-based compounds such as annealing, stereocomplexing and combination of nucleating agent and nanoparticles. To generate toughened PLA with high mechanical performances and high thermal stability, several key-parameters involving the matrix polymer (*i.e.* miscibility, concentration), the matrix-rubber adhesion (*i.e.* domain size and shape, distribution) and process modification (*i.e.* annealing temperature and time) must be properly controlled. Furthermore, another objective of this thesis is to select the most promising compound offering an appropriate balance between different properties such as ductility, strength and stiffness, impact toughness, good thermal stability and a content of bio-sourced polymer in the blend at least equal to 50% with the aim to be industrialized for use in technical parts subjected to severe loading conditions.

To achieve these objectives, different approaches have been explored during this Ph.D. degree to elaborate PLA materials suitable for technical application. In particular, works focus on improvement of both mechanical and thermal properties as well as on the scaling-up of the promoted PLA-based compound towards industrialization prospective. The final performance of compound subjected to severe loading conditions is checked and its durability under severe thermal conditions is studied. Furthermore, a special emphasis is put on the “structure - properties - process” relationship about the performances of the as-produced PLA-based materials.

The body of this thesis is organized into 5 chapters. In details, Chapter II is a background review about the development of PLA based blends and the different modifications that may enhance PLA performances in terms of mechanical properties (ductility combined with high rigidity and strength), high heat-resistance, durability and good processability, even under high-

rate production. Based on previous researches carried out in our laboratory group, we had the idea to combine a commercial impact modifier Biomax Strong and a petrosourced polymer poly(methyl)methacrylate (PMMA) to overcome toughness limitation and improve thermal stability of PLA blends. To reach our objectives, the determination of prevailing parameters is necessary for endowing PLA-based materials with high-toughness and thermal resistance as described in Chapter III. Among these key-parameters, some concern the matrix phase (*i.e.* miscibility of the matrix, crystallinity), the impact modifier phase (*i.e.* immiscibility with the matrix) or again the phase morphology (*i.e.* mean size of rubber, shape and related distribution of the dispersed phase). However, the crystallization ability of these blends remained inferior to what it is required for their industrial processing, for instance, by injection techniques. In chapter IV, different strategies to promote PLA crystallization were therefore investigated with the objective of increasing both crystalline rate and content in order to improve thermal stability ultimately. Three different methods are tested, namely annealing process, addition of silica nanoparticles and nucleating agent or finally stereocomplexation by adding PDLA to PLA blends.

Keeping in mind a future industrialization of PLA-based composition, Chapter V covers the scaling up, the evaluation of mechanical performances under severe loadings and finally the durability of best compounds. In details, the selected compound is processed at “industrial scale” by extrusion and injection molding, while controlling the prevailing parameters (feeding rate, residence time governed by rotation speed and feeding rate), which are necessary for keeping interesting thermo-mechanical properties. Then, tensile behavior of resulting blends is investigated under high-strain-rate loadings, for the moment at ambient temperatures in order to verify the suitability of the promising compound for use in technical parts subjected to severe loading conditions. Finally, suitability of the selected material for automotive application must be evaluated regarding long-term performances under severe conditions (high temperature). Through these different approaches, the present thesis will highlight the best approach strategy offering a suitable PLA based material for automotive application and responding in terms of properties, durability and environmental regulation, to the requirement of automotive industry.

CHAPTER III

DESIGN OF HIGHLY TOUGH POLY (L-LACTIDE)-BASED
TERNARY BLENDS

Design of highly tough poly(L-lactide)-based ternary blends for automotive applications

INTRODUCTION

Renewable and biodegradable plastics are being more and more appealing due to the growing concerns on sustainability and end-of-life aspects [1]. Among them, polylactide (PLA) is definitely the most promising bioplastics for numerous applications [2-4]. Several key-points contribute to the success of PLA as a renewable alternative to traditional petroleum-based plastics, especially its excellent biocompatibility, bioresorbability, (bio)degradability as well as its attractive physical and mechanical properties such as high rigidity, strength and easy processability [5]. Yet, for automotive applications, some properties of PLA-based materials have still to be improved, in particular durability, flexibility in the design, ductility, resiliency and thermal properties, while keeping an affordable cost. Several strategies have thereby been carried out to overcome those drawbacks and to improve limited mechanical properties of PLA (see Chapter II).

In that context, blending PLA with another (partially) miscible thermoplastic polymer (petro-sourced or not) often appears as a promising strategy to improve PLA thermal and/or mechanical properties [6-15]. In particular, Poly(methyl methacrylate) (PMMA) is often viewed as an excellent polymer partner with PLA, yielding blends of high miscibility, excellent thermal stability with higher heat deflection temperature (HDT), high mechanical properties, sustainability and good ageing behavior [7,16-18]. However, toughness and ductility of the blend still need some improvement to make PLA-based compositions suitable for engineering applications.

To overcome toughness limitation and reduce brittleness, the use of impact modifier is of high interest, as it allows to impart greater energy dissipation pathways throughout the materials, without affecting stiffness and thermal stability [19]. Many commercially available impact modifiers such as Biomax Strong are specifically designed in order to toughen PLA [20-23] as dispersed rubbery microdomains (with an average size around 0.1–1.0 μm) within the PLA matrix able to absorb the energy upon an impact [24]. Their toughening effects are of varying magnitudes, depending on their miscibility extent within the PLA matrix, their thermal stability under PLA processing temperatures, the interfacial adhesion between the dispersed rubbery phase and the continuous PLA matrix within the blend, *etc.*

Impact modifiers providing an appropriate balance of these properties are therefore fundamental for these intended applications.

The present contribution aims at designing rubber-toughened PLA/PMMA-based formulations with enhanced heat deflection temperature (HDT) suitable for injection-molding process via the addition of a commercially-available impact modifier. Among different tested impact modifiers (PARALOID™ BPM-520, Biostrength®150, Biomax® Strong 120, Nanostrength®M53, Nanostrength®E20, LOTADER®AX8900 and Biomax®PTT 1100) Biomax® Strong 120 (BS) was selected as an efficient impact modifier commercially available from Dupont™, yielding, e.g., PLA-based materials with the best balance between rigidity and ductility (2.5 GPa and 116% respectively) and the highest value of impact strength ($\approx 44\text{kJ/m}^2$) comparable to the other commercial impact modifiers. (see Appendix I Figure III.A.1 and Figure III.A.2)

Then, various PLA/PMMA formulations were melt-blended with a fixed BS content (17 wt%) and characterized by means of mechanical, thermo-mechanical and morphological analyses. The miscibility between each partner, the mechanical performances (toughness and ductility) and related morphologies are specifically addressed. Interfacial adhesion and coupling reactions in the melt-state are revealed in PLA-rich formulations and correlated with mechanical performances in terms of toughness and ductility. A mechanical mapping is finally set between the best PLA-based formulations and an ABS/PC blend, frequently used in automotive industry [25-27] and bio-based ternary blends appear as promising alternatives to petro-sourced blends such as ABS-based blends in engineering injection-molding parts.

EXPERIMENTAL

Materials

Commercial extrusion grade poly(L-lactide) NatureWorks 4032D (hereafter called PLA) was used as received ($\overline{M}_n = 133,500 \pm 5,000 \text{ g/mol}$, $D = 1.94 \pm 0.06$ as determined by size-exclusion chromatography in chloroform at 35°C upon a relative polystyrene calibration, $1.4 \pm 0.2 \%$ D-isomer content as determined by the supplier). Poly(methyl methacrylate) (Plexiglas® 8N, hereafter called PMMA) was supplied by Evonik ($\overline{M}_n = 50,000 \text{ g/mol} \pm 2,000 \text{ g/mol}$, $D = 2.1 \pm 0.1$). Biomax® Strong 120, hereafter called BS, was provided by Dupont™. As presented before, BS is an ethylene acrylate impact modifier bearing epoxy moieties specially designed for PLA. Ultrinox 626A (GE Specialty Chemicals) was used as a stabilizer at a content of 0.3 wt% in all PLA-based blends. For comparative purposes, a commercial ABS/PC blend

(Novodur H801) designed for automotive interior and exterior parts, was supplied by Styrolution ($\overline{M}_n = 32,900 \text{ g/mol} \pm 3,000 \text{ g/mol}$, $D = 3.4 \pm 0.1$).

Blend preparation and compounding

Seven different PLA/PMMA/BS were studied with different ratio of PLA/PMMA at a constant impact modifier concentration of 17 wt% and both neat PLA and PMMA were also processed. All formulations are gathered in Table III.1.

Table III.1 Designation of as-prepared PLA-based ternary formulations

Sample Code	PLA content (wt%)	PMMA content (wt%)	BS content (wt%)
Neat PLA	100	0	0
PLA/BS	83	0	17
PLA80/PMMA20/BS	66.4	16.6	17
PLA70/PMMA30/BS	58	25	17
PLA50/PMMA50/BS	41.5	41.5	17
PLA30/PMMA70/BS	25	58	17
PLA20/PMMA80/BS	16.6	66.4	17
PMMA/BS	0	83	17
Neat PMMA	0	100	0

Prior to mixing, polymeric components were dried overnight at 60 °C in a vacuum oven to remove any residual water before processing. The additives were first pre-mixed in a plastic container and then melt-blended in a Brabender internal mixer (model 50EHT) with 3 min pre-mixing at 30 rpm followed by 7 min of mixing at 70 rpm. Normalized samples of resulting PLA-based materials were then prepared by injection molding using DSM Mini Injection Molding apparatus upon the following procedure: 3 min at 210°C and injection within a mold at 45°C, except for PMMA content higher than 70 wt% (3 min at 220°C and injection within a mold at 55°C).

Characterizations

Differential scanning calorimetry (DSC) was performed using a DSC Q2000 from TA Instruments at both heating and cooling rates of 10 °C/min under nitrogen flow. The glass transition temperature (T_g), melting temperature (T_m), cold-crystallization temperature (T_{cc}), enthalpy of cold-crystallization (ΔH_{cc}) and melting enthalpy (ΔH_m) were evaluated from the resulting DSC thermograms at the second heating scan. Crystallinity index of PLA (X_{c-PLA}) was determined using the following relation (1): [28]

$$X_{c-PLA}(\%) = \frac{\Delta H_m - \Delta H_{cc}}{X_{PLA} \cdot \Delta H_m^0} \times 100 \quad (1)$$

with X_{PLA} the weight fraction of PLA in the sample and ΔH_m^0 (93 J/g) the melting enthalpy for 100% crystalline PLA.

Tensile tests were carried out on Tensile Universal testing Machine UTM (LR 100 K, Lloyds Instruments, UK) according to ASTM-D-638 norm, at a crosshead speed of 1 mm/min. Tensile data are derived from the machine software (For elastic modulus, a linear regression is applied to the initial linear part of the behavior curve, i.e. nominal axial stress vs. average axial strain, for values of average axial strain varying from 0.05 to 0.25%). Notched Izod Impact tests (5 tests per composition) were performed according to ASTM D256 norm using a Ray-Ran pendulum impact tester ($E=3.99J$, $m=0.668$ kg, $speed=3.46m/s$). Resiliency here is obtained by dividing the energy required to break the sample by its cross-section area at notch location.

Dynamic mechanical thermal analysis (DMTA) was carried out using a DMTA Q800 from TA Instruments mounted in a dual cantilever mode at a constant frequency of 1 Hz, an amplitude of 20 μm and a heating rate of 2°C/min. To determine the heat deflection temperature (HDT), a constant load of 0.45 MPa was applied at the center of a 3-point bending flexural bar sample (dimensions of 55 \times 12 \times 2mm³), which was heated at the rate of 2°C/min from room temperature to 130°C. The temperature when the specimen reached a deflection of 250 μm was reported as the HDT value. [7]

Impact-fractured surfaces of specimens were examined for morphological investigations through scanning electron microscopy (SEM) using a Hitachi SU8020 (100 V–30 kV) apparatus. Samples were cryofractured under liquid nitrogen and then coated using a gold sputtering technique to avoid any charging effect during the electron beam scanning. For the determination of particle size of dispersed BS microdomains within the blends, 100 to 300 diameters from 2 independent SEM images (5 \times 5 μm^2) were measured using “Image J” software. The cross-sectional area (A_i) of each individual particle (i) was measured and converted into

an equivalent sphere diameter by the equation ($d_i = (4A_i/\pi)^{0.5}$). Number-average particle diameter (d_n) and volume average particle diameter (d_v) which are usually thought to give a correlation with notched impact strength, were determined from the following equations:

$$d_n = \frac{\sum n_i d_i}{\sum n_i} \quad (2)$$

$$d_v = \frac{\sum n_i d_i^4}{\sum n_i d_i^3} \quad (3)$$

where n_i is the number of particles having the apparent particle diameter d_i .

RESULTS AND DISCUSSION

The incorporation of PMMA into PLA by melt-blending techniques was previously investigated by our group and PLA/PMMA miscible blends display significant improvements in term of heat deflection temperature (HDT) [12]. PLA/PMMA blends could be suitable for injection-molded parts in automotive or electronic industry. However, the low toughness and ductility still remain important challenges to be overcome with the use of impact modifiers. In this context, ternary PLA/PMMA/BS blends are developed and investigated by means of thermal, mechanical, thermo-mechanical and morphological analyses. PLA/PMMA formulations all over the composition range were investigated to highlight the influence of PMMA on final properties. Rubber-toughening was ensured by BS at a fixed content of 17 wt-% (based on the total weight) based on the literature. Actually, BS allows reaching a right balance between rigidity and toughness of neat PLA [22, 29-31].

III.1. Miscibility of ternary blends

Miscibility between components is an important requirement to achieve interesting mechanical properties for the final blends [32]. Miscibility extent of PLA/PMMA binary blends may depend on the processing techniques (solvent casting or extrusion technique) [7, 33-35]. Thermal treatments, process conditions and molecular parameters of each component must be controlled to ensure a good miscibility of PLA/PMMA blends and reach the full benefits in terms of thermo-mechanical improvements. Addition of impact modifier into a PLLA/PMMA blends to produce ternary PLLA/PMMA/BS blends can however lead to some change in the miscibility of PLA/PMMA blends. To investigate this point, glass transition temperatures, T_g , of PLA/PMMA/BS ternary blends were determined using DSC technique and corresponding mechanical relaxations (with the temperature at the $\tan\delta$ peak, $T_{\tan\delta}$) were evaluated using DMTA. Figure III.1 shows typical DSC thermograms of the PLA/PMMA/BS blends (arrows indicate the glass transition). Corresponding T_g values and crystallinity index of PLA are

reported in Table III.2. All curves exhibit a single glass transition, located at an intermediate temperature between those of pure PLA (61°C) and pure PMMA (116°C) and shifting towards higher values when increasing PMMA content. Similar trends were reported, for example by Zhang *et al.*[18] reporting the evolution of T_g for miscible P(D,L-LA)/PMMA blends obtained by solution/precipitation at different compositions. They confirm that the blends of both polymers exhibit a single T_g in a range between the T_g of the individual components. The location of the blend T_g appears to be more or less proportional to the composition of the blend, which is a clear indication for the miscibility of blends. In our work, such observations confirm the miscibility between PLA and PMMA in ternary formulations, *i.e.* in the presence of BS. It can be noted out that the glass transition temperature of the impact modifier in ternary blends (expected at around -35°C) could not be detected by DSC because of the imprecision of DSC machine.

The crystallinity ratio of PLA/PMMA/BS blends reduces gradually as the PMMA content increases (Table III.2) and above 50 wt% of PMMA, the blends become fully amorphous. It is worth noting that the addition of impact modifier BS to PLA results in a nucleation effect with the increase of crystallinity ratio from 3% for neat PLA to 19% for PLA/BS (17 wt% of BS).

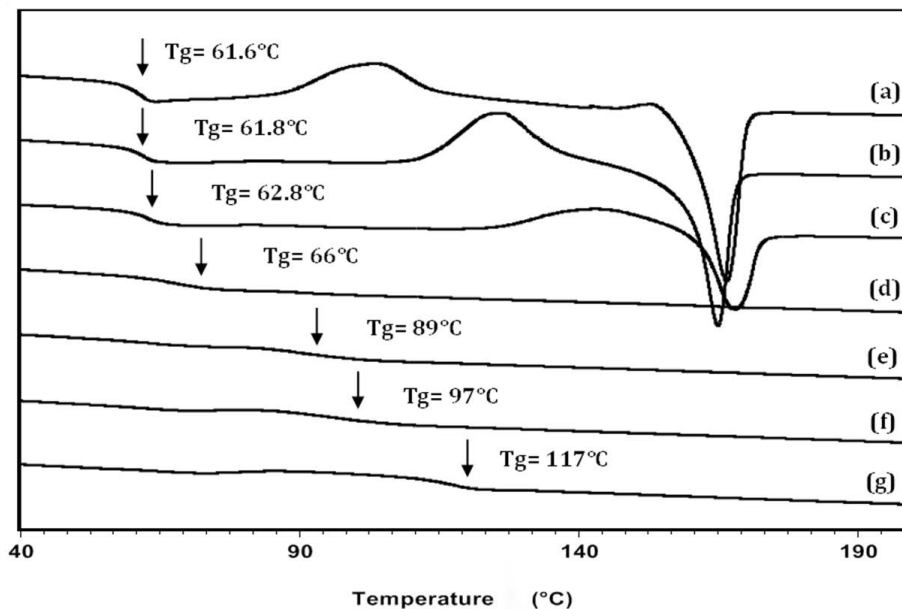


Figure III.1. DSC thermograms recorded during the second heating scan for (a) PLA/BS, (b) PLA80/PMMA20/BS, (c) PLA70/PMMA30/BS, (d) PLA50/PMMA50/BS, (e) PLA30/PMMA70/BS, (f) PLA20/PMMA80/BS, (g) PMMA/BS blends (heating rate 10°C/min).

Table III.2 Glass transition temperature, crystallinity index, relaxation temperature and HDT for PLLA/PMMA/BS blends determined from DSC and DMTA analyses.

Sample Code	T _g [*] (°C)	X _c [*] (%)	T _{tanδ1} ^{**} (°C)	T _{tanδ2} ^{**} (°C)	HDT ^{**} (°C)
Neat PLA	61	3	57	-42	54
PLA/BS	61.6	19	60	-42	53
PLA80/PMMA20/BS	61.8	9	64	-43	57
PLA70/PMMA30/BS	62.8	3	67	-43	58
PLA50/PMMA50/BS	66	-	76	-40	63
PLA30/PMMA70/BS	89	-	93	-40	70
PLA20/PMMA80/BS	97	-	100	-33	72
PMMA/BS	117	-	115	-	84
Neat PMMA	116	-	118	-	-
Neat BS	-	-	-	-35	-

* As determined by DSC

** As determined by DMTA

Mechanical relaxation at high and low temperatures was also investigated and Figure III.2 displays DMTA thermograms of PLA/PMMA/BS blends. Two distinct $\tan\delta$ peaks were systematically observed for all ternary compositions. The high-temperature relaxation corresponds to the α -relaxation of miscible PLA/PMMA fraction, *i.e.* located at an intermediate temperature between those of the respective homopolymers in accordance with DSC results. The low-temperature relaxation appearing between -33 and -42°C could be ascribed to α -relaxation of BS ($T_{\tan\delta} = -35^\circ\text{C}$ for neat BS). The presence of these two distinct $\tan\delta$ peaks therefore suggests that the PLA/PMMA matrix and the impact modifier are (partly) phase-separated. Table III.2 presents the temperature at $\tan\delta$ peaks for the high- and the low-temperature relaxation ($T_{\tan\delta1}$ and $T_{\tan\delta2}$, respectively) with the heat deflection temperature (HDT) determined from DMTA analyses for each PLA/PMMA/BS formulations. Related to their good miscibility and in accordance with the literature, [7] $T_{\tan\delta1}$ of the matrix PLA/PMMA increases slightly with PMMA content until 30wt% PMMA (reaching an improvement of 7°C for $T_{\tan\delta}$ of 70/30PLA/PMMA). At PMMA content higher than 30wt%, $T_{\tan\delta1}$ increases significantly, *e.g.* by 16°C between 30 wt-% and 50 wt-% of PMMA. In addition, HDT smoothly increases with the amount of PMMA into the ternary blend (an increase of 10°C at

50% of PMMA) and the beneficial effect of PMMA on thermo-mechanical properties is also confirmed in ternary formulations. The incorporation of BS into a PLA/PMMA miscible blend has a limited influence on HDT. These ternary PLA/PMMA/BS formulations are therefore comparable to binary PLA/PMMA blends developed by Samuel *et al.* [7], in terms of improved HDT, and a progressive increase of heat deflection temperature up to 61.9 °C with 50% PMMA is noticed.

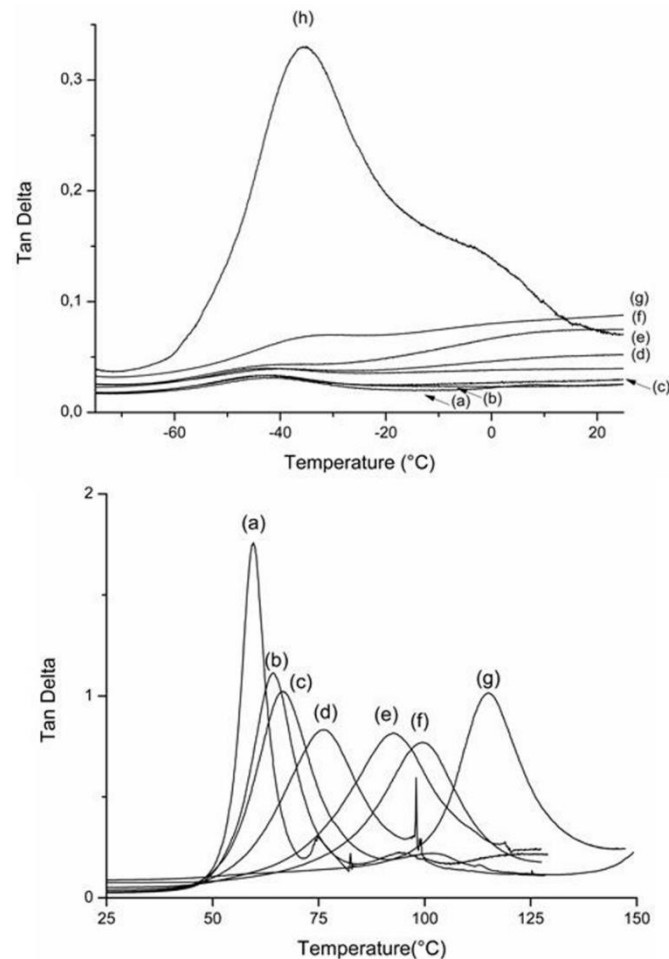


Figure III.2. Tan δ curves of (a) PLA/BS, (b) PLA80/PMMA20/BS, (c) PLA70/PMMA30/BS, (d) PLA50/PMMA50/BS, (e) PLA30/PMMA70/BS, (f) PLA20/PMMA80/BS, (g) PMMA/BS, (h) neat BS.

III.2. Mechanical properties of PLA-based blends

Nominal strain-stress curves at a displacement rate of $1\text{mm}\cdot\text{min}^{-1}$ for PLA homopolymer and all investigated PLA/PMMA/BS blends are shown in Figure III.3. PLA is known for its high rigidity and tensile strength but low elongation at break, even at low deformation rate [12]. The present results confirm this behavior for neat PLA with a very high rigidity of ≈ 3.2 GPa, a tensile strength of 68 MPa and a low elongation at break of 2.8%. The addition of BS strongly modifies the mechanical properties of PLA, as shown in Figure III.3 and Table III.3. A high

level of ductility is reached (elongation at break $\approx 148\%$) with the addition of BS at 17-wt% and a brittle-to-ductile transition is clearly observed. Nevertheless, the apparent rigidity and yield stress decrease of about 30% and 35% respectively with respect to neat PLA. The same phenomena were reported by Taib *et al.* [22] who have designed PLA blends with different amounts (0-50%) of a commercially ethylene acrylate copolymer impact modifier (Biomax[®] Strong). They show that adding 20% of impact modifier can improve ductility of blends (128% of elongation at break) with a decrease of yield stress and apparent rigidity of about 34% and 36% respectively with respect to neat PLA. The ductile behavior of the ternary blends is not altered with the addition of PMMA up to 80-wt%. Both tensile modulus (E) and tensile strength (σ) increases while strain at break decreases. It can be noted out that PMMA/BS binary blend shows a brittle behavior (2% of elongation at break) together with a low rigidity (1.6 GPa).

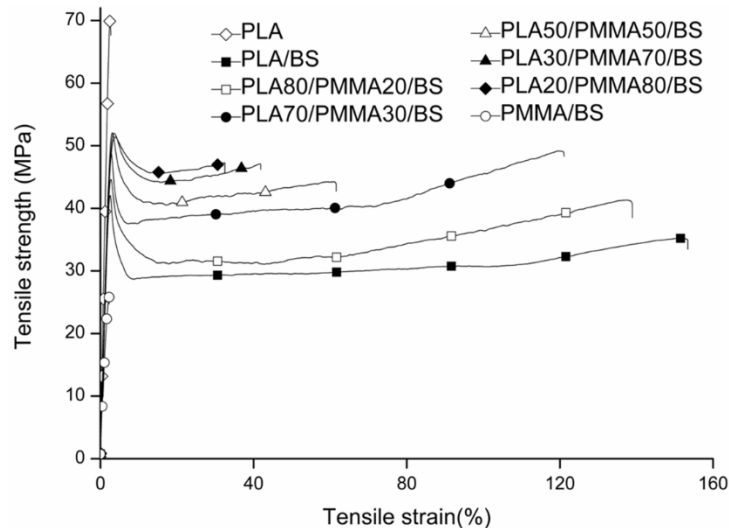


Figure III.3. Tensile stress-strain curves of PLA and PLA/PMMA/BS blends

Table III.3 Tensile properties of neat PLA and PLA/PMMA/BS blends (standard deviations into brackets)

Sample Code	Tensile Strength (MPa)	Apparent Elastic Modulus (GPa)	Elongation at break (%)
Neat PLA	68 (2)	3.2 (0.1)	2.8 (0.2)
PLA/BS	44 (2)	2.3 (0.1)	148 (28)
PLA80/PMMA20/BS	46 (1)	2.4 (0.1)	133 (11)
PLA70/PMMA30/BS	49 (3)	2.5 (0.1)	116 (4)

Sample Code	Tensile Strength (MPa)	Apparent Elastic Modulus (GPa)	Elongation at break (%)
PLA50/PMMA50/BS	52 (1)	2.6 (0.1)	66 (26)
PLA30/PMMA70/BS	53 (1)	2.5 (0.1)	44 (7)
PLA20/PMMA80/BS	52 (1)	2.4 (0.1)	33 (5)
PMMA/BS	23 (5)	1.7 (0.2)	2 (0.3)

Aiming at designing injection-molded parts for engineering applications in automotive, high impact toughness is also needed in addition to high tensile strength, rigidity and ductility. Figure III.4 illustrates the effect of PMMA content on the notched impact strength of ternary PLA-based blends. Neat PLA presents low impact strength of around 3.4 kJ/m² and adding 17 wt-% of impact modifier to neat PLA results in a significant improvement of toughness up to 24 ± 0.1 kJ/m² in accordance with literature [22]. A synergistic effect of BS and PMMA is surprisingly evidenced with an optimum impact toughness close to 44 ± 2.5 kJ/m² observed with the addition of 30% wt-% PMMA to PLA/BS blends. The same impact strength (42.8 kJ/m²) was also measured by Notta-Cuvier *et al.* [4] when performing PLA-plasticizer-impact modifier-nanoclay quaternary composition (80/10/10/1) designed for automotive applications. Nevertheless, mechanical tensile properties were much lower (1.74 GPa and 22.81 MPa, respectively for apparent rigidity and maximal nominal axial stress) compared to results obtained for ternary PLA70/PMMA30/BS17% blend). Further increase of PMMA content without sacrificing impact toughness is possible up to 50 wt-%. However, PMMA-rich formulations display a dramatic reduction of the material toughness, likely due to a lack of affinity between BS and matrix. Tensile and impact tests point out that BS has a strong positive effect on toughness and ductility for PLA-rich formulations (Figure III.3 and III.4). The formulation PLA70/PMMA30/BS can be selected with an optimum stiffness-toughness balance and improved HDT for high-performance applications, together with a high content of biobased material (58 wt%).

Mechanical properties of the most efficient bio-based composition, *i.e.* PLA70/PMMA30/BS, are compared to those of a commercial ABS/PC blend. Blend of polycarbonate (PC) and Acrylonitrile-Butadiene-Styrene (ABS) has encountered a great attention for the last decade, in particular in automotive applications, thanks to appealing properties and affordable cost. Indeed, these blends combine the best properties of both constituents: mechanical and thermal properties are improved by the presence of PC, while

processability and impact resistance are improved by the ABS. Adding a small amount of ABS to PC improves blend processability and impact strength. On the other hand, adding a small amount of PC to ABS increases its thermal properties [36-38]. These blends are recommended for the manufacture of large automotive parts, *e.g.* dashboards, interior trims, seat and glove box components, which require the use of high strength materials [39,40]. Table III.4 presents some mechanical properties (elastic modulus, tensile strength, elongation at break and impact strength) obtained for ABS/PC and PLA70/PMMA30/BS. Based on these results, it can be concluded that PLA70/PMMA30/BS has better mechanical properties than ABS/PC blend. In fact, the PLA70/PMMA30/BS blend shows comparable yield stress and tensile modulus, but better elongation at break (+84%) and enhanced impact strength (+55%) compared to ABS/PC blend, which make this selected composition interesting for automotive application.

Table III.4 Summary of all mechanical properties of PLA70/PMMA30/BS compared to those of ABS/PC

Compounds	ABS/PC	PLA70/PMMA30/BS
ElasticModulus (GPa)	2.3 (0.1)	2.5 (0.1)
UltimateStrength (MPa)	52 (1)	49 (3)
Elongation at break (%)	19 (5)	116 (4)
Impact Strength (KJ/m²)	20 (1)	44 (2)

For information purpose, different blending procedures to form the ternary blends were initially tested. Interestingly, the direct blending of all components gives the best results in terms of impact strength and ductility. More precisely, two-stage blending processes such as mixing BS in a pre-formed PLA/PMMA blend result in lower mechanical performances (see Appendix II Figures III.A3 and III.A4, TableIII.A1 and TableIII.A2).

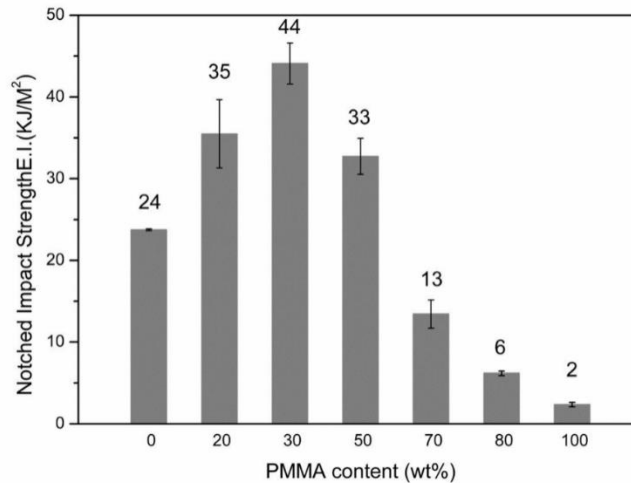


Figure III.4. Effect of relative content of PMMA on the notched impact strength of PLA/PMMA/BS blends

III.3 Morphology of rubber-toughened blends

The microstructure of rubber-toughened polymer is of prime importance on toughening mechanisms and the relationship between average size and distribution of rubbery microdomains, on one hand, and toughness, on the other hand, are often considered [19,41]. According to Perkinset *al.* [19], an optimum range of particle sizes leading to the best toughness improvement exists for each polymeric matrix. However, the interfacial adhesion between rubber particles and the matrix also plays a key role. Therefore, in order to understand the evolution of toughness in PLA/PMMA/BS blends, microstructures were analyzed by scanning electron microscopy (SEM). In particular, the influence of PMMA content on the average size of dispersed rubbery micro-domains of BS within PLA was first investigated. Figure III.5 shows SEM micrographs of cryofractured surfaces of PLA/PMMA/BS ternary blends at different PMMA content.

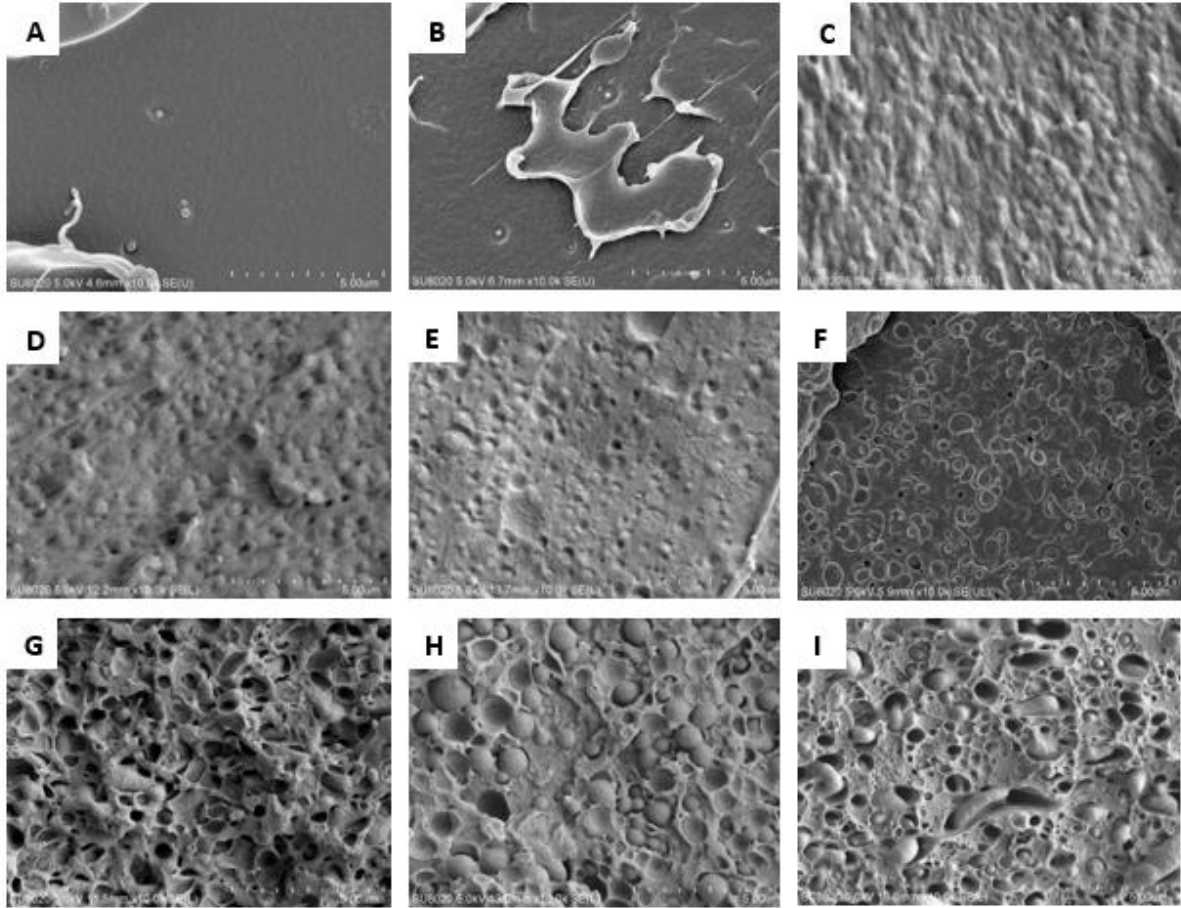


Figure III.5. SEM micrographs of impact-fractured surfaces of (A) neat PLA, (B) PLA70/PMMA30, (C) PLA/BS, (D) PLA80/PMMA20/BS, (E) PLA70/PMMA30/BS, (F) PLA50/PMMA50/BS, (G) PLA30/PMMA70/BS, (H) PLA20/PMMA80/BS, (I) PMMA/BS

As shown in Figure III.5A, neat PLA specimen exhibits a smooth surface and a relatively brittle morphology after fracture. The SEM micrograph of PLA70/PMMA30, without BS, also shows a homogenous morphology (Figure III.5B), in accordance with the miscibility extent achieved within this brittle blend. In contrast, all PLA/PMMA/BS blends display phase-separated morphology, which is a necessary condition for toughening [42,43], with dispersed BS droplets into PLA/PMMA matrices (Figures III.5C – I). These morphologies confirm the immiscibility of BS into the matrix as previously concluded by DSC and DMA (see sections III.1 and III.2). However, a strong influence of PMMA is clearly noticed on the morphology of cryofractured PLA/PMMA/BS blends. A large amount of plastically-deformed material is observed for the PLA/BS binary blend. BS droplets with diameter lower than 500 nm are homogeneously dispersed into PLA and a strong adhesion of BS to PLA matrix is noticed (Figure III.5C). This observation was in agreement with results reported by Afrifah *et al.*[23] who performed

PLA/EAC impact modifier (Ethylene acrylate copolymer). They confirmed that for blends at 10 wt.-% or more impact modifier, the fracture mechanisms included impact modifier debonding, fibrillation, crack bridging, and matrix shear yielding resulting in a ductile behavior. Adding PMMA to PLA/BS binary blends preserves the plastic deformation and a good interfacial adhesion for blends containing up to 50wt-% of PMMA is noticed. At higher PMMA content, ternary blends also show phase-separated morphologies but larger BS microdomains of irregular shapes and large interfacial voids, caused by mechanical debonding of BS from matrix, are revealed. Significant differences in terms of interfacial adhesion and BS microdomain size are therefore clearly evidenced in PLA/PMMA/BS ternary blends. PLA-rich blends, up to 50 wt-% PMMA, are specifically marked by a high interfacial adhesion. PLA-rich blends also seem to display smaller BS microdomains and a deeper analysis of BS droplet size was performed.

The number-average diameter of dispersed rubbery microdomains within PLA (d_n), the volume-average diameter (d_v) and the full size distribution curve were established. The spherical shape of particles rubber was first verified by longitudinal and transversal morphological views (see Appendix III Figure III.A5). Figure III.6 displays the evolution of BS droplet diameter with the amount of PMMA within PLA/BS blends.

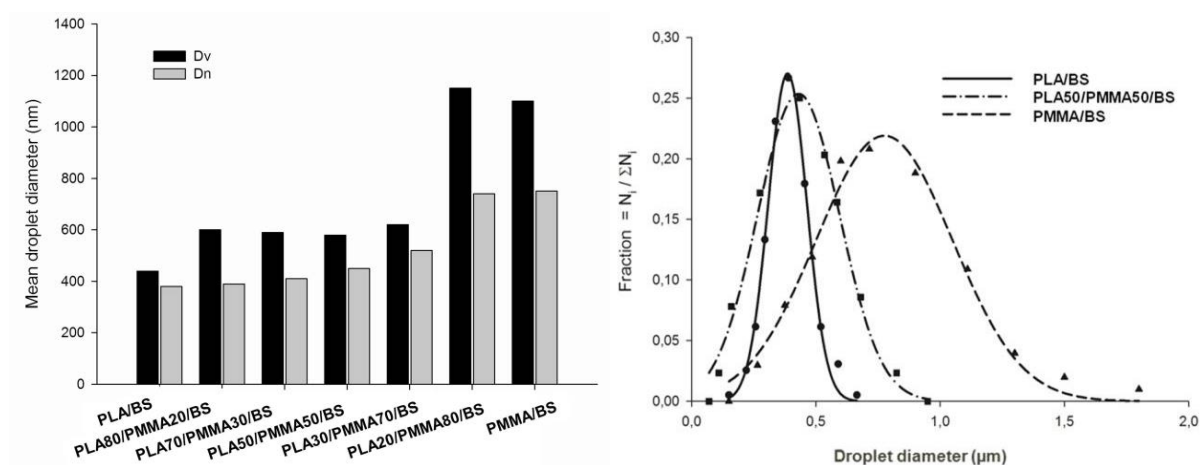


Figure III.6. BS droplet diameter as a function of PMMA content (left) and associated size distributions of the rubbery BS microdomains (right) for various PLA/PMMA/BS formulations.

In the absence of PMMA, *i.e.* in PLA/BS blends, spherical BS droplets with diameter close to 400 nm (for d_v and d_n) are observed, in agreement with a study based on toughened PLA formulations (PLA/ PBAT compounds) reported by Jiang *et al.*[44]. The blend comprised an immiscible two-phase system with the PBAT evenly dispersed in PLA with an average particle

size at the level of 0.3–0.4 μm . In our work, BS droplet diameter slightly tends to increase upon the addition of miscible PMMA into PLA/BS blends up to 70 wt-% PMMA, but the diameter of BS micro-domains droplet size remains lower than 600 nm. On the contrary, at PMMA content higher or equal to 80 wt%, blends morphology is marked by the presence of larger BS microdomains ranging from 0.5 μm to 1.5 μm . Figure III.6 also displays the size-distributions of BS microdomains for different PLA/PMMA/BS ternary blends. PLA-rich blends exhibit BS droplets with narrow size distribution reflecting a good dispersion of BS into PLA-rich blends. The size distribution of BS droplets significantly broadens with the addition of PMMA, and PMMA-rich blends are marked by a very broad distribution reflecting a poor dispersion of BS into PMMA-rich blends.

In this context, the interfacial energy between BS and the matrix plays a key role on the morphology developed during compounding. For less than 50% of PMMA, a high interfacial adhesion between BS and the matrix are observed (Figure III.5 C, D and E). A clear relationship can be established between the dispersion of BS, its adhesion to the matrix and the final mechanical performances [44, 45]. High toughness and ductility are observed for PLA-rich blends and mainly arise from a good dispersion of small BS droplets with a strong adhesion to PLA. The addition of PMMA up to 50 wt-% remains possible without detrimental effect on BS droplet size and interfacial adhesion. However, significant differences are observed in terms of ductility and impact toughness for PLA-rich formulations with an optimum PMMA content close to 30 wt-%. The size of rubbery domains also represents a key-parameter, affecting the final ductility and toughness [30, 46]. It is generally accepted that an optimum in energy dissipation appears for particle diameter of 0.5 to 0.55 μm [47]. This optimum particle size for our toughened PLA system seems reasonable. Beyond the optimum particle size, the plastic deformation behavior of PLA-rich blends changes to a debonding fracture mechanism due to the phase-separated morphology generated with increased PMMA content (more than 50%). Increasing the PMMA amount can affect the morphology of blends and cause a poor adhesion of the matrix, resulting in restrained mechanical properties. Such trend is due to the poor affinity of impact modifier to the PMMA matrix. The low affinity of impact modifier with PMMA leads to the presence of BS microdomains with different sizes in these blends. This can be explained by the occurrence of crazing fracture as among the most important energy dissipation process involved in the impact fracture of toughened polymer systems [19, 48, 49].

Another explanation could be more likely related to the *in situ* formation of “graft copolymers” as compatibilizers through coupling reactions between the functional end-groups

(hydroxyl and carboxylic) of PLA chains and the complementary functional groups (epoxy functions) of the impact modifier (Figure III.7). This hypothesis was also mentioned in different studies [22, 50].

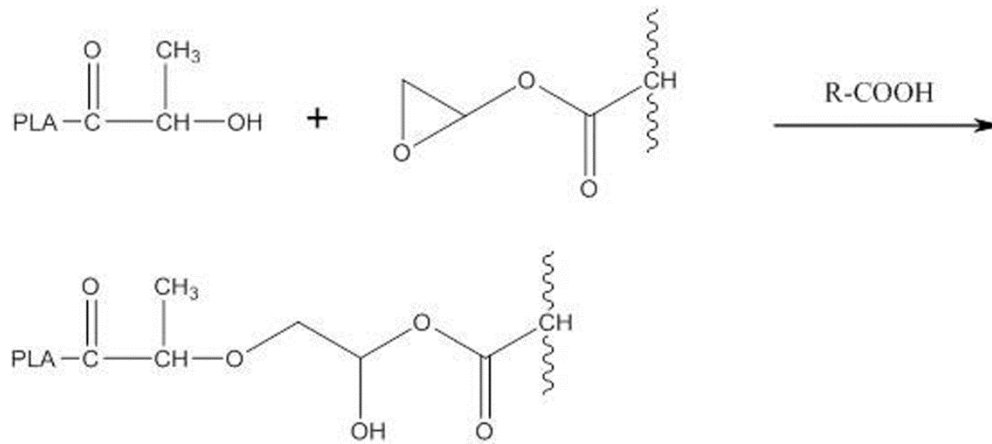


Figure III.7. Likely coupling reaction between BS and PLA (COOH residues as catalysis could be derived from the hydrolysis and/or presence of acid end-groups of PLA chains). [22]

As a result, improved interfacial adhesion and hence fine dispersion are achieved in these blends. Quantitatively, reducing the relative amount of PLA in PLA/PMMA/BS blends affects the formation of the *in situ* generated copolymers and can subsequently alters both morphological and mechanical features of the blends, leading to a poor interfacial adhesion between all components. These results are in good agreement with the mechanical experiments and indicate that the impact modifier in the presence of PLA leads to the formation of compatibilizers, resulting to a good interfacial adhesion between the different components of the blend.

CONCLUSIONS

Thanks to its biodegradability, easy processability, affordable cost and high stiffness, poly(lactic) acid (PLA) is regarded as the most promising bio-based alternatives to petropolymers. However, its use in automotive applications remains a challenge due to its low thermal stability and inherent brittleness. In this chapter, many efforts have been performed to enhance ductility of PLA through addition of ethylene-acrylate impact modifier and to improve the thermal stability in the presence of PMMA. New PLA/PMMA/BS ternary blends were successfully prepared using melt blending and injection molding processes. Miscibility extent was checked using DMTA, confirming the presence of two distinct $\tan \delta$ peaks, the first one for the miscible PLA/PMMA matrix and the second one for the dispersed impact modifier. It was suggested that the miscible PLA/PMMA matrix and the impact modifier BS were phase-separated and formed immiscible blends. Thermal stability of the blends slightly increases depending on amount of PMMA in the blend. Regarding the mechanical properties, a significant gain in tensile elongation and impact toughness were reached with a slight decrease in rigidity and tensile strength. The most promising composition was selected as the one that presents the better balance between ductility and stiffness and contains at least 50% of bio-sourced polymer in the blend. This way, PLA70/PMMA30/BS was selected and a comparative study between PLA70/PMMA30/BS and commercial ABS/PC was established and confirmed that the PLA-based ternary blend could represent a very promising bio-sourced alternative for automotive applications. Finally, using morphological analysis, size-distribution of rubber micro-domains was studied for a better understanding of impact strength results, in particular. It revealed that impact toughness and fracture mechanisms of blends depend on rubber particle size with an optimum in the range of 0.5 to 0.55 μm , achieved at 30 wt-% PMMA. PMMA contents higher than 50% led to poor mechanical properties and low interfacial adhesion between PLA/PMMA matrix and BS nodules due to the low affinity of impact modifier with PMMA. In this respect and based on the slight increase of heat resistance of the selected PLA70-PMMA30-BS blend, the next chapter will aim at improving crystallization ability of PLA based blends in order to enhance heat resistance while keeping the advantageous mechanical properties of the blends.

REFERENCES

1. Flieger, M.; Kantorova, M.; Prell, A.; Rezanka, T.; Votruba, J. *Folia Biol.* 2003, **48**, 27
2. Avérous, L. *Polylactic Acid: Synthesis, Properties and Applications*; Elsevier: Amsterdam 2008, 433–450.
3. Notta-Cuvier, D.; Murariu, M.; Odent, J.; Delille, R.; Bouzouita, A.; Raquez, J. M.; Lauro, F.; Dubois, P. *Macromol. Mater. Eng.* 2015, **300**, 684.
4. Notta-Cuvier, D.; Odent, J.; Delille, R.; Murariu, M.; Lauro, F.; Raquez, J. M.; Bennani, B.; Dubois, P. *Polym. Test.* 2014, **36**, 1.
5. Bhardwaj, R.; Mohanty, A. K. *J. Biobased Mater. Bio.* 2007, **1**, 191
6. Wang, Y.; Chiao, S. M.; Hung, T. F.; Yang, S. Y. *J. Appl. Polym. Sci.* 2012, **125**, 402.
7. Samuel, C.; Raquez, J. M.; Dubois, P. *Polymer* 2013, **54**, 3931.
8. Takagi, Y.; Yasuda, R.; Yamaoka, M.; Yamane, T. *J. Appl. Polym. Sci.* 2004, **93**, 2363.
9. Anderson, K. S.; Schreck, K. M.; Hillmyer, M. A. *Polym. Rev.* 2008, **48**, 85.
10. Jiang, L.; Wolcott, M. P.; Zhang, J. *Biomacromolecules* 2005, **7**, 199.
11. Lee, J. B.; Lee, Y. K.; Choi, G. D.; Na, S. W.; Park, T. S.; Kim, W. N. *Polym. Degrad. Stab.* 2001, **96**, 553.
12. Li, Y.; Shimizu, H. *Eur. Polym. J.* 2009, **45**, 738.
13. Loureiro, N. C.; Ghosh, S.; Viana, J. C.; Esteves, J. L. *Polym. Plast., T. Eng.* 2014, **60**, 603.
14. Park, J. W.; Im, S. S. *J. Appl. Polym. Sci.* 2002, **86**, 647.
15. Simões, C. L.; Viana, J. C.; Cunha, A. M. *J. Appl. Polym. Sci.* 2009, **112**, 345.
16. Eguiburu, J. L.; Iruin, J. J.; Fernandez-Berridi, M. J.; San Román, J. *Polymer* 1998, **39**, 6891.
17. Li, S. H.; Woo, E. M. *Polym. Int.* 2008, **57**, 1242.
18. Zhang, G.; Zhang, J.; Wang, S.; Shen, D. *J. Polym. Sci. Part B: Polym. Phys.* 2003, **41**, 23.
19. Perkins, W. G. *Polym. Eng. Sci.* 1999, **39**, 2445.
20. Scaffaro, R.; Morreale, M.; Mirabella, F.; La Mantia, F. P. *Macromol. Mater. Eng.* 2011, **296**, 141.
21. Ito, M.; Abe, S.; Ishikawa, M. *J. Appl. Polym. Sci.* 2010, **115**, 1454.
22. Taib, R. M.; Ghaleb, Z. A.; MohdIshak, Z. A. *J. Appl. Polym. Sci.* 2012, **123**, 2715.
23. Afrifah, K.; Matuana, L. *Macromol. Mater. Eng.* 2010, **295**, 802.
24. NatureWorks, *Technology Focus Report: Toughened PLA* 2007, accessed: January, 2015.
25. Marketsandmarkets, Available at: www.marketsandmarkets.com/Market-Reports/automotive-plastics-market-passenger-cars-506.html, accessed: April, 2015.
26. Khan, M. M. K.; Liang, R. F.; Gupta, R. K.; Agarwal, S. *Korea-Aust. Rheol. J.* 2005, **17**, 1.
27. PlasticPortal.eu, Available at: www.plasticportal.eu, accessed: April, 2015.
28. Fortunati, E.; Armentano, I.; Zhou, Q.; Iannoni, A.; Saino, E.; Visai, L.; Berglund, L. A.; Kenny, J. M. *Carbohydr. Polym.* 2012, **87**, 1596.
29. Dupont™, *Biomax® Strong: PLA TOUGHENING MODIFIER* 2010, accessed: February, 2015.
30. Liu, H.; Zhang, J. *J. Polym. Sci., Part B: Polym. Phys.* 2011, **49**, 1051.
31. Pluta, M.; Murariu, M.; Dechief, A. L.; Bonnaud, L.; Galeski, A.; Dubois, P. *J. Appl. Polym. Sci.* 2012, **125**, 4302.
32. Pukánszky, B.; Tüdös, F. *Makromol. Chem. Macromol. Symp.* 1990, **38**, 221.

33. Eckelt, J.; Enders, S.; do CarmoGonçalves, M.; Queiroz, D. P.; Wolf, B. A. *Fluid Phase Equilib.* 2000, **171**, 219.
34. Le, K. P.; Lehman, R.; Remmert, J.; Vanness, K.; Ward, P. M. L.; Idol, J. D. *J. Biomater. Sci. Polym. Ed.* 2006, **17**,121.
35. Shirahase, T.; Komatsu, Y.; Tominaga, Y.; Asai, S.; Sumita, M. *Polymer* 2006, **47**, 4839.
36. Balakrishnan, S.; Neelakantan, N. R.; Saheb, D. N.; Jog, J. P. *Polymer* 1998, **39**, 5765.
37. Lombardo, B. S.; Keskkula, H.; Paul, D. R. *J. Appl. Polym. Sci.* 1994, **54**, 1697.
38. Krache, R. *Mater. Sci. Appl.* 2011, **02**.
39. Helps, I. *Plastics in European Cars 2000-2008*, RAPRA Technology, 2001.
40. Van de Grambel, H. T. *Blends and Alloys of Engineering Thermoplastics*. Rapra Technology Ltd.: Shrophshire, UK, 1991, Report 49, Vol. **5**, 1.
41. Weiss, P. *J. Polym. Sci. Polym. Lett. Ed.* 1978, **16**, 376.
42. Ratna, D.; Banthia, A. K. *Polym. Int.* 2000, **49**, 309.
43. Das, V.; Pandey, A. K.; Krishna, B. *J. Reinf. Plast. Compos.* 2008, **28**, 2879
44. Jiang, L.; Wolcott, M. P.; Zhang, J. *Biomacromolecules* 2006, **7**, 199.
45. Kfoury, G.; Raquez, J. M.; Hassouna, F.; Odent, J.; Toniazzo, V.; Ruch, D.; Dubois, P. *Front Chem* 2013, 1.
46. Walker, I.; Collyer, A. *Rubber Toughening Mechanisms in Polymeric Materials*, In *Rubber Toughened Engineering Plastics*, Ed.; Chapman and Hall: London, UK, 1994, 29–56.
47. Gramlich, W. M.; Robertson, M. L.; Hillmyer, M. A. *Macromolecules* 2010, **43**, 2313.
48. Ikeda, R. M. *J. Appl. Polym. Sci.* 1993, 619
49. Narisawa, I.; Yee, A. *Materials Science and Technology: Crazing and Fracture of Polymers*, Wiley-VCH Verlag GmbH & Co. KGaA: 2006. DOI: 10.1002/9783527603978.mst0146.
50. Murariu, M.; Ferreira, A. D. S.; Duquesne, E.; Bonnaud, L.; Dubois, P. *Macromol. Symp.* 2008, **272**, 1.

APPENDIX I: Selection of impact modifier

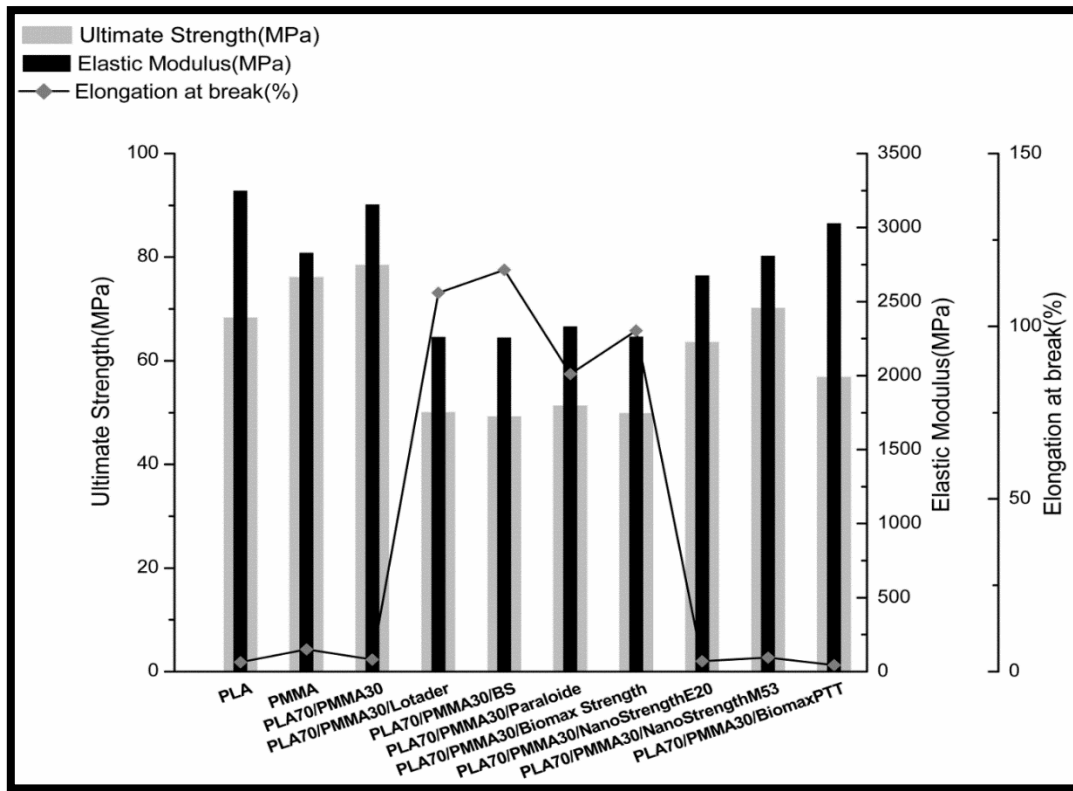


Figure III.A.1 Tensile properties of PLA/PMMA/IM blends

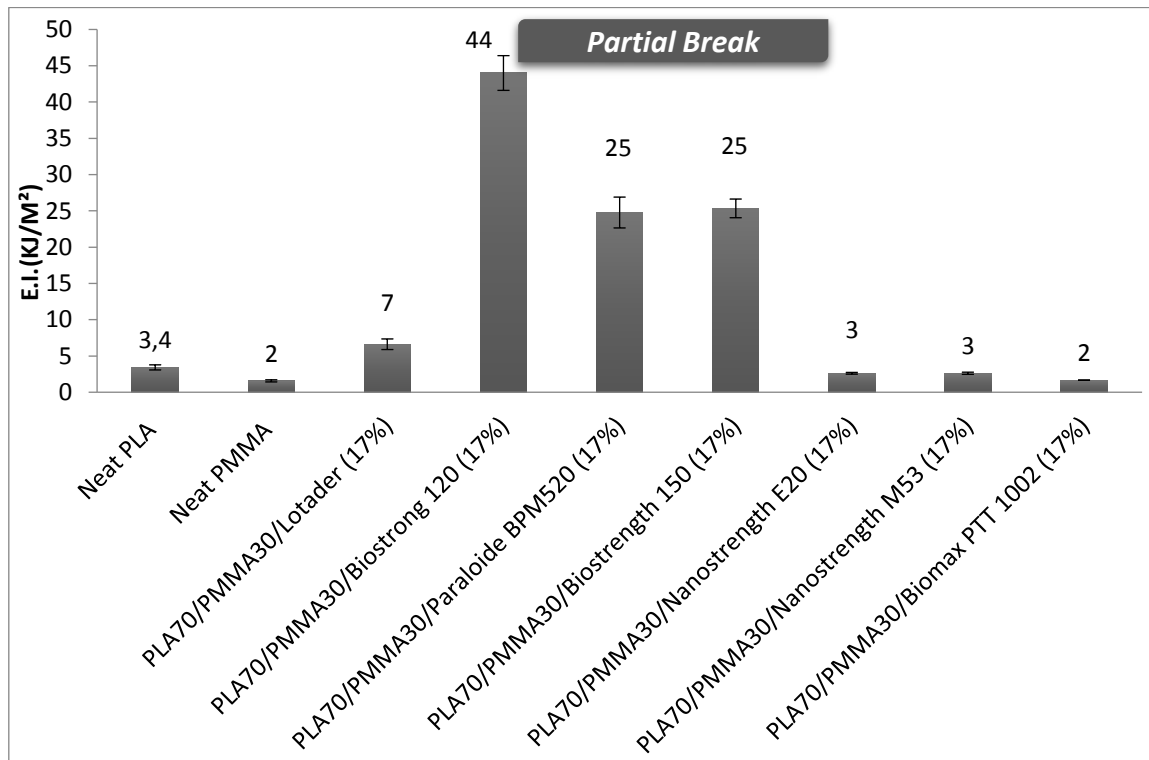


Figure III.A.2. Notched impact strength of PLA/PMMA/IM blends

APPENDIX II: Process modification**Table III.A.1.** Sample Compositions

Compounds	Sample Code	Process
PLA70/PMMA30/BS17%	1	Mixing in one step
PLA70/PMMA30+BS17% (10')	2	1st step:mixing PLA70/PMMA30(5min) 2nd step: Adding BS (5min)
PLA70/PMMA30+BS17% (15')	3	1st step:mixing PLA70/PMMA30(5min) 2nd step: Adding BS (10min)
PLA70+ BS17%/PMMA30	4	1st step:mixing PLA70/BS 17%(5min) 2nd step: Adding PMMA(5min)

Table III.A.2. Mechanical properties of PLA/PMMA/BS blends

Sample Code	E (MPa)	Yield Strength (MPa)	Elongation at break (%)
1	2467±35	49±3	116±4
2	2271±35	43±0.1	17±2
3	2376±41	47±1	37±15
4	2355±41	48±1	97±14

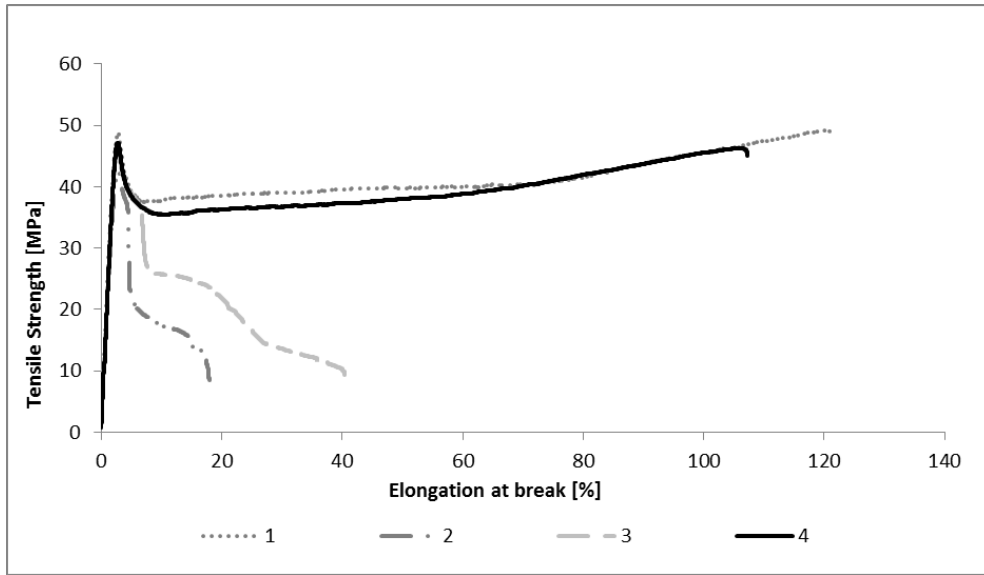


Figure III.A.3 Tensile curves of PLA/PMMA/BS blends (for sample codes 1 to 4, see Table III.A.1)

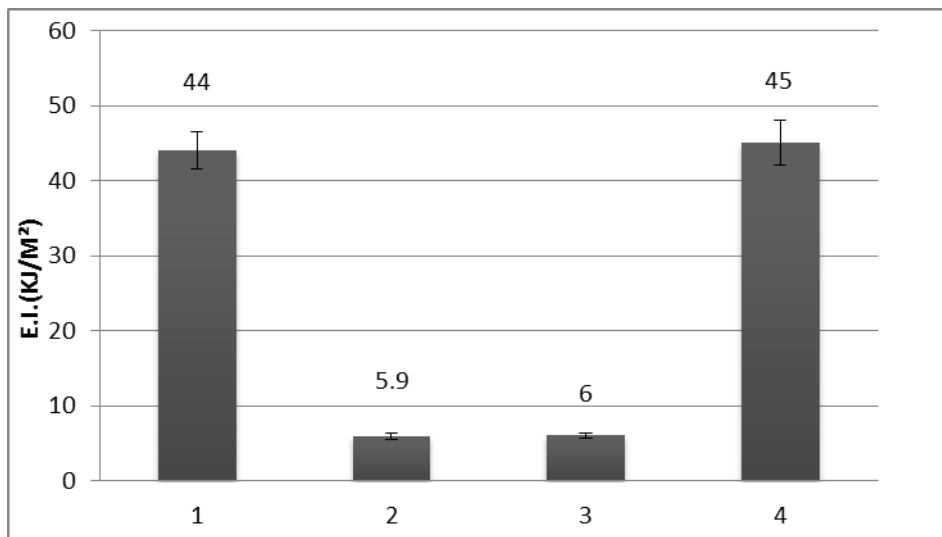


Figure III.A.4. Notched impact strength of PLA70/PMMA30/BS blends (for sample codes 1 to 4, see Table III.A.1)

APPENDIX III: Spherical shape of particles rubber

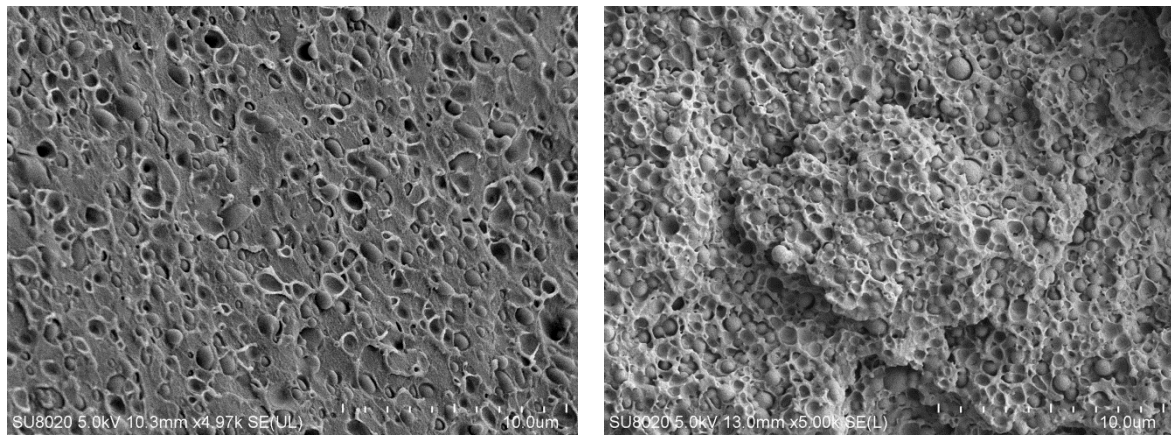


Figure III.A.5. SEM micrographs of impact fractured surfaces of PLA30/PMMA70/BS blends (Left: longitudinal view; Right transversal view)

CHAPTER IV

IMPROVING CRYSTALLINITY OF HIGHLY TOUGH POLY
(L-LACTIDE)-BASED TERNARY BLENDS

Effect of annealing process, stereocomplexation and nucleation on performances of highly tough Polylactide-based materials for automotive applications

INTRODUCTION

Renewable poly(L-lactide) (PLLA)-based materials represent excellent candidates to design engineering and environmentally friendly polymers for automotive applications. However, broader use of PLLA is still impeded by its poor thermal stability, brittle behavior and low crystallization ability [1]. Considerable efforts are therefore necessary to improve the properties of PLA under extreme loadings that may be encountered in automotive applications. The use of impact modifier is generally preferred, as it imparts greater energy dissipation pathways throughout the material, without affecting stiffness and heat resistance [2]. In the previous chapter, we successfully developed a ductile PLLA bio-based blend with enhanced impact strength and improved heat resistance by blending PLLA with PMMA and 17 wt% of Biomax® Strong120 (BS). However, heat resistance was still limited and crystallization ability of these blends remained inferior to what is required for their industrial post-processing, for instance, by injection techniques. Obtaining a highly crystalline injection-molded PLLA part remains difficult due to PLLA slow crystallization rate. Beside this aspect, polymer crystallinity plays a significant role in the material performance. For example, an increase in overall crystallinity leads to improved stiffness, strength, heat deflection temperature, and chemical resistance [3,4]. Different strategies to promote PLLA crystallization of blends were investigated with the objective of increasing the crystalline content [5-7]. Interestingly, annealing treatments play a decisive role to improve thermal stability of PLLA-based materials, giving rise to the crystallization of PLLA matrix and also a dramatic increase in the notched impact strength of the resulting materials [8-10]. Moreover, performing PLLA-PDLA stereocomplexes, can also be a promising solution to obtain sc-PLA materials with high thermal resistance. Their fast crystallization from the melt state [11,12], their nucleating effect in neat PLLA [13,14], their superior thermomechanical properties [15], and their lower thermal and hydrolytic degradation rates [16] are the most fascinating properties that clearly highlight the high potential of PLA stereocomplexes to develop semicrystalline PLA grades with enhanced properties for long-lasting applications.

Compared to the long-term annealing-induced crystallization of PLLA matrix, the dramatically accelerated crystallization rate upon the addition of efficient nucleating agents is largely preferred in industry. Addition of nucleating agents into semi-crystalline polymers not only decreases the crystallization time, but also increases the mechanical properties of resulting materials [17,18]. Accordingly, an increase in the overall crystallinity can lead to improvements in stiffness, toughness and heat-deflection temperature. In this way, numerous works have been devoted to improve PLLA crystallization kinetics by adding nucleating agents. Particularly lots of research efforts have been paid to the elaboration and characterization of polylactide-based nanocomposites with the aim of combining both the nucleating and the mechanical reinforcing effects brought by the fillers [19-21,7].

The present contribution aims to improve crystallization ability of the optimum compound PLLA70-PMMA30-BS following three different methods, namely after annealing process, stereocomplexation by adding PDLA to the toughened PLLA blends or finally by adding a combination of silica nanoparticles and nucleating agent (SiO_2/EBS) as nucleating agent. Crystallization behavior of those PLLA blends was investigated using wide angle X-ray diffraction (WAXS) and differential scanning calorimetry (DSC) techniques. Mechanical properties such as rigidity, ductility and impact behavior of all the samples were evaluated and compared to assess the effect of each method on these properties. Heat deflection temperature was determined using dynamic mechanical analysis in order to highlight the thermal resistance of blends.

EXPERIMENTAL

Materials

A commercially available extrusion-grade poly(L-lactide) (NatureWorks 4032D, hereafter called PLLA) was used as received ($\overline{M}_n = 133,500 \pm 5,000$ g/mol, $\text{Đ} = 1.94 \pm 0.06$ as determined by size-exclusion chromatography in chloroform at 35°C upon a relative polystyrene calibration, 1.4 ± 0.2 % D-isomer content as determined by the supplier). Poly(D-lactide), hereafter called PDLA, was supplied by Purac and used as received ($\overline{M}_n = 42,000 \pm 4,000$ g/mol, $\text{Đ} = 2.1 \pm 0.2$). Poly(methyl methacrylate) (Plexiglas® 8N, hereafter called PMMA) was supplied by Evonik ($\overline{M}_n = 50,000$ g/mol ± 2,000 g/mol, $\text{Đ} = 2.1 \pm 0.1$). Biomax® Strong 120,

hereafter called BS, was provided by Dupont™. Ultrinox 626A (GE Specialty Chemicals) was used as a stabilizer at a content of 0.3 wt% in all PLA-based blends.

N,N'-Ethylenebis(stearamide), is a commercial polymer additive known as EBS produced by Sigma-Aldrich. CAB-O-SIL M5 (SiO₂, 200m²/g) is an untreated fumed silica, supplied by Cabot (Massachusetts, USA) and was used as received.

Blend preparation and compounding

Prior to mixing, polymeric components were dried overnight at 60 °C in a vacuum oven to remove any residual water before processing. The additives' pellets were first pre-mixed in a plastic container and then melt-blended in a Brabender internal mixer (model 50EHT) with 3 min of pre-mixing at 30rpm followed by 7 min of mixing at 70 rpm. Normalized samples of resulting PLA-based materials were then prepared by injection molding using DSM Mini Injection Molding apparatus upon the following procedure: 3 min at 210°C and injection within a mold at 45°C. Blends were processed as aforementioned at a constant concentration of impact modifier and PMMA at 17 wt% and 25wt% respectively. All formulations are gathered in Table IV.1.

PLLA70-PMMA30-BS17% and PLLA/BS17% were melt blended on brabender and injected. Annealing process was performed at 120°C (this temperature was fixed after the study of crystallization kinetics), after 10, 20 and 30 min for both compounds (PLLA-BS and PLLA-PMMA-BS blends)

Table IV.1 Designation of as-prepared PLLA-based materials

Compounds	PLLA (wt%)	PMMA (wt%)	BS (wt%)	PDLA (wt%)	EBS (wt%)	SiO ₂ (wt%)
PLLA-BS	83	0	17	-	-	-
PLLA70-PMMA30-BS	58	25	17	-	-	-
PLLA95-PDLA5	95	-	-	5	-	-
PLLA90-PDLA10	90	-	-	10	-	-
PLLA95-PDLA5-BS	78.15	-	17	4.15	-	-
PLLA90-PDLA10-BS	74.7	-	17	8.3	-	-
PLLA95-PDLA5-PMMA-BS	55.1	25	17	2.9	-	-
PLLA90-PDLA10-PMMA-BS	52.2	25	17	5.8	-	-

Compounds	PLLA (wt%)	PMMA (wt%)	BS (wt%)	PDLA (wt%)	EBS (wt%)	SiO ₂ (wt%)
PLLA70-PDLA30-PMMA-BS	40.6	25	17	17.4		
PLLA50-PDLA50-PMMA-BS	29	25	17	29		
PLLA-EBS	99.25	-	-	-	0.75	
PLLA-SiO ₂ -EBS	96.25	-	-	-	0.75	3
(PLLA-SiO ₂ -EBS) /PMMA/BS	55.825	25	17	-	0.435	1.74

Characterizations

Differential scanning calorimetry (DSC) was performed using a DSC Q2000 from TA Instruments at both heating and cooling rates of 10 °C/min under nitrogen flow. The glass transition temperature (T_g), melting temperature (T_m), cold-crystallization temperature (T_{cc}), enthalpy of cold-crystallization (ΔH_{cc}) and melting enthalpy (ΔH_m) were evaluated from the resulting DSC thermograms at the second heating scan. Crystallinity index of PLA (X_{c-PLLA}) was determined using the following relation (1)[33]:

$$X_{c-PLLA}(\%) = \frac{\Delta H_m - \Delta H_{cc}}{X_{PLLA} \cdot \Delta H_m^0} \times 100 \quad (1)$$

with X_{PLA} the weight fraction of PLLA in the sample and ΔH_m^0 (93 J/g) the melting enthalpy for 100% crystalline PLLA.

The specimens for WAXS characterization were produced by injection molding. The WAXS analysis was performed on a Siemens D5000 diffractometer using Cu K α radiation (wavelength, 1.5406 Å) at room temperature. The samples were step-scanned from 10 to 25° in 2 θ with steps of 0.02° with a fixed time sampling of 4 s (40 kV and 30 mA).

Tensile tests were carried out on Tensile Universal testing Machine UTM (LR 100 K, Lloyds Instruments, UK) according to ASTM-D-638 norm, at a crosshead speed of 1 mm/min. Tensile data are derived from the machine software (For elastic modulus, a linear regression is applied to the initial linear part of the behavior curve, i.e. nominal axial stress vs. average axial strain, for values of average axial strain varying from 0.05 to 0.25%). Notched Izod Impact tests (5 tests per composition) were performed according to ASTM D256 norm using a Ray-Ran pendulum impact tester (E=3.99J, m=0.668 kg, speed=3.46m/s).

Dynamic mechanical thermal analysis (DMTA) was carried out using a DMTA Q800 equipment from TA Instruments mounted in a dual cantilever mode at a constant frequency of

1 Hz, an amplitude of 20 μm and a heating rate of 2°C/min. To determine the heat deflection temperature (HDT), a constant load of 0.45 MPa was applied at the center of a 3-point bending flexural bar sample (dimension of 55 \times 12 \times 2mm³), which was heated at the rate of 2°C/min from room temperature to 130°C. The temperature when the specimen reached a deflection of 250 μm was reported as the HDT value.[22]

Impact-fractured surfaces of specimens were examined for morphological investigations through scanning electron microscopy (SEM) using a Hitachi SU8020 (100 V–30 kV) apparatus. Samples were cryo-fractured under liquid nitrogen and then coated using a gold sputtering technique to avoid any charging effect during the electron beam scanning.

RESULTS AND DISCUSSIONS

IV.1 Annealing:

Simultaneously improving PLLA crystallization and PLLA toughness is an appealing challenge. Following this objective, we first considered the effect of annealing process on the crystallinity of composition PLLA70-PMMA30-BS, which has been determined as the most promising composition in terms of ductility and toughness, high to moderate biobased content and improved HDT for high-performance applications (cf Chapter III). In the present chapter, the crystallization kinetics of a commercial grade of PLLA is studied to select the most suitable annealing temperature for improving thermo-mechanical properties of PLLA-BS and PLLA-PMMA-BS. In order to study isothermal crystallization, samples were heating up to 220°C, then cooled from 220°C directly to isothermal testing temperature (crystallization temperature), at a cooling rate of 10°C/min. Isothermal crystallization kinetics were investigated at different temperatures, namely 100°C, 110°C and 120°C. As mentioned in literature, neat PLA has a crystallization half time with the range of 17-45 min [18,23]. When semi-crystalline PLLA is processed, its overall crystallization rate is reduced, resulting to a shear-induced crystallinity and giving rise to a crystallization half time of 5 min [24]. As expected and seen in Figure IV.1, the isothermal crystallization half time of processed PLA at 120 °C decreased by adding the impact modifier BS reaching 2 min. This indicates an enhancement effect of PLLA crystallization promoted by the nucleating effect of impact modifier. By adding PMMA to PLLA-BS the isothermal crystallization half time increased to reach 13 min at 120°C due to the amorphous character of polymer which slows the crystallization of the blend. The isothermal step at 110°C and 120°C (Figure IV.1) show that there is no noticeable effect of isothermal

temperature on the crystallization half time ($t_{1/2}$) of PLLA-BS, which always ranges from 90 to 120 s. However, for PLLA-PMMA-BS blend, increasing the isothermal temperature leads to a shift of isotherms curves to the left side and causes a significant decrease of $t_{1/2}$ from 13 min to almost 6 min. Based on these results, the selected annealing temperature was at 120°C. The effect of annealing time will be studied afterwards.

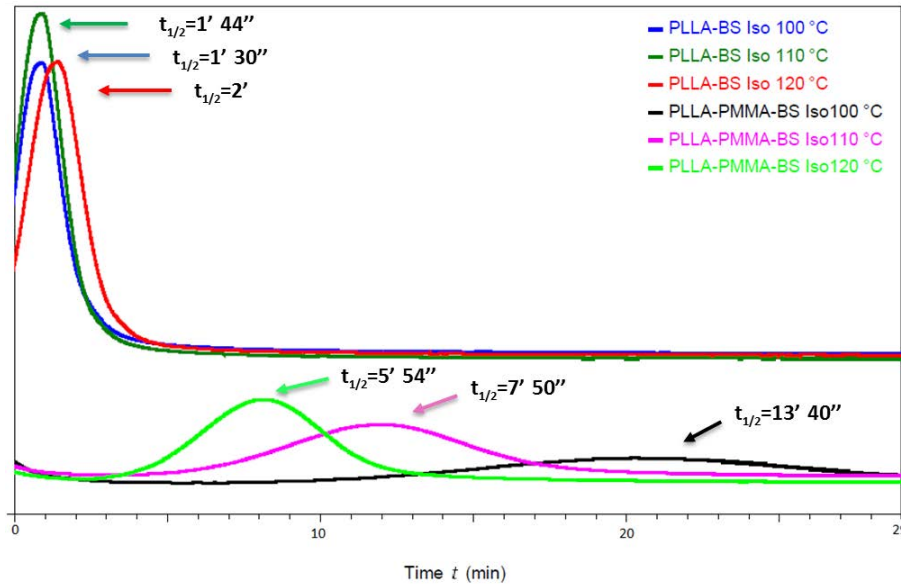


Figure IV.1. Crystallization isotherm curves of PLLA-PMMA-BS and PLLA-BS blends (100, 110 and 120°C)

The crystallinity of annealed PLA blends was investigated by DSC and WAXS. Figure IV.2 shows the WAXS profiles of the PLLA-BS and PLLA-PMMA-BS blends with various annealing times at 120°C. The non-annealed injected PLLA-BS sample presented a significant peak on its WAXS profile at 16.5° and an interesting value of crystallinity (10% instead of 5% for non-annealed PLLA-PMMA-BS - Table IV.2). In addition to a sharp diffraction peak at 16.5°, which is attributed to the diffraction of α form crystal planes for the crystallized PLA [25], four noticeable small peaks were also observed at 14.7°, 19°, 22.3° and 28.9° after 10 min annealing. The same peaks also appear after 10 min annealing of PLLA-PMMA-BS blend indicating that the materials were pronounced to form more perfect crystals at high annealing temperature under these conditions [26]. As shown in Table IV.2, the crystallinity of PLLA-PMMA-BS significantly increased ($\chi_c=28\%$) after 10 min annealing and reached a maximum of 49% after 30 min annealing. This phenomenon is due to the enhancement of mobility of molecular chains when the samples are annealed above their glass transition temperature (T_g). This is conducive to a preferred orientation arrangement of molecular chains, resulting in an

increase of crystallinity ratio, χ_c [27]. Consequently, the rearrangement of the molecular chains into the crystal lattice is favored when the samples are annealed above T_g . The intensity of the WAXS peaks of PLLA-PMMA-BS increased with annealing time, which was likely caused by the development of ordered crystallites and the formation of crystalline structures throughout the annealing process [28,29]. In contrast, crystallinity ratio of PLLA-BS blends decreased with annealing time to attain 34% after 30 min. This may be attributed to the formation of PLA-BS copolymers inducing some defects on rearrangement of macromolecular chain confirmed by the increase of M_n of PLA-BS blends after 30 min annealing (results not shown)

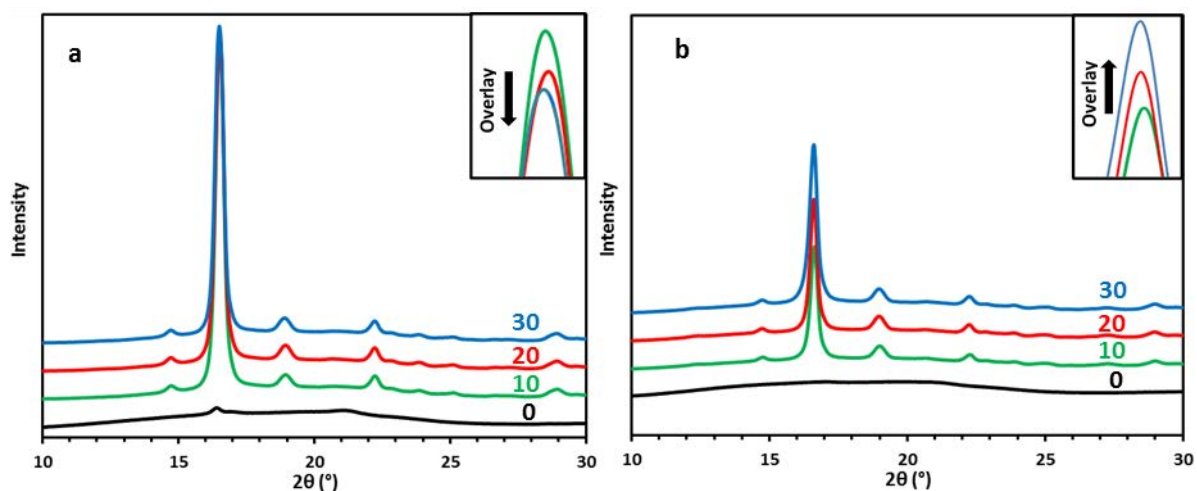


Figure IV.2. The WAXS profiles with various annealing times at 120 °C of (a) PLLA-BS and (b) PLLA-PMMA-BS blends and normalized overlay data (Numbers stand for annealing time in min).

Table IV.2 Crystallinity ratio, temperature and enthalpy of non-annealed and annealed specimens

Compounds	Annealing time (min)	ΔH_m (J/g)	ΔH_{cc} (J/g)	T_m (°C)	T_{cc} (C°)	T_g (°C)	χ_c (%)
Non-annealed PLLA-BS	0	31.91	24,45	166	88	60.5	10
PLLA-BS	10	33.3	0	167	-	NO	43
PLLA-BS	20	29.71	0	166	-	64	38
PLLA-BS	30	25.93	0	166	-	65	34
Non-annealed PLLA70-PMMA30-BS	0	20.11	17.47	166	125	62.6	5
PLLA70-PMMA30-BS	10	16.72	1.729	165	83	NO	28
PLLA70-PMMA30-BS	20	26.55	0	165	-	NO	49
PLLA70-PMMA30-BS	30	26.42	0	168	-	NO	49

NO: not observed

As can be seen in Table IV.2, some values of T_g could not be characterized by DSC due to the decrease of the quantity of amorphous phase after the annealing process [27]. As illustrated in Table IV.2, the cold crystallization peak cannot be seen for annealed PLLA-BS and PLLA-PMMA-BS. Thereby, it clearly suggests that the annealing time has a prominent effect on the cold crystallization behavior of the PLA blends.

The results obtained by WAXS confirm that annealing process was efficient to increase crystallinity after injection molding. Therefore, the effect of annealing on the dynamic mechanical properties and thermal resistance properties of PLLA blends will be discussed.

Table IV. 3 Relaxation temperatures, storage modulus and HDT of PLLA based blends before and after annealing process

Compounds	Annealing time (min)	Ttan δ ($^{\circ}$ C)	E(MPa) T=25 $^{\circ}$ C	HDT($^{\circ}$ C)
Non-annealed PLLA-BS	0	60	1355	52.5
PLLA-BS	10	63.7	2345	77
PLLA-BS	20	64.3	2523	66
PLLA-BS	30	65.9	2452	66
Non-annealed PLLA70-PMMA30-BS	0	67	1613	57.5
PLLA70-PMMA30-BS	10	101	2315	76.5
PLLA70-PMMA30-BS	20	98	2448	75
PLLA70-PMMA30-BS	30	100	2318	70

Storage modulus (E), temperature at tan δ peak ($T_{\tan\delta}$) and HDT values of PLLA based blends with/without annealing treatment against time are given in Table IV.3 (see Figure IV.3). It shows that the storage modulus was dramatically enhanced with annealing process for both binary and ternary blends (e.g. from 1.63GPa for non-annealed PLLA-PMMA-BS blend to 2.31 GPa after 10 min annealing), mainly due to the gradual increase of crystallinity. Similar trends were reported in literature for injected PLA samples [6]. The storage modulus showed almost the same value independently of annealing time, as illustrated in Figure. IV.3b. The high relaxation temperature corresponds to the α -relaxation of the miscible PLLA-PMMA fraction and was therefore located at an intermediate temperature between those of the homopolymers (see chapter III). It can be clearly observed that after annealing process, Tan δ shifted to a higher temperature (from 67 $^{\circ}$ C for non-annealed PLLA-PMMA-BS blend to 100 $^{\circ}$ C after 30 min annealing), which can be attributed to the limitation of chain mobility within the polymer matrix due to the increase of crystallinity fraction [6]. To evaluate the thermal stability, or the heat

resistance of developed PLLA blends, HDT was determined using DMTA analyses. Thanks to enhanced crystallinity of PLLA based blends, HDT significantly increased after annealing treatment (an increase of 20°C after 10 min annealing for binary and ternary blends) to reach 77°C for PLLA-PMMA-BS blend, confirming a better heat resistance resulting from annealing treatment.

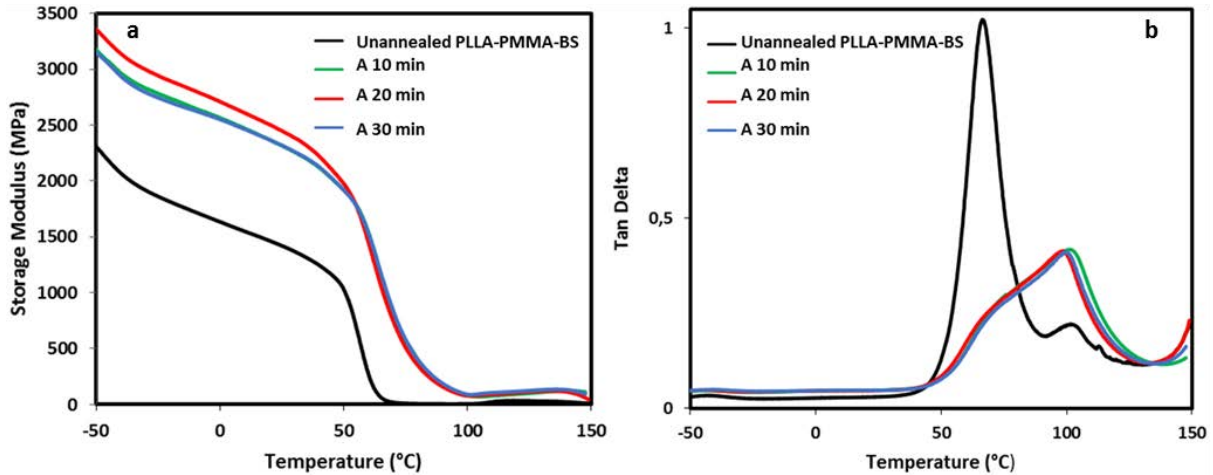


Figure IV.3. Exploitation of DMTA of non-annealed and annealed PLLA-PMMA-BS after different annealing times (a) Comparison of storage modulus of PLLA based blends (b) Comparison of $\text{Tan}\delta$ of PLLA based blends.

As a conclusion, annealing process improved the thermal stability (increase of HDT and $\text{Tan}\delta$) of blends independently of annealing time thanks to improved crystallinity. The best performance in terms of high HDT value and $\text{Tan}\delta$ were obtained in the case of PLLA-PMMA-BS blends annealed for 10 min at 120°C.

It is well known that improving crystallinity of polymers can modify their mechanical properties, in particular their rigidity while decreasing their ductility. To assess that trend, mechanical properties were characterized using tensile and notched impact tests. Mechanical properties after tensile tests at a displacement rate of 1 mm min⁻¹ for binary and ternary PLLA based blends are shown in table IV.4.

Table IV.4 Tensile Properties of PLLA-BS and PLLA-PMMA-BS blends before and after annealing process

Compounds	Annealing time (min)	χ_c (%)	Tensile strength (MPa)	Elastic modulus (GPa)	Elongation at break (%)
Non-annealed PLLA-BS	0	10	44±2	2.3±0.07	148±28
PLLA-BS	10	43	47±0.5	2.7±0.04	27±9

Compounds	Annealing time (min)	χ_c (%)	Tensile strength (MPa)	Elastic modulus (GPa)	Elongation at break (%)
PLLA-BS	20	38	49±1.3	2.8±0.03	53±14
PLLA-BS	30	34	49±1	3.±0.07	31±5
Non-annealed PLLA70-PMMA30-BS	0	5	49±3	2.5±0.1	116±4
PLLA70-PMMA30-BS	10	28	49±3	2.5±0.03	35±5
PLLA70-PMMA30-BS	20	49	50±4	2.7±0.06	16±3
PLLA70-PMMA30-BS	30	49	52±0.1	2.7±0.07	13±4

By referring to the previous chapter III, both binary and ternary non-annealed PLLA-based blends reached a high level of ductility with the addition of BS at 17 wt % and a brittle-to-ductile transition is clearly observed. As can be seen in Table IV.4, following annealing process, the elastic modulus of the annealed PLLA based blends was noticeably higher compared to as-molded specimens (from 2.3GPa for non-annealed PLLA-BS to 2.7 GPa after 10 min annealing). Nevertheless, elongation at break decreased of about 80% after 10 min annealing compared to the as-molded PLA-BS blend. The same trend was found for PLLA-PMMA-BS blends with better mechanical performances in terms of tensile strength and elongation at break after 10 min annealing (respectively 49 MPa and 35%). Additionally, when increasing the annealing time, rigidity of PLLA blends increased while elongation at break decreased but with the preservation of a ductile behavior up to 30 min of annealing process (further increase of annealing time up to 120 min caused a brittle behavior of PLLA-PMMA-BS blend with 7% of elongation at break but led to an improved HDT of 116°C - results not shown).

The effect of annealing time on impact strength was also studied on binary and ternary blends. Figure IV.4 displays that PLLA-PMMA-BS blends kept approximately the same impact strength after annealing process (e.g., 44kJ/m² after 10 min annealing) contrary to PLA/BS blends that showed a dramatic increase of impact strength, reaching 74 kJ/m² after 10 min annealing. This improvement can be due to a change in failure mode of fractured PLLA-BS blends (from debonding mechanism to shear yielding mechanism) that does not appear for PLLA-PMMA-BS specimen, which can explain that this composition kept the same impact strength values (Figure IV.5). As attested by scanning electron microscopy (SEM), macroscopic localized zones of micro-voids and micro-fibrils are found by annealing PLLA-BS blend (Figure IV.5b). Therefore, these highly localized plastic deformation triggered by the dispersed rubbery phase, refer to the possible toughening mechanisms: *i.e.* shear yielding as the prevalent mechanism.

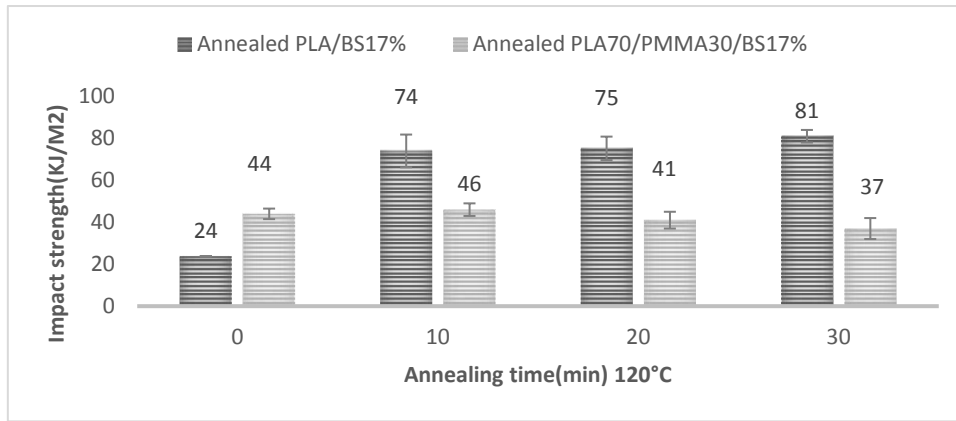


Figure IV.4. Effect of annealing time on impact strength of PLLA based blends

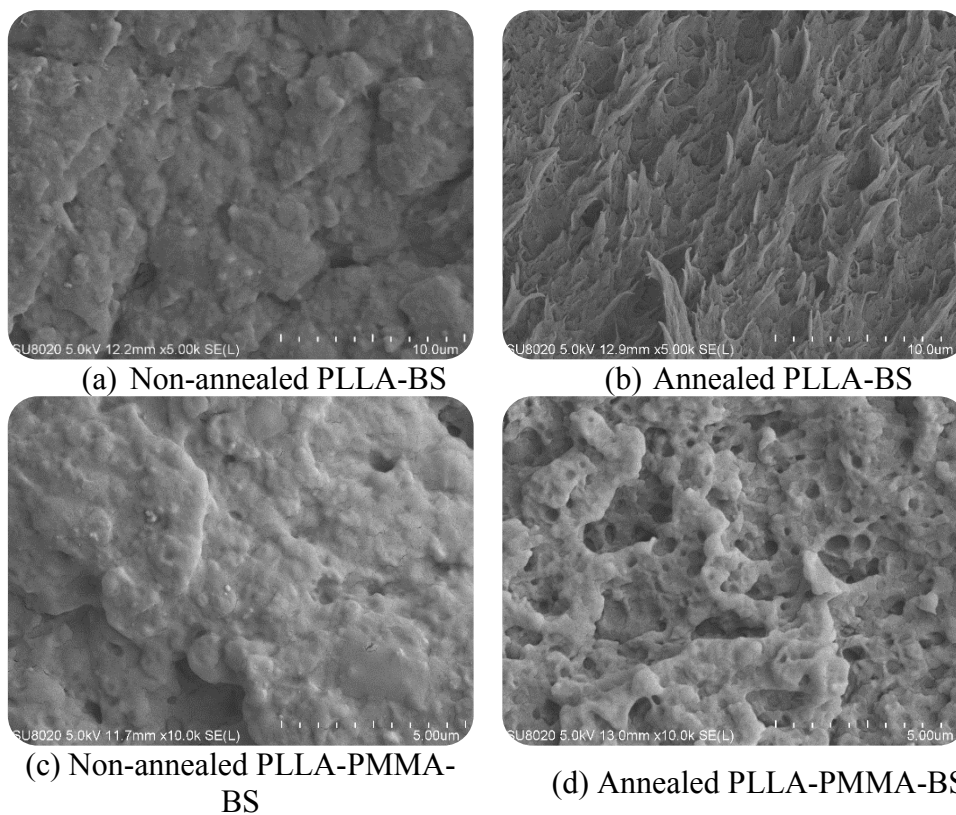


Figure IV.5. SEM micrographs of PLLA based blends before and after annealing for 30 min at 120°C

As a conclusion, we can conclude that annealing process is a promising approach to enhance heat resistance of PLA based blends while improving toughness and rigidity. However, ductility can be affected depending on annealing parameters. A second approach will be developed in the next section in order to enhance crystallinity.

IV.2 Stereocomplexing PLA-based materials

Performing PLLA-PDLA stereocomplexes can be a promising solution to obtain PLA materials with high thermal resistance and improved crystallinity. Therefore, numerous PLLA-PDLA blends were studied in this section. PLLA-PDLA binary, ternary (impact modifier was added to PLLA-PDLA blends) and quaternary blends (both impact modifier and PMMA were added to PLLA-PDLA blends) cited in table V.1 were melt blended in an internal mixture chamber at 210°C for 10 min. In these blends, four different ratio of PLLA/PDLA was studied (95/5), (90/10), (70/30) and (50/50), while PMMA and BS weight content were maintained respectively at 25% and 17%, i.e., at the optimal contents leading to the best mechanical performances (see chapter III). WAXS profiles were recorded on these injection-molded stereocomplexed PLA (sc-PLA) blends to assess their crystallinity (Figure IV.6). In all cases, a broad amorphous halo covering the entire 2θ range was observed, together with superposition of a couple of crystalline diffraction peaks. The diffraction peaks for binary sc-PLA blends (PLLA95/PDLA5 and PLLA90/PDLA10) appeared at ca. 12, 16, 21 and 24°. These two blends displayed peaks corresponding to both stereocomplex and homopolymer crystallites in accordance with the literature [30]. According to Schmidt et al.[30] the diffraction peaks of pure PLLA homopolymer indeed appear at ca. 16, 18.5, 22.5, 24, and 29°, whereas diffraction peaks of the PLLA50/PDLA50 blend corresponding to the stereocomplex appear at ca. 12, 21, and 24°. In the case of PLLA90/PDLA10 blend, different peaks are displayed, corresponding to both stereocomplex and homopolymer crystallites. When increasing the amount of PDLA, the intensity of the diffraction peaks associated to PLA stereocomplex increased progressively to reach a crystallinity ratio of 15%. However, the introduction of impact modifier had a strong influence on the WAXS profiles. In presence of BS, the four diffraction peaks decreased progressively when increasing PDLA amount and crystallinity was affected to attain 5% for sc-PLA. Addition of PMMA to the ternary PLLA95/PDLA5/BS blends affected the formation of sc-PLA due to the very low amount of PDLA related to PLLA. At higher PDLA amount, small diffractions peaks of PLLA90-PDLA10-PMMA-BS blend appeared at approximately 12, 21, and 24° (2θ) and can be attributed to crystals of PLA stereocomplexes [31]. Crystallinity of PLLA-PDLA-PMMA-BS blend increased when increasing PDLA content (Table IV.5). In this blend, no diffraction peak attributed to PLLA was observed, thus indicating the absence of PLLA homocrystallization.

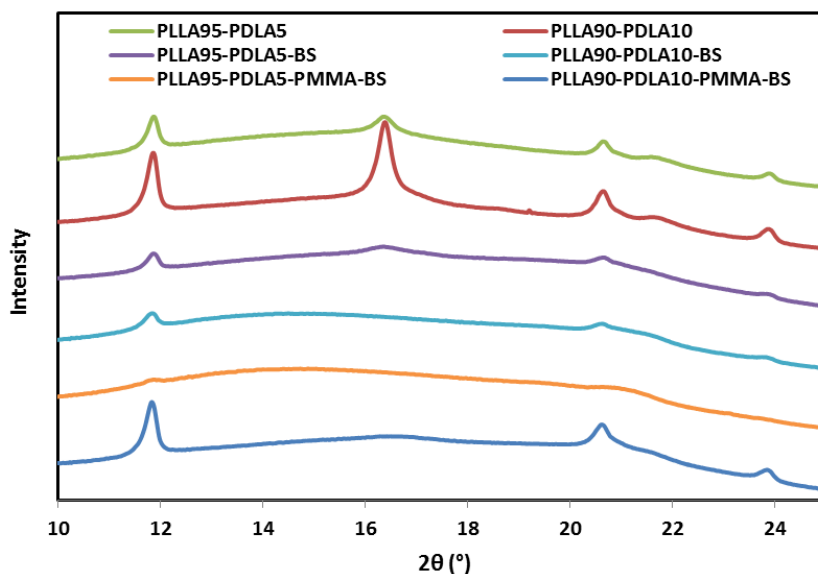


Figure IV.6. WAXS profiles of binary (PLLA-PDLA), ternary (PLLA-PDLA-BS) and quaternary (PLLA-PDLA-PMMA-BS) blends

DSC analyses were also performed to investigate the thermal behavior of sc-PLA blends. Results presented in table IV.5 show two melting temperatures for all sc-blends. The peak at around 164-168°C for sc-PLA blends is ascribed to the melting of PLLA or PDLA homo-crystallites, while the new melting peak at around 216°C is attributed to the melting of stereocomplex crystallites. Note that PLLA-PDLA-PMMA-BS blends with 10, 30 and 50% of PDLA present only one melting temperature at around 216°C, which corresponds to the melting temperature of stereocomplex crystallites. The present results confirm WAXS profiles interpretation with the absence of diffraction peaks related to PLLA homopolymer for PLLA90-PDLA10-PMMA-BS blends (the same results are found for both PLLA70-PDLA30-PMMA-BS and PLLA50-PDLA50-PMMA-BS—WAXS profiles are not shown). When increasing PDLA contents on sc-PLA-PMMA-BS blends, the melting enthalpy of sc-PLA increases (2 J/g with 5% of PDLA to 12.5 J/g with 30% of PDLA), while the melting enthalpy of homocrystallites is affected by increasing PDLA content. The same trend was reported in literature [32-34].

Table IV.5 Glass transition, Crystallization and Melting Temperature and Enthalpy for PLA Stereocomplexes and PLA Homocrystallites in sc-PLA blends

Compounds	T _g (°C)	ΔH _m scPLA (J/g)	ΔH _m homocrystallites PLLA (J/g)	T _m sc- PLA (°C)	T _m homocrystallites PLLA (°C)	ΔH _{cc} (J/g)	T _{cc} (C°)	X _c * (%)
PLLA95- PDLA5	62	8	30	217	168	28	105	8
PLLA90- PDLA10	62	10	30	217	168	24	105	15
PLLA95- PDLA5-BS	62	4	23	216	164	23	117	4.7
PLLA90- PDLA10-BS	62	8	19	216	164	20	116	5
PLLA95- PDLA5- PMMA-BS	63	2	0.3	214	168	1.5	149	2.4
PLLA90- PDLA10- PMMA-BS	63	5	-	216	-	3	150	8
PLLA70- PDLA30- PMMA-BS	63	12.5	-	216	-	5.4	125	—
PLLA50- PDLA50- PMMA-BS	63	11.7	-	216	-	5	126	—

*Crystallinity ratio calculated from WAXS profile.

In order to evaluate the stereocomplexation effect of PLA based blends on the thermomechanical properties, the storage modulus and tan δ were recorded as a function of the temperature for all injection-molded sc-PLA blends. Values of tan δ, storage modulus and HDT are presented in Table IV.6. PLLA-PDLA blends presented a high value of storage modulus (≈ 2.2 GPa with 10%wt of PDLA). It can be seen that the addition of BS impact modifier to sc-PLA decreased its storage modulus (≈1.6GPa, in part because of the low stiffness of impact modifier (12 MPa at 25°C)). Adding PMMA to sc-PLA/BS blend increased the rigidity of the blend up to 100 MPa. Regarding the tan δ profiles, a unique peak associated to the α-relaxation transition was detectable for all injection molded ternary blends (59°C for sc-PLA, enhanced up to 69°C thanks to addition of PMMA for sc-PLA blends). Unfortunately, the sc-PLA blends maintained the same performances like PLLA-BS and PLLA70-PMMA30-BS (presented in chapter III). Indeed, there is no enhancement of thermo-mechanical properties in terms of

storage modulus, $Tan\delta$ and HDT value due to the limited improvement of crystallinity ratio. In the same context, Nam et al.[35] succeeded to perform sc-PLA with improved thermal resistance (HDT= 110°C) by simply adding 8% PDLA to PLLA but with the use of different process for making sc-PLA (extrusion process at 180° C and screw speed of 200 rpm). Yet, adding impact modifier to sc-PLA blends can affect their thermal resistance and HDT value of toughened sc-PLA blends decreased by 35°C to reach 65°C when adding 20% of Biomax Strong. Concerning our study, many reasons can explain the limited crystallinity and HDT of sc-PLA such as the presence of impact modifier as aforementioned, since there is a formation of “graft copolymers” as compatibilizers through coupling reactions between the functional end-groups (hydroxyl and carboxylic) of PLA chains and the complementary functional groups (epoxy functions), which can affect the formation of sc-PLA. Another reason concerns the molecular weight between PLLA and PDLA. When there is a significant difference of molecular weight between PLLA and PDLA and even if they are mixed at their equitable ratio, there will be an excess of homopolymer crystallites of the polymer having the low molecular weight (in our case PDLA) or a limited racemic crystallites depending on the critical molecular weight of sc-PLA[36,11].(see Appendix Figure A1)

Table IV. 6 Relaxation temperatures, storage modulus and HDT of sc-PLA based blends

Compounds	Ttanδ(°C)	Storage Modulus E(MPa) _{T=25°C}	HDT(°C)
Neat PLLA	57	3100	54
PLLA95-PDLA5	59	2251	53
PLLA90-PDLA10	57	2165	54
PLLA-BS	60	1355	53
PLLA95-PDLA5-BS	59	1522	51
PLLA90-PDLA10-BS	56	1623	52
PLA70-PMMA30-BS	67	1613	58
PLLA95-PDLA5-PMMA-BS	67	1748	56
PLLA90-PDLA10-PMMA-BS	69	1706	57
PLLA70-PDLA30-PMMA-BS	70	1723	56
PLLA50-PDLA50-PMMA-BS	71	1689	56

Mechanical properties of sc-PLA based blends were studied in terms of tensile tests at a displacement rate of 1 mm min⁻¹ and notched impact tests. Table IV.7 shows the mechanical properties of sc-PLA blends and toughened PLA blends obtained in the previous chapter for comparison. First, compared to PLLA-BS blend, the toughened sc-PLA blends presented the same mechanical properties. Stereocomplexation therefore maintained the good mechanical

properties of blend (ductile behavior with high rigidity and good impact strength). When increasing the PDLA content, impact strength of PLLA90-PDL10-BS increased to reach 50kJ/m². Nevertheless, adding PMMA to toughened sc-PLA blends affected the toughness both at 5 wt% and 10 wt% of PDLA to reach 27 kJ/m². Tensile modulus and strength showed values of 2.4 GPa and 48 MPa, respectively. In conclusion, compared to PLA based blend analyzed in Chapter III, the sc-PLA based blends maintained almost the same mechanical properties excepting the impact properties. It is well known that the overall material toughness is mainly governed by a variety of factors such as the composition and crystallization behavior of the matrix, the rubber particle size and size distribution, the rubber-matrix interfacial adhesion or the blend morphology. This latter is therefore investigated in the next paragraph.

Table IV.7 Mechanical properties of sc-PLA blends

Compounds	E (MPa)	Maximal stress (MPa)	Elongation at break (%)	Impact Strength (kJ/m ²)
Neat PLLA	3200±100	68±2	2.8± 0.2	3.4±0.1
PLLA-BS	2288±72	44±2	148±38	24±0.1
PLLA95-PDLA5-BS	2298±71	48.7±0.4	158.78±10	25±2
PLLA90-PDLA10-BS	2172±260	48.1±0.8	169.86±4	50±7
PLLA70-PMMA30-BS	2467±35	49±3	116±4	44±2
PLLA95-PDLA5-PMMA-BS	2443±78	46.8±1.7	129.84±4	27±1
PLLA90-PDLA10-PMMA-BS	2486±42	48.2±1.2	126.39±6	27±2

Figure IV.6 shows SEM micrographs of cryofractured surfaces of sc-PLLA (L/D 95/5)-PMMA-BS ternary blends and PLLA-PMMA-BS blend. As shown in Figure IV.7a and already mentioned in Chapter III, PLLA-PMMA-BS blend presented a phase separated morphology with plastic deformation of the surface and a good interfacial adhesion. Sc-PLA-PMMA-BS blend (Figure IV.7b) also shows a phase-separated morphology but with a coarse dispersion of BS microdomains of irregular shape and large interfacial voids caused by mechanical debonding of BS from matrix. This low interfacial adhesion can explain the decrease of impact strength of about 40% when adding 5 wt% of PDLA.

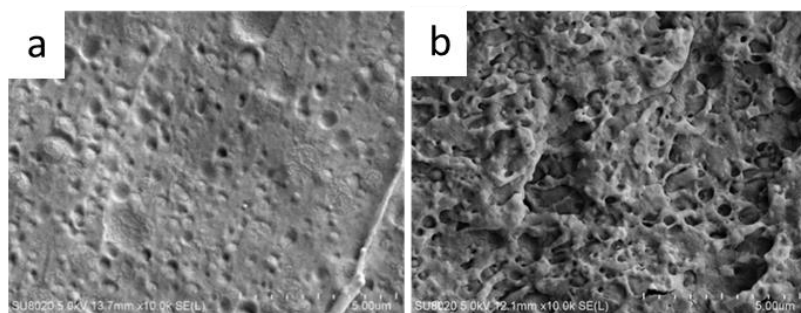


Figure IV.7. SEM micrographs of impact-fractured surfaces of (a) PLLA70-PMMA30-BS; (b) PLLA95-PDLA5-PMMA-BS

Concerning PLA stereocomplexation, the ratio of stereocomplex crystallites to homocrystallites may be affected by numerous parameters, such as the molecular weights, melting temperature and time, mixing ratio of the isomeric chains, etc, as reported in the literature [37,38,16]. Therefore, mastering the process parameters is required to control the stereocomplexation of PLA blends.

It is investigated whether further improvements in properties can be reached by optimizing processing of sc-PLA blends [31,39]. In our study, it appeared that the level of tensile strength, rigidity or impact resistance can be tuned up by modifying the blending process of sc-PLA blends, while maintaining advanced crystallization properties. More precisely, two-stage blending processes, i.e. mixing BS and PMMA in a pre-formed PLLA/PDLA blend, resulted in improved impact strength while maintaining good mechanical properties in terms of rigidity, tensile strength and ductility (results not shown). As shown in Figure IV.8, the impact strength of sc-PLA blends increased when making blends in two steps ($\approx 50\%$ of improvement), except for PLLA90-PDLA10-BS which had almost the same impact strength. SEM micrographs were then performed to see the morphology of the cryo-fractured surface of blends. As can be seen in Figure IV.9, the surface was regular and a good adhesion between rubber BS micro-domains and matrix with the absence of voids was noticed for both sc-PLA-PMMA-BS blends processed in two steps, which explains the improvement in toughness for these blends.

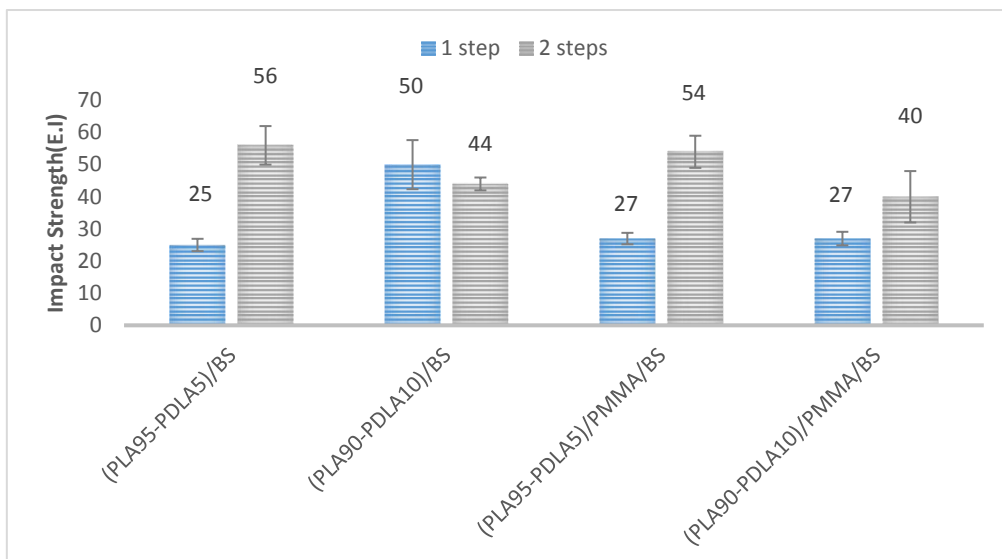


Figure IV.8. Effect of modified process on the notched impact strength of sc-PLA blends

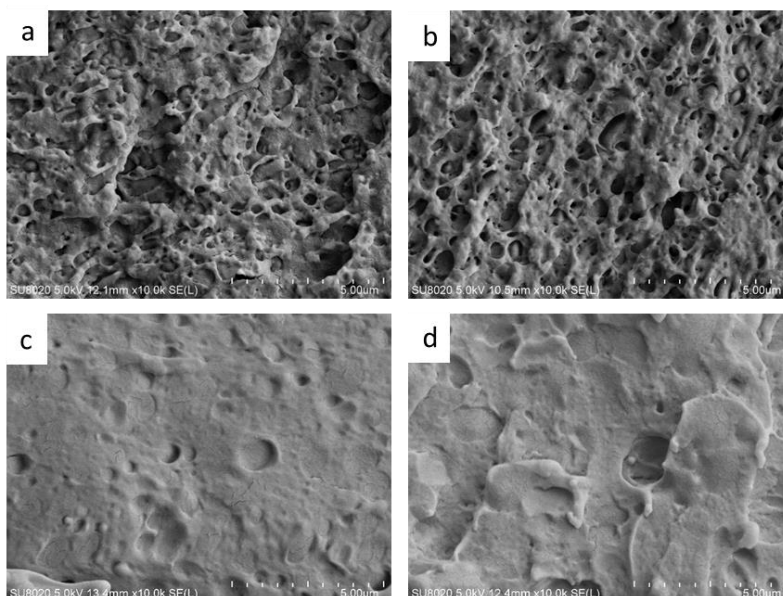


Figure IV.9. SEM micrographs of impact-fractured surfaces of (a) (PLA95-PDLA5)/PMMA/BS 1 step, (b) (PLA90-PDLA10)/PMMA/BS one step, (c) (PLA95-PDLA5)/PMMA/BS 2 steps, (d) (PLA90-PDLA10)/PMMA/BS 2 steps.

To conclude, stereocomplexation between PLLA and PDLA is an interesting approach to improve crystallinity of compounds together with good processability. However, in the present study PLLA/PDLA molecular weight was different, which led to limited crystallinity improvement for the resulting sc-PLA with a partial crystallization of homopolymers. Therefore, studying different molecular weight of PLLA and PDLA can be interesting to promote complete stereocomplexation. Finally, the presence of PMMA and BS also affects the

stereocomplexation, as well as processing parameters, which have a significant influence on the improvement of crystallinity and related HDT.

IV.3 Combination of Nucleating agent and nanoparticles:

To simultaneously improve PLA crystallization and PLA toughness, nanocomposites were produced by melt blending PLA with untreated silica 3D-nanofiller (SiO_2). An ethylene bis-stearamide (EBS) was added to promote both nucleating ability and chain mobility in the melt. The combination of silica nanoparticles and nucleating agent could result in a synergistic effect and behave as remarkable nucleating agents to endorse PLA crystallization rate with improved mechanical properties[7]. Only SiO_2/EBS ratio of 80/20 was studied, at a total nanofiller content of 3 wt%, based on the optimum highlighted by previous studies of PLA nanocomposites of our research group[7]. For the sake of comparison, PLLA-EBS and PLLA-EBS- SiO_2 blends were performed. The effect of EBS and silica nanoparticles on the crystallization of PLA blends was investigated using differential scanning calorimetry (DSC) techniques. The DSC profiles and corresponding data of resulting PLA-based materials are shown in Figure IV.10 and Table IV.8. The peak of the crystallization exotherm was denoted as T_{cc1} . (see Figure IV.10a) On cooling from the melt, some samples showed a sharp crystallization exotherm, which was denoted T_{cc2} (see Figure IV.10b).

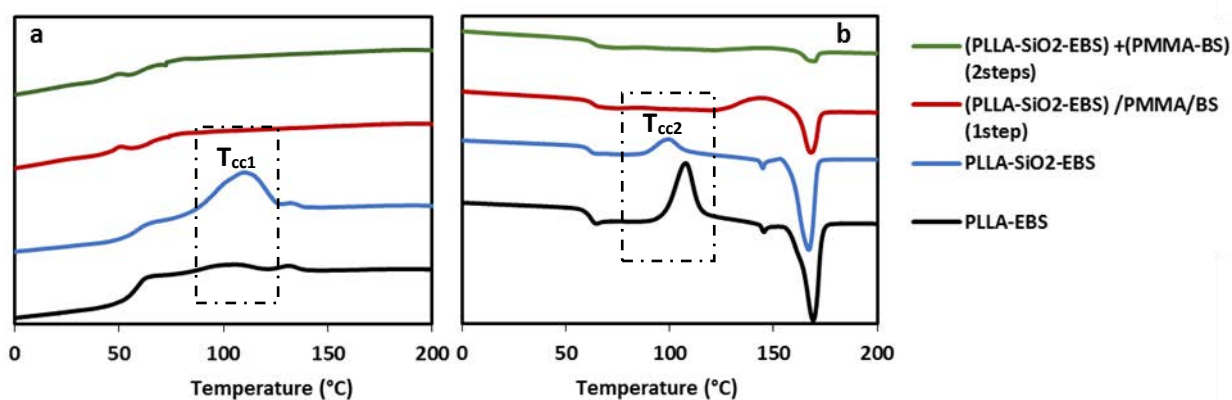


Figure IV.10. DSC thermograms of PLA-based materials as they were recorded (a) during cooling and (b) during second heating.

While PLLA-EBS blend showed a weak and broad exothermic crystallinity (T_{cc1}) (Figure IV.10 a), addition of silica nanoparticles led to a clear PLA crystallization during cooling (ΔH_{cc1} of 15.9 J/g instead of 4 J/g for PLLA-EBS). A small sharper peak was observed within the

temperature range 131°C-133°C, which was attributed to the crystallization of EBS itself. Similar results were reported by Murariu et al.[7] following the development of nanocomposites PLA with EBS as a nucleating agent.

As expected, the glass transition temperatures (T_g) of PLA-based materials remained unchanged at 61 °C upon the addition of EBS. However, a new endothermic peak related to the melting of EBS has been evidenced at around 144 °C (Figure IV.10b). Moreover, cold crystallization exotherm (T_{cc2}) was observed prior to the melting endotherm on heating at around 107 °C for PLLA-EBS and 99°C when adding silica nanoparticles. The cold crystallization peak of PLA in the blends decreased significantly when adding nanoparticles (ΔH_{cc2} decreased from 24.3 to 8 J/g), indicating an enhancement of PLA crystallization induced by the presence of silica nanoparticles (as shown in Table IV.8). Additionally, with the addition of silica nanoparticles, the degree of crystallinity (χ_c) remarkably increased reaching 25%, demonstrating that the combination of SiO₂ and EBS behave as an efficient nucleating agent for PLLA, if using a processing method appropriate to promote crystallization[40]. In this respect, relationship between processing (the order of mixing of compounds) and crystallization behavior was investigated for PLLA nanocomposite-based materials containing 17 wt% of BS impact modifier and 25 wt% of PMMA (PLLA-PMMA-BS-SiO₂-EBS). For doing so, blends were performed using a one-step process (i.e. BS and PMMA were added simultaneously with nanofillers into the blend) or a two-step process (BS and PMMA were added after, in the preformed PLLA-SiO₂-EBS blend).

First, as shown in Table IV.8, crystallinity of nanocomposites PLA with addition of PMMA and BS performed in one step dramatically decreased to reach 6% instead of 25% for PLLA-SiO₂-EBS but still higher than PLA-PMMA-BS blend. Thereby nucleating effect of SiO₂-EBS was no more highlighted in this blend and it was even poorest for the blend processed in two steps, which crystallinity decreased to reach 1%, thus confirming that process parameters can control crystallinity behavior of compounds. Compared to PLLA-PMMA-BS blend prepared in chapter III, nanocomposite PLA-PMMA-BS blend presented the same T_g , T_{cc2} and T_m (around 63°C, 143°C and 168°C, respectively), which are typical thermal properties for miscible toughened PLLA-PMMA based blends.

Table IV.8 Thermal properties of PLA and toughened PLA-PMMA nanocomposites containing EBS

Compounds	ΔH_m (J/g)	ΔH_{cc2} (J/g)	T_m (°C)	T_{cc2} (C°)	T_g (°C)	χ_c (%)*
PLLA-EBS(Ref)	32.4	24.3	169	107	61	9
PLLA-SiO ₂ -EBS	30.5	8	166	99	61	25
PLLA-PMMA-BS (Ref)	11.5	10	168	143	62.8	3
(PLLA-SiO ₂ -EBS) /PMMA/BS (1step)	12.5	9.3	168	143	63	6
(PLLA-SiO ₂ -EBS) + (PMMA/BS) (2 steps)	2.797	2.253	169	145	63.7	1

The effect of crystallinity ratio on mechanical performance and thermal stability was respectively measured through tensile test, notched impact test and HDT. Table IV.9 summarizes mechanical properties and HDT values of different nanocomposites PLA blends. Surprisingly, the ductility of PLLA-EBS and PLLA- SiO₂-EBS increased (elongation at break of 10 % and 6% respectively) compared to neat PLA (2.8%). Unfortunately, HDT did not increase even when adding combined SiO₂/EBS. In particular, PLLA-PMMA-BS blend maintained the same thermal stability in presence of SiO₂/EBS. Note that annealing process was recommended by Harris et al. [18] to enhance HDT by upwards of 30°C for post –annealed PLA-EBS blend at 80°C for 60 min.

Table IV.9 Mechanical properties of nanocomposites PLA blends.

Compounds	Apparent rigidity E (MPa)	Ultimate Strength (MPa)	Elongation at break (%)	Impact Strength (kJ/m²)	HDT(°C)
PLLA-EBS	3221±34	68±2	10±6	3±0.1	53
PLLA-SiO ₂ -EBS	3287±2	68±3	6±2	3±0.3	54
(PLLA-SiO ₂ -EBS) /PMMA/BS (1step)	2263±15	46±0.1	122±3	35±1	58
(PLLA-SiO ₂ -EBS) + (PMMA/BS) (2 steps)	2100±29	44±0.4	105±1	13±0.2	56

Finally, nanocomposites PLLA-PMMA-BS blend processed in one step presented interesting impact strength compared to the blend made in two steps (35 kJ/m² instead of 13 kJ/m² for 2 steps blend). The morphological characteristic features, a key-element of this study,

may explain how processing methods affect toughness. Indeed, as already mentioned, the overall shape and average dimensions of dispersed rubbery phase must be properly controlled to form compositions with optimal mechanical properties. SEM micrographs of PLLA-EBS and PLLA-SiO₂-EBS and PLLA-PMMA-BS nanocomposites are shown in Figure IV.11.

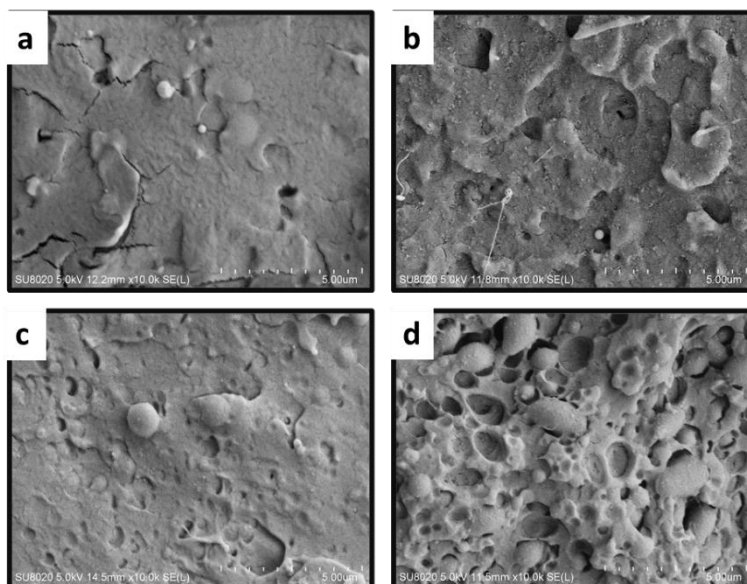


Figure IV.11. SEM micrographs of impact-fractured surfaces of (a) (PLLA-EBS)/PMMA/BS, (b) PLLA-SiO₂-EBS, (c) PLLA-SiO₂-EBS-PMMA-BS 2 steps, (d) PLLA-SiO₂-EBS/PMMA/BS 2 steps.

In PLLA-SiO₂-EBS (Figure IV.11 b), the white bright spots of nano-silica particles can be clearly seen. Silica particles were dispersed in PLLA-EBS blend with good compatibility. A phase separated morphology with plastic deformation of the surface and a good interfacial adhesion between matrix and rubber microdomains was observed in PLLA-SiO₂-EBS-PMMA-BS processed in one step (Figure IV.11c), which explain the high impact strength of the blend. In addition, it was observed that many of the rubber droplets contained many silica nanoparticles inside. TEM micrographs confirm the presence of silica nanoparticles on the rubber droplets of impact modifier (Figure IV.12). With the presence of impact modifier into PLLA-SiO₂-EBS matrix, silica nanoparticles migrate from the matrix to the interior of the rubber microdomains, which can negatively affect the nucleating effect of nanoparticles. This can explain the decrease of crystallinity of (PLLA-SiO₂-EBS) /PMMA/BS blend after adding PMMA and BS. By contrast, nanocomposite PLA-PMMA-BS made in 2 steps (Figure IV.11d) showed a phase-separated morphology of irregular shapes of BS microdomains and large

interfacial voids caused by mechanical debonding of BS from matrix. This low interfacial adhesion can explain the decrease of impact strength of about 60% that was measured. As a conclusion, achieving good mechanical properties by controlling morphology and crystallinity behavior requires to find the optimum process parameters.

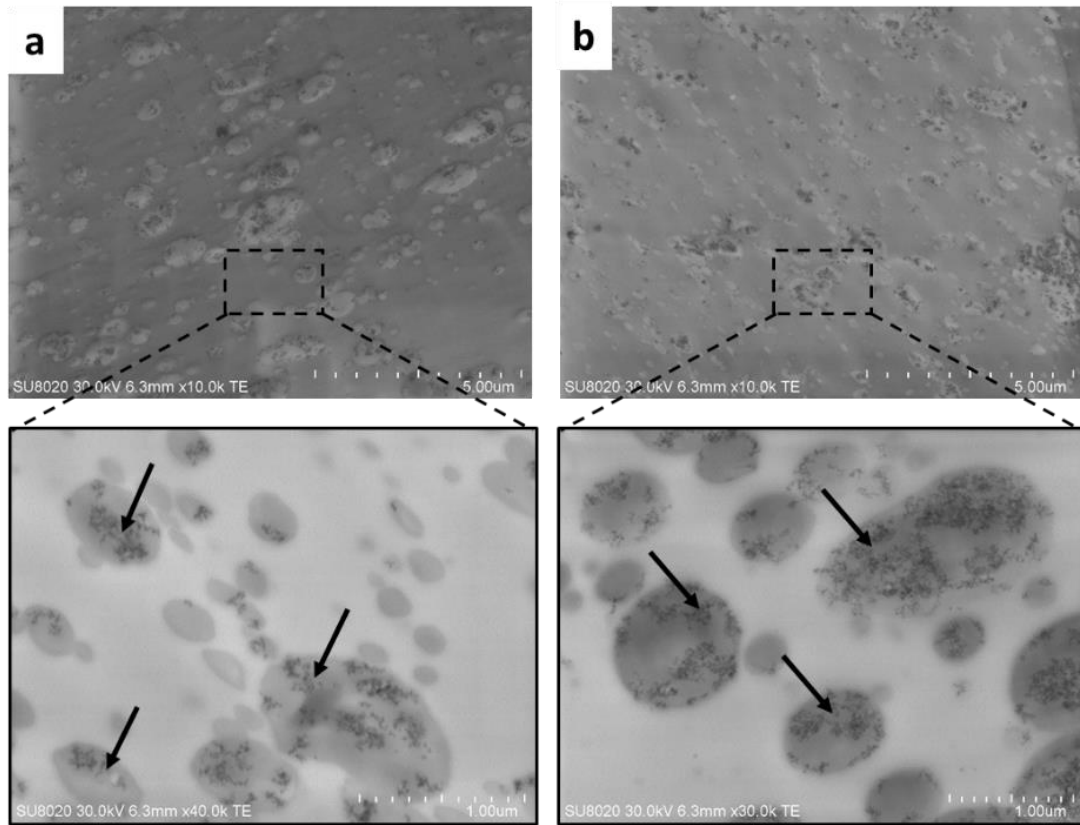


Figure IV.12. TEM micrographs of impact-fractured surfaces of (a) PLLA-SiO₂-EBS-PMMA-BS 2 steps, (b) PLLA-SiO₂-EBS/PMMA/BS 2 steps.(arrows indicate the nanoparticles)

CONCLUSIONS

The use of PLA in automotive application is currently limited because PLA shows a slow crystallization rate under the same process conditions, leading to limited thermal resistance in particular. Among several investigated approaches to overcome this problem, annealing was revealed as a good solution to improve heat resistance by improving crystallinity ratio (28%) against time (HDT around 80°C after 10 min at 120°C). However, time and temperature of pre-heat treatment should be optimized to not affect the ductility of PLA-PMMA-BS blend. Unfortunately, annealing process can be expensive and involves longer production time. Therefore, it cannot be seen as a promising solution for mass production characterizing the automotive industry. Stereocomplexing PLA can also improve heat resistance but, in our case, process parameters should be still optimized in order to make sc-PLA complete. Otherwise, impact toughness can be affected, and heat deflection temperature is not enhanced. Concerning the enhancement of crystallinity behavior of PLA-PMMA-BS blend thanks to the combination of nucleating agent and nanoparticles, a limited improve of crystallinity ratio (6%) was revealed with unenhanced . According to literature, PLA nanocomposites need a post treatment such as annealing to improve heat deflection temperature, which is again not reasonable for making PLA-based blends suitable for automotive application.

Finally, based on promising results obtained in Chapter III, PLLA70-PMMA30-BS was selected as the one that presents the better balance between ductility and stiffness, improved thermal properties and contains at least 50% of bio-sourced polymer, without any additional processing or filling. In this respect, the next chapter will aim at scaling up that selected composition towards industrialization, i.e. assessing whether the material can be processed at an “industrial scale” while keeping interesting thermo-mechanical properties. The performance of the blend under severe loading conditions and its durability after thermal aging will be investigated.

REFERENCES

1. Rasal RM et al. (2010) Poly(lactic acid) modifications. *Progress in Polymer Science* 35 (3):338-356.
2. Perkins WG (1999) Polymer toughness and impact resistance. *Polymer Engineering & Science* 39 (12):2445-2460. doi:10.1002/pen.11632
3. Srithep Y et al. (2011) Processing and characterization of recycled poly(ethylene terephthalate) blends with chain extenders, thermoplastic elastomer, and/or poly(butylene adipate-co-terephthalate). *Polymer Engineering & Science* 51 (6):1023-1032. doi:10.1002/pen.21916
4. Osswald TA (2006) *International Plastics Handbook: The Resource for Plastics Engineers*. Hanser,
5. Xu H et al. (2006) Improvements of thermal property and crystallization behavior of PLLA based multiblock copolymer by forming stereocomplex with PDLA oligomer. *Polymer* 47 (11):3922-3928.
6. Srithep Y et al. (2013) Effects of annealing time and temperature on the crystallinity and heat resistance behavior of injection-molded poly(lactic acid). *Polymer Engineering & Science* 53 (3):580-588. doi:10.1002/pen.23304
7. Murariu M et al. (2015) Recent advances in production of poly(lactic acid) (PLA) nanocomposites: a versatile method to tune crystallization properties of PLA. *Nanocomposites* 1 (2):71-82. doi:10.1179/2055033214y.0000000008
8. Oyama HT (2009) Super-tough poly(lactic acid) materials: Reactive blending with ethylene copolymer. *Polymer* 50 (3):747-751.
9. Takayama T et al. (2011) Effect of annealing on the mechanical properties of PLA/PCL and PLA/PCL/LTI polymer blends. *Journal of the Mechanical Behavior of Biomedical Materials* 4 (3):255-260.
10. Turng L-S, Srithep Y Annealing conditions for injection molded poly (lactic acid). *Society of Plastics Engineers (SPE)*
11. Tsuji H et al. (1991) Stereocomplex formation between enantiomeric poly(lactic acid)s. 4. Differential scanning calorimetric studies on precipitates from mixed solutions of poly(D-lactic acid) and poly(L-lactic acid). *Macromolecules* 24 (20):5657-5662. doi:10.1021/ma00020a027
12. Tsuji H, Tezuka Y (2004) Stereocomplex Formation between Enantiomeric Poly(lactic acid)s. 12. Spherulite Growth of Low-Molecular-Weight Poly(lactic acid)s from the Melt. *Biomacromolecules* 5 (4):1181-1186. doi:10.1021/bm049835i
13. Yamane H, Sasai K (2003) Effect of the addition of poly(d-lactic acid) on the thermal property of poly(l-lactic acid). *Polymer* 44 (8):2569-2575.
14. Tsuji H et al. (2006) Isothermal and non-isothermal crystallization behavior of poly(l-lactic acid): Effects of stereocomplex as nucleating agent. *Polymer* 47 (11):3826-3837.
15. Tsuji H, Ikada Y (1999) Stereocomplex formation between enantiomeric poly(lactic acid)s. XI. Mechanical properties and morphology of solution-cast films. *Polymer* 40 (24):6699-6708.

16. Tsuji H, Fukui I (2003) Enhanced thermal stability of poly(lactide)s in the melt by enantiomeric polymer blending. *Polymer* 44 (10):2891-2896.
17. Tang Z et al. (2012) The crystallization behavior and mechanical properties of polylactic acid in the presence of a crystal nucleating agent. *Journal of Applied Polymer Science* 125 (2):1108-1115. doi:10.1002/app.34799
18. Harris AM, Lee EC (2008) Improving mechanical performance of injection molded PLA by controlling crystallinity. *Journal of Applied Polymer Science* 107 (4):2246-2255. doi:10.1002/app.27261
19. Ouchiar S et al. (2016) Influence of the Filler Nature on the Crystalline Structure of Polylactide-Based Nanocomposites: New Insights into the Nucleating Effect. *Macromolecules* 49 (7):2782-2790. doi:10.1021/acs.macromol.5b02746
20. Sinha Ray S (2012) Polylactide-Based Bionanocomposites: A Promising Class of Hybrid Materials. *Accounts of Chemical Research* 45 (10):1710-1720. doi:10.1021/ar3000376
21. Liu Z-W et al. (2014) Mechanical and thermal properties of thermoplastic polyurethane-toughened polylactide-based nanocomposites. *Polymer Composites* 35 (9):1744-1757. doi:10.1002/pc.22828
22. Samuel C et al. (2013) PLLA/PMMA blends: A shear-induced miscibility with tunable morphologies and properties? *Polymer* 54 (15):3931-3939.
23. Yu F et al. (2012) Effects of talc on the mechanical and thermal properties of polylactide. *Journal of Applied Polymer Science* 125 (S2):E99-E109. doi:10.1002/app.36260
24. Fang H et al. (2013) Shear-Induced Nucleation and Morphological Evolution for Bimodal Long Chain Branched Polylactide. *Macromolecules* 46 (16):6555-6565. doi:10.1021/ma4012126
25. Das K et al. (2010) Crystalline morphology of PLA/clay nanocomposite films and its correlation with other properties. *Journal of Applied Polymer Science* 118 (1):143-151. doi:10.1002/app.32345
26. Tabi T et al. (2010) Crystalline structure of annealed polylactic acid and its relation to processing. *Express Polym Lett* 4 (10):659-668
27. Lv S et al. (2015) Effect of annealing on the thermal properties of poly (lactic acid)/starch blends. *International Journal of Biological Macromolecules* 74:297-303.
28. Chou PM et al. (2011) Changes in the crystallinity and mechanical properties of poly(l-lactic acid)/poly(butylene succinate-co-l-lactate) blend with annealing process. *Polymer bulletin* 67 (5):815-830. doi:10.1007/s00289-011-0456-5
29. Kim JY et al. (2003) Effects of annealing on structure and properties of TLCP/PEN/PET ternary blend fibers. *Macromolecular Research* 11 (1):62-68
30. Schmidt SC, Hillmyer MA (2001) Polylactide stereocomplex crystallites as nucleating agents for isotactic polylactide. *Journal of Polymer Science Part B: Polymer Physics* 39 (3):300-313. doi:10.1002/1099-0488(20010201)39:3<300::aid-polb1002>3.0.co;2-m
31. Tsuji H (2007) Poly(lactide) Stereocomplexes: Formation, Structure, Properties, Degradation, and Applications. *Macromolecular Bioscience* 7 (12):1299-1299. doi:10.1002/mabi.200700275

32. Wei X-F et al. (2014) Stereocomplex Crystallite Network in Asymmetric PLLA/PDLA Blends: Formation, Structure, and Confining Effect on the Crystallization Rate of Homocrystallites. *Macromolecules* 47 (4):1439-1448. doi:10.1021/ma402653a
33. Rahman N et al. (2009) Effect of Polylactide Stereocomplex on the Crystallization Behavior of Poly(l-lactic acid). *Macromolecules* 42 (13):4739-4745. doi:10.1021/ma900004d
34. Samuel C et al. (2013) Stereocomplexation of Polylactide Enhanced by Poly(methyl methacrylate): Improved Processability and Thermomechanical Properties of Stereocomplexable Polylactide-Based Materials. *ACS Applied Materials & Interfaces* 5 (22):11797-11807. doi:10.1021/am403443m
35. Nam B-U, Lee B-S (2012) Toughening of PLA stereocomplex by Impact modifiers. *Journal of the Korea Academia-Industrial cooperation Society* 13 (2):919-925
36. Tsuji H et al. (1991) Stereocomplex formation between enantiomeric poly(lactic acid)s. 3. Calorimetric studies on blend films cast from dilute solution. *Macromolecules* 24 (20):5651-5656. doi:10.1021/ma00020a026
37. Tsuji H (2005) Poly(lactide) Stereocomplexes: Formation, Structure, Properties, Degradation, and Applications. *Macromolecular Bioscience* 5 (7):569-597. doi:10.1002/mabi.200500062
38. Ikada Y et al. (1987) Stereocomplex formation between enantiomeric poly(lactides). *Macromolecules* 20 (4):904-906. doi:10.1021/ma00170a034
39. Takasaki M et al. (2003) Development of Stereocomplex Crystal of Polylactide in High-Speed Melt Spinning and Subsequent Drawing and Annealing Processes. *Journal of Macromolecular Science, Part B* 42 (3-4):403-420. doi:10.1081/mb-120021570
40. Jun CL (2000) Reactive Blending of Biodegradable Polymers: PLA and Starch. *Journal of Polymers and the Environment* 8 (1):33-37. doi:10.1023/a:1010172112118

APPENDIX: Thermal analysis of equitable ratio of PLLA-PDLA blends

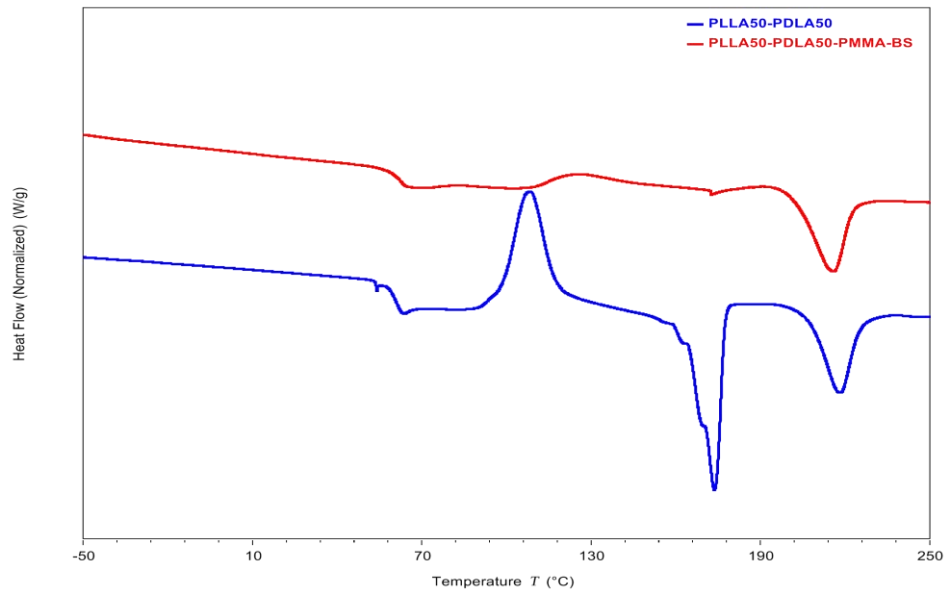


Figure A.1. DSC curves of equitable ratio of PLLA-PDLA blends

CHAPTER V

HIGHLY TOUGH POLY (L-LACTIDE) BASED TERNARY
BLENDS TOWARD INDUSTRIALIZATION

Highly tough poly(L-Lactide)-based ternary blends toward industrialization

INTRODUCTION

Nowadays, due to increasing environmental consciousness as well as more and more stringent regulations concerning the use of recyclable materials in cars, many R&D works aim to find sustainable alternatives to fossil based plastics. In that context, the use of PLA is undoubtedly appealing thanks to its high strength and rigidity. Today, PLA can already be found in a couple of non-technical automotive interior parts such as door trim [1], and its use should significantly increase in a near future. Contrary to non-technical interior parts, automotive technical exterior parts can be subjected to severe loading conditions, in terms of high strain rate, combined with harsh conditions of temperature, hygrometry, etc. Thereby, some PLA properties still have to be improved in order to compete with traditional petro-sourced polymers like mineral-filled polypropylene (PP) or acrylonitrile butadiene styrene (ABS)/polycarbonate (PC) blends. Indeed, PLA presents significant obstacles such as its brittleness, low thermal and hydrolysis resistance, impact strength and crystallization rate, impeding its use in parts subjected to severe loading and/or environmental conditions. In this respect and as shown in Chapter III, significantly improved thermal stability, evaluated in terms of heat deflection temperature (HDT), has been proven for PLA/poly(methyl methacrylate) (PMMA) blends depending on PMMA content, together with high miscibility and good aging behavior[2-6]. Based on those results, we developed ternary blends made of PLA/PMMA matrix in association with impact modifier Biomax® Strong 120 [2]. We have demonstrated in Chapter III that combining PLA/PMMA blend with Biomax® Strong 120 (BS) was a successful strategy to dramatically increase the ductility and the impact toughness of the material, thanks to the addition of the impact modifier, without altering the thermal properties of PLA/PMMA matrix. Several formulations of PLA/PMMA matrix in association with a constant content of impact modifier (17% of total weight) were characterized by means of mechanical, thermo-mechanical and morphological analyses. Good interfacial adhesion and coupling reactions in the melt-state were unveiled in PLA-rich formulations and correlated with excellent mechanical performances in terms of toughness and ductility. From these studies, the composition 58 wt% PLA-25 wt% PMMA-17 wt% BS (hereafter simply called PLA-PMMA-BS composition) was selected as the most promising one (see chapter III). Comparison of mechanical and thermal properties of

PLA-PMMA-BS composition with those of an ABS-PC blend, frequently used in automotive industry, revealed that this composition can be highly suitable for use in technical applications.

The current chapter will aim to investigate the performances of PLA-PMMA blends for automotive applications and, more generally when subjected to high loading rate under a wide range of temperature (typically -40°C to 80°C in automotive sector). This chapter focuses on the analysis of mechanical behavior of PLA-PMMA-BS composition over a wide range of loading rate, from quasi-static to dynamic loading conditions, at ambient and high temperature. In addition, dynamic mechanical behavior of PLA-PMMA-BS composition will be investigated over a wider range of temperature and frequencies.

An important step toward the industrialization of PLA based composition is to assess whether the material can be processed (extrusion followed by injection molding) at an “industrial scale” while keeping interesting thermomechanical properties. Indeed, reactive extrusion is obviously impacted by several parameters such as feeding rate, residence time, shearing in the melt (governed by screw profile and rotation speed, etc.). In the same way, mechanical and thermal properties of an injected part also depend on process parameters such as mold and melt temperature, injection pressure, cycle time, etc. In this study, some PLA-based compositions were here prepared using industrial type facilities for the extrusion and the injection molding phases (section V.1). Tensile tests under quasi-static loading conditions at ambient temperature were first performed in order to assess whether PLA-PMMA-BS samples produced in this industrial way present interesting mechanical properties in line with those of samples produced at “laboratory scale”. The next step is to verify that appealing properties of PLA-PMMA-BS compositions processed at laboratory scale are kept when the same material is processed using industrial facilities, i.e. as obtained using extrusion technology and subjected to more severe loading conditions (here in terms of high strain rate and high temperature). The resulting materials will be then investigated as technical parts subjected to high-strain-rate loadings and/or high temperature, typical of those encountered by technical exterior automotive parts, such as bumpers. Dynamic tensile tests, at high strain rate, are therefore performed (here at ambient temperature - section V.2), as well as quasi-static tensile tests at high temperature (50°C - section V.3). It is worth noting that, at authors’ knowledge, any PLA based composition have been never tested under high loading rate before. Dynamic mechanical analyses (i.e. loading/unloading cyclic tests) were also performed under a wide range of temperature and frequency (section V.4). In order to evaluate whether PLA-PMMA-BS blend can be a valuable alternative to classical petrosourced polymers for use in technical parts subjected to high loading rate and/or high temperature, mechanical properties of PLA based compositions, in

terms of tensile strength, rigidity, strain at break and volume energy of deformation and storage modulus (E'), are compared to those of an ABS/PC blend, being considered as a reference for use in automotive parts. Finally, durability of PLA based blends is studied under thermal aging (section V.5).

MATERIALS AND EXPERIMENTS

Materials

Commercial grade poly(L-lactide) 4032D, supplied by NatureWorks and hereafter called PLA, was used as received. Its principal characteristics are $\overline{M}_n = 133,500 \pm 5,000$ g/mol, $\overline{D} = 1.94 \pm 0.06$ (as determined by size-exclusion chromatography in chloroform at 35°C, upon a relative polystyrene calibration) and a D-isomer content of $1.4 \pm 0.2\%$ as determined by the supplier. Poly(methyl methacrylate), hereafter called PMMA, was supplied by Evonik, under commercial name Plexiglas[®] 8N. Its principal characteristics are $\overline{M}_n = 50,000 \pm 2,000$ g/mol and $\overline{D} = 2.1 \pm 0.1$.

Biomax[®] Strong 120, here after called BS, was provided by Dupont. Ultrinox[®] 626A (from GE Specialty Chemicals) was used as a stabilizer at a content of 0.3 wt % in all PLA-based blends. For comparative purposes, a commercial ABS/PC blend (Novodur[®] H801) designed for automotive interior and exterior parts, was supplied by Styrolution ($\overline{M}_n = 32,900 \pm 3,000$ g/mol and $\overline{D} = 3.4 \pm 0.1$).

Optimal Composition PLA-PMMA-BS

PLA-PMMA-BS compositions are developed in order to improve PLA impact toughness and ductility (thanks to the addition of BS) and thermal resistance (thanks to blending with PMMA), without altering too much the inherent high rigidity and strength of PLA.

In chapter III, the optimal composition of PLA-PMMA-BS has been determined, based on dynamic mechanical-thermal analyses (DMTA), Differential Scanning Calorimetry (DSC) analyses, tensile and notched impact tests. Polymeric components and additives were melt-blended in a Brabender internal mixer (model 50EHT; premixing at 30 rpm then 70 rpm) and samples were then prepared using a DSM Mini Injection Molding apparatus. As already mentioned, the composition 58 wt% PLA - 25 wt% PMMA - 17 wt% BS was selected as the one presenting the best compromise between impact toughness, tensile strength and rigidity, on

the one hand, and ductility and thermal properties (in terms of heat deflection temperature - HDT), on the other hand (see chapter III).

RESULTS AND DISCUSSIONS

V.1 Industrialization of Processes

As described in the previous section, preliminary characterizations and mechanical tests on PLA-PMMA-BS were performed on samples processed at “laboratory scale” (Brabender and DSM Mini Injection Molding apparatus). Yet, in order to evaluate the possibility to use this composition for industrial applications, it must be verified that it can be processed using industrial facilities while keeping mechanical properties satisfying. For the present chapter, the extrusion step was performed on an industrial extrusion device (Leistritz ZSE twin-screw co-rotating extruder). All compounds were blended together at different feeding rates and using different screw speeds in order to fit the feeding rate, following the temperature profile given in Table V.1. In order to select the most suitable screw speed and feeding rate, preliminary tests were conducted where both parameters varied simultaneously from 30 to 200 rpm and 0.6 to 4 kg.h⁻¹, respectively.

Table V.1 Temperature profile during extrusion of compounds

Distance in the barrel to feeding area	Set
0 to 90 mm	160°C
90 to 180 mm	190°C
180 to 270 mm	210°C
270 to 360 mm	210°C
360 to 450 mm	210°C
450 to 540 mm	210°C
540 to 630 mm	210°C
Die	190°C

Extruded materials were then injection molded to form impact specimens (mini injection molding apparatus) and the evolution of impact strength in function of the residence time was studied, as this parameter is likely able to affect impact strength. Indeed, we state out in chapter III that the good interfacial adhesion between the matrix PLA-PMMA and impact modifier, leading to a good impact strength, is due to the formation of “grafted copolymers”, acting as compatibilizers, through coupling reactions between the functional end-groups (hydroxyl and carboxylic groups) of PLA chains and the complementary functional groups (epoxy functions)

along the impact modifier. Yet, residence time can affect the formation of such grafted polymers, the morphology of compounds and so the toughness of blends.

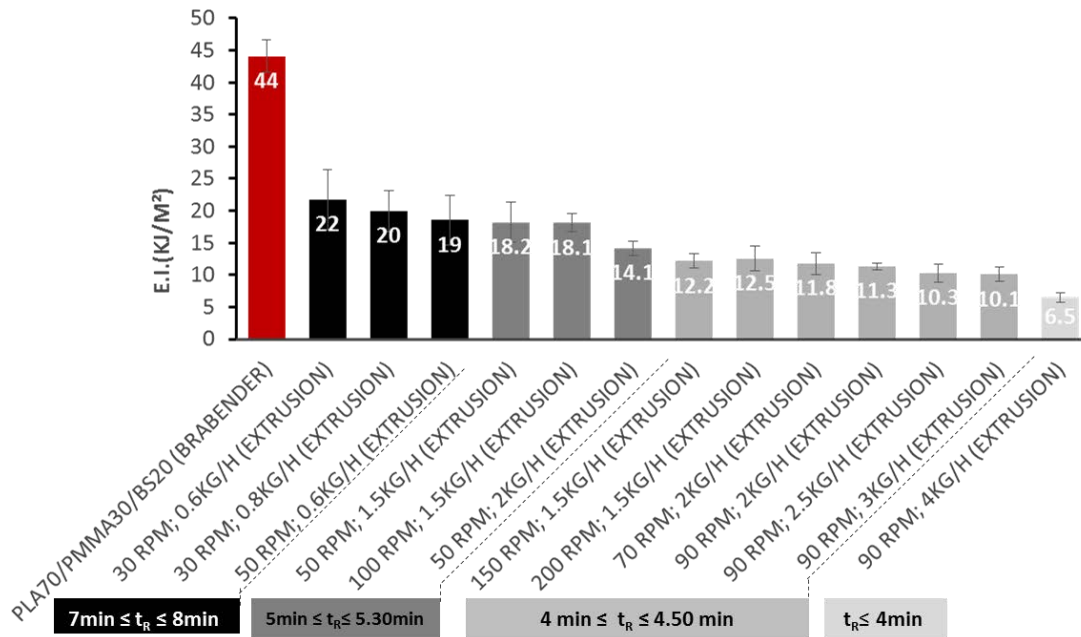


Figure V.1. Evolution of impact resistance of PLA70-PMMA30-BS20 blend in function of residence time in extruder

The evolution of impact strength of differently produced PLA-PMMA-BS compositions in function of the residence time of the blends during extrusion process is presented in Figure V.1. It shows that impact strength increases when increasing the residence time (t_r) in the extruder and specially with increasing the feeding rate (from 6.5 kJ/m² for less than 4 min to 18.2 kJ/m² for more than 5 min), which confirms that coupling reaction between PLA and impact modifier needs some time to be fully achieved. Moreover, the microstructure of rubber-toughened polymer is of prime importance on toughening mechanisms. This was highlighted by scanning electron microscopy (SEM) where the microdomain size and size distribution of the impact-fractured surfaces of specimens were estimated (Figure V.2 and V.3). Whereas the PLA-PMMA-BS extruded for a residence time (t_r) of 4.50 min (1.5 kg/h; 200 rpm) shows dispersed microdomains characterized by an average diameter of about 1.15 μm (Figure V.2.b and V.3), different distribution of micodomains were observed for the PLA-PMMA-BS extruded for $t_r = 5.30$ min (1.5 kg/h; 50 rpm) with a mean diameter for the dispersed microdomains of about 0.85 μm (Figure V.2.a and V.3). The difference may explain the increase of impact strength when increasing the residence time. With a longer residence time, the fractured surface of the blends presents an optimum range of size distribution and regularity of the size of microdomains leading to a higher impact strength.

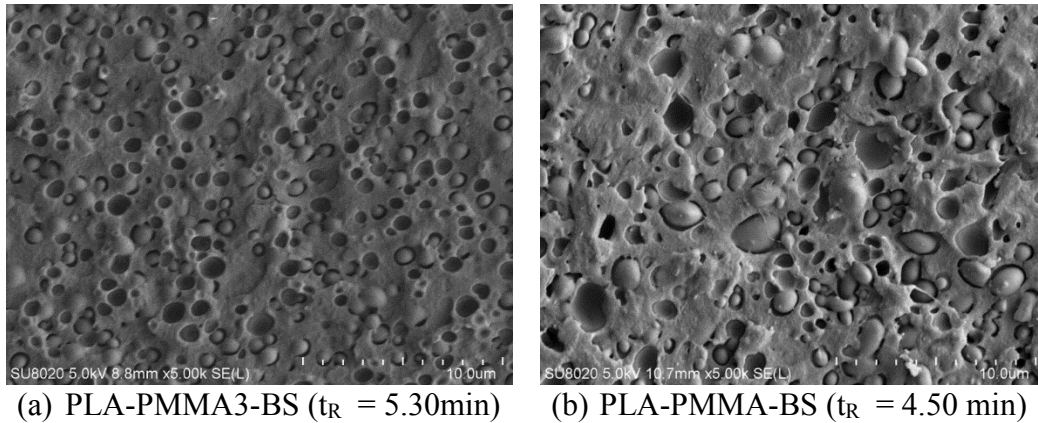


Figure V.2. SEM micrographs of impact-fractured surfaces of PLA-PMMA-BS blends

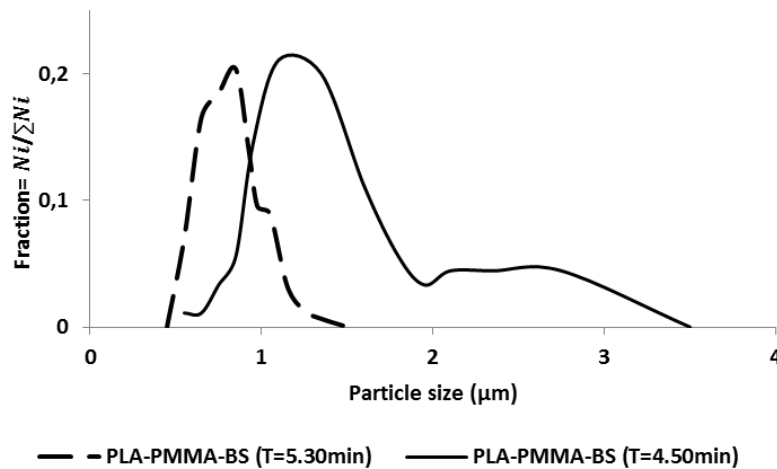


Figure V.3. Associated size distributions of the rubbery BS for PLA-PMMA/BS blends with different process parameters

The most suitable extrusion parameters, 1.5 kg/h for feeding rate and screw speed of 50 rpm, were thus selected in the subsequent part of the part, leading to the highest notched impact toughness (18.2 kJ/m^2). It is worth noting that the lowest feeding rates ($< 1 \text{ kg/h}$) were not taken into account since they are unsuitable for mass production. Moreover, this optimal value of impact toughness decreased drastically compared to the impact toughness of the material prepared at lab scale by Brabender (44 kJ/m^2) (Figure V.1). It may be explained by the significant reduction of the residence time (5 min against 10 min) that may prevent the full achievement of as-formed graft copolymers (in terms of PLA-BS bonding, e.g.). In any case, sensitivity of impact toughness to process parameters was evidenced, thus reinforcing the need for studying material properties based on industrially manufactured samples. For comparative purposes, the same extrusion parameters were applied when processing PLA-BS.

After extrusion, PLA-based materials were cut into pellets and conditioned into hermetically closed bags. Pellets of extruded PLA-based compositions and of as-received ABS-

PC were then conditioned for 24h at 50°C (uncontrolled ambient hygrometry). They were then injection molded into rectangular thin plates (dimensions of about 96*166 mm², thickness of 3 mm) using facilities of Reydel, an automotive supplier. During injection process, melt and mold temperature were respectively of 210°C and 40°C for PLA-PMMA-BS, 210°C and 45°C for PLA-BS, and 250°C and 80°C for ABS-PC (following the recommendation of the supplier).

V.2 Quasi-Static and Dynamic Tensile Tests at ambient temperature:

To judge about the relevance of using PLA-PMMA-BS composition for the manufacturing of technical parts subjected to high-strain-rate loadings, it is crucial to study its tensile behavior under a wide range of strain-rate. As mentioned in section V.1, behavior of ABS-PC will be taken as a reference, since this material shows high strength, rigidity and energy of deformation, even under high strain rate. It is therefore commonly used in technical parts, in particular in automotive industry. For comparative purposes, tests are also performed on PLA-BS blend. All the following information is common to tensile tests of all materials. Tensile specimens were cut by water jet on the injected plates.

Quasi-static tensile tests are performed at room temperature using Instron E3000 electromagnetic jack (3 kN load cell sensor). The geometry of quasi-static tensile specimens follows ISO527 norm (Figure V.4a), with a cross-section of about 13 mm². Quasi-static tests are carried out at displacement rates of 1, 10 and 100 mm.min⁻¹. Those displacement rates correspond to average strain rates of about $5.55 \cdot 10^{-4}$, $5.55 \cdot 10^{-3}$ and $5.55 \cdot 10^{-2} \text{ s}^{-1}$, respectively, since the region of interest (ROI) is 30 mm high. Five tests per displacement rate are performed. Dynamic tensile tests are carried out at room temperature using Instron 65/20 hydraulic jack (i.e. 65 kN load cell sensor, maximum speed 20 m.s⁻¹). For the present tests on polymeric materials, a piezoelectric load cell sensor, calibrated in the range 0-5kN, with a precision of 2.5 N, is fixed on the rigid frame of the jack. A specific set-up for dynamic test, developed at LAMIH, is used to clamp the specimen. This set-up allows in particular reducing device resonance during high speed tests and ensuring that specimen loading does not begin before imposed test velocity is achieved and stabilized. Geometry of dynamic tensile specimens is specially designed according to this set-up (Figure V.4b). Length of the ROI is reduced to 20 mm instead of 30 mm for quasi-static tensile specimens in order to reach higher strain rates. Displacement rates of 100 and 1000 mm.s⁻¹ are imposed (average strain rate of about 5 and 50 s⁻¹). At least 5 tests per displacement rate are performed.

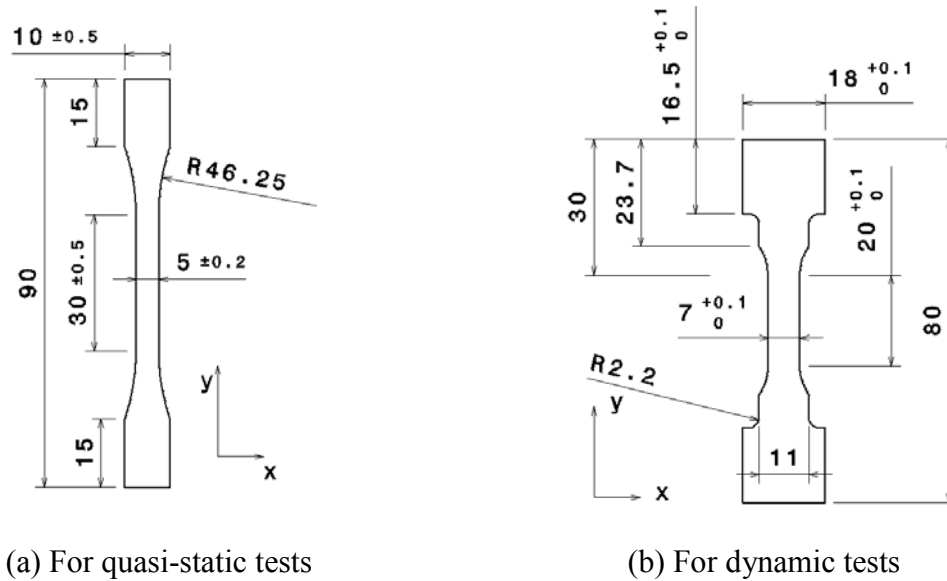


Figure V.4. Geometry of specimens for tensile tests (in mm)

In both quasi-static and dynamic tensile tests, the nominal axial stress, σ , is computed by the ratio of the load that is applied to the specimen, F , (measured by load cell sensor) by the initial cross-section area of the specimen, S_0 , so that $\sigma = F/S_0$. True in-plane strains are computed from displacement field measurements by digital image correlation (DIC) [7]. A random pattern is created on the whole specimen ROI by applying sprays of black paint after specimen surface is painted in white. Grayscale images of the pattern are recorded throughout the loading, at constant time interval (Table V.2), by a camera. For DIC analysis, a reference image is chosen for each tensile test as the last one recorded at a non-deformed stage, i.e. just before load is applied to the specimen. Sets of image are then analyzed using a DIC Software (VIC2D software here). First, the random pattern of the reference image is divided into square facets, of a few pixels size, each of them being characterized by a unique signature in gray level (Figure V.5). This unique signature allows the tracking of facets by DIC software, using a correlation algorithm between each image, recorded at a given instant of loading, and the reference image. This way, in-plane displacements of all facet centers, with respect to the reference image, are determined. In plane strains are finally computed at the center of each facet by spatial derivation.

It is worth noting that the size of facets has an influence on the signal/noise ratio and therefore on the accuracy of strain computation. In a few words, noise level tends to increase when the facet size decreases. Yet, because strains are averaged over the facet size, a too high size of facet leads to an inaccurate strain computation in case of high strain gradient. To analyze the sensitivity of the signal/noise ratio to size of facets for the current experiments, rigid body

motion tests were performed prior to tensile tests, at all the investigated displacement rates. Rigid body motion does not generate any strain in the specimen. The “strains” that are computed by DIC in that case are therefore representative of the noise level. For both quasi-static and dynamic tests, size of facets of 15x15, 17x17, 19x19 and 21x21 pix² were tested.

Noise levels were similar for all components (i.e. axial, transverse and shear “strain”) for all facet sizes, for rigid body motions recorded at all displacement rates. Therefore, the lowest facet size of 15x15 pix² was selected, with a step size (distance between two consecutive points of measurement) equal to 7 pixels, for the analysis of all quasi-static and dynamic tests. It can be noted that a distance of 7 pixels on recorded images corresponds to an actual distance of 435 and 437 μm on the specimen during quasi-static and dynamic tests, respectively. Technical information about tensile tests is given in Table V.2.

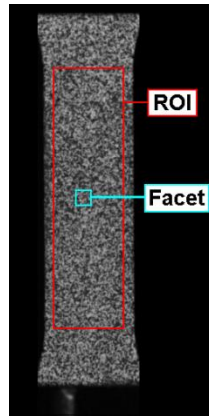


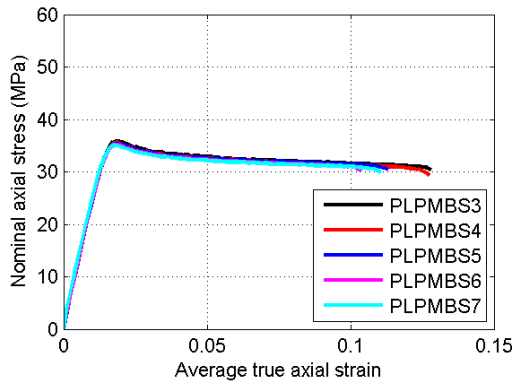
Figure V.5. Black and white pattern for DIC tracking (example of dynamic specimen of PLA-PMMA-BS before loading)

Table V.2. Tensile tests specifications

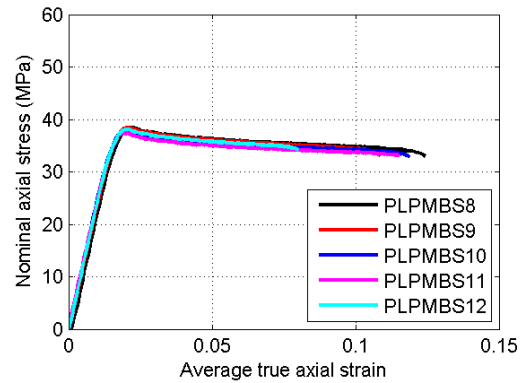
Displacement rate	Engineering strain-rate (s ⁻¹)	Load frequency of acquisition (Hz)	Camera frame rate (fps)
1 mm.min ⁻¹	5.55 10 ⁻⁴	50	1
10 mm.min ⁻¹	5.55 10 ⁻³	500	5
100 mm.min ⁻¹	5.55 10 ⁻²	2000	15
100 mm.s ⁻¹	5	100000	6000
1 m.s ⁻¹	50	1000000	22500

Up to now, dynamic tensile tests were never performed on any PLA-based composition. The material capacity to bear high strain-rate loadings therefore remains unknown. In that framework, the present tensile tests provide very insightful results. Indeed, PLA-based

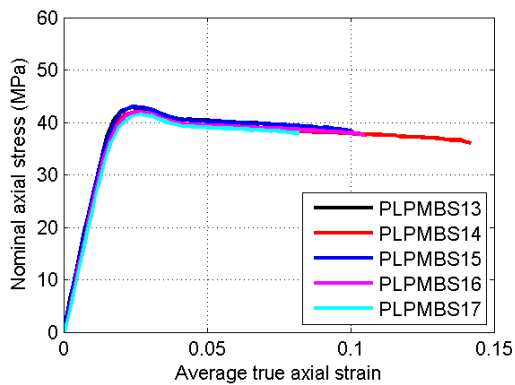
compositions show high stress levels, at all displacement rates, including dynamic ones, together with high levels of ductility (Figure V.6 and V.7). In addition, the reproducibility of tensile behavior is excellent at all test speeds, thus making results trustworthy and indicating a good homogeneity of material properties in injected plates. Tensile behavior of PLA-based compositions is compared to that of ABS-PC in Figure V.8. Since the behavior of the three materials showed good repeatability, a curve per test speed, arbitrarily chosen among available data, is represented for each material (i.e. these are not average curves).



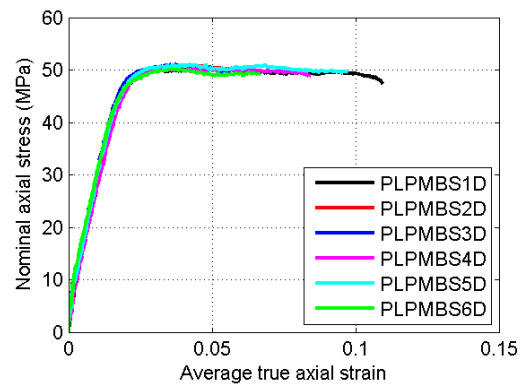
(a) 1 mm/min



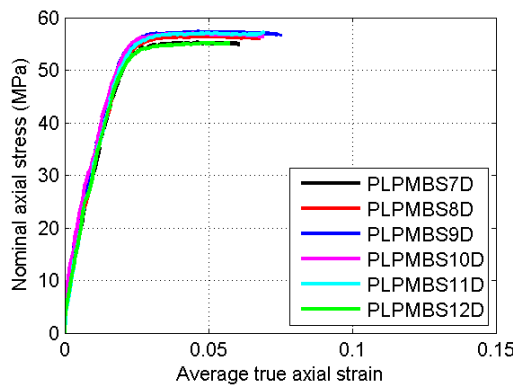
(b) 10 mm/min



(c) 100 mm/min



(d) 100 mm/s



(e) 1 m/s

Figure V.6. Quasi-static and dynamic tensile behavior of composition PLA-PMMA-BS

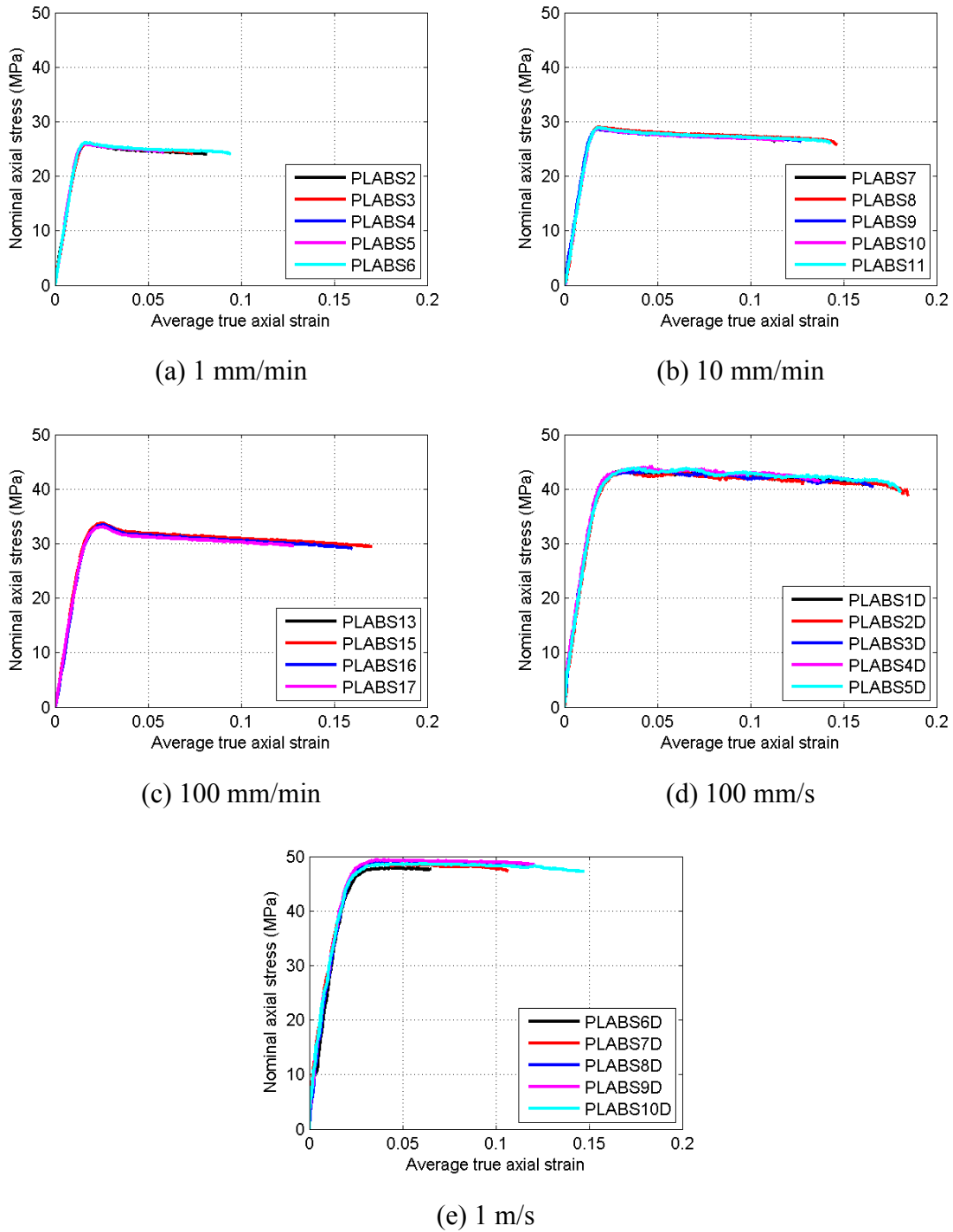


Figure V.7. Quasi-static and dynamic tensile behavior of composition PLA-BS

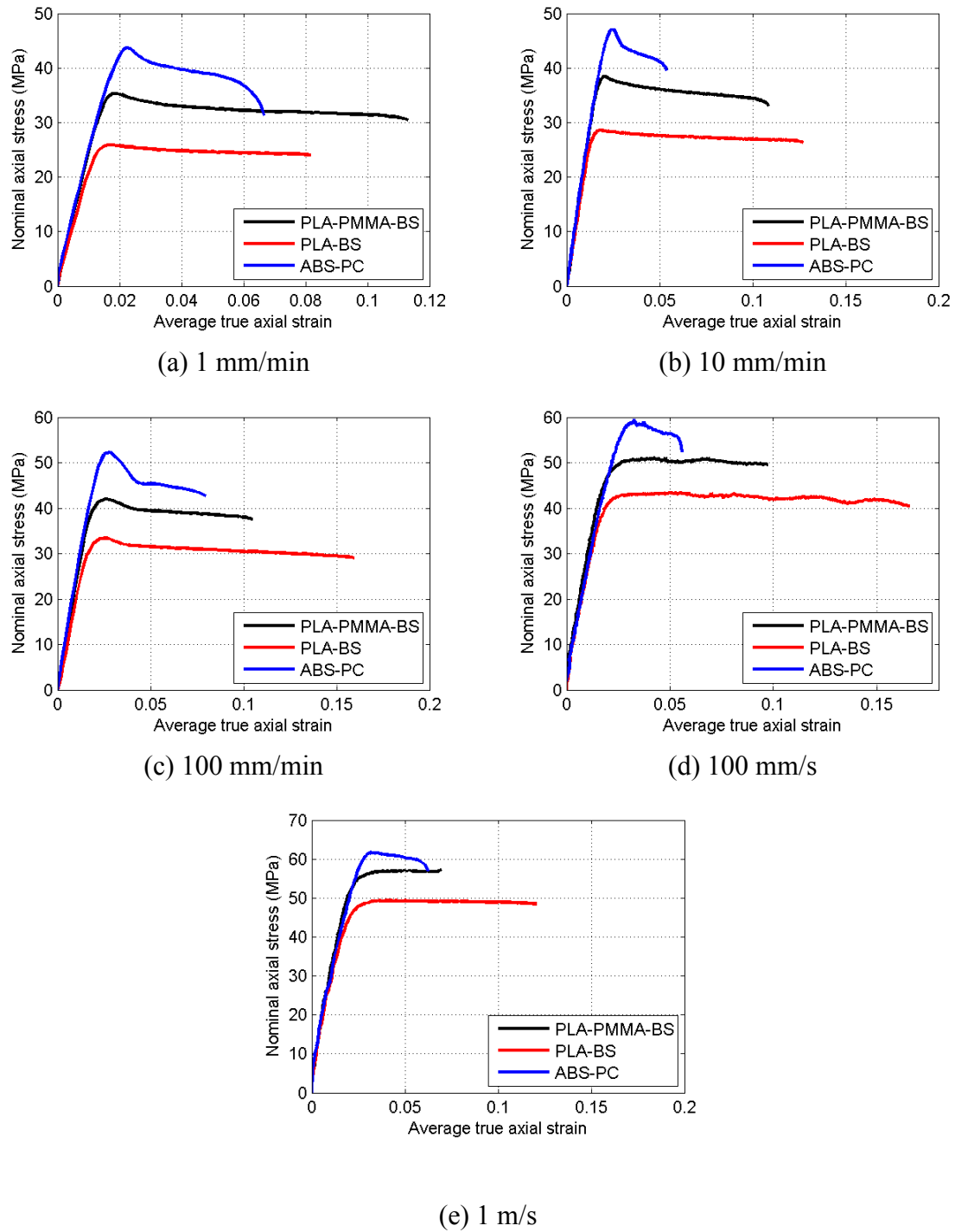


Figure V.8. Comparison of tensile behavior of PLA-PMMA-BS, PLA-BS and ABS-PC

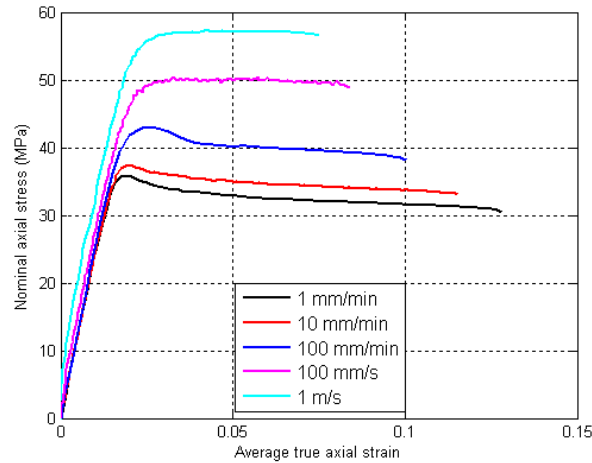


Figure V.9. Comparison of tensile behavior of PLA-PMMA-BS at different tensile displacement rate

In order to compute the elastic modulus, a linear regression is applied to the initial linear part of the behavior curve, i.e. nominal axial stress vs. average axial strain, for values of average axial strain varying from 0 to 1%. The average axial strain is the average of true axial strain computed for all the facets in specimen's ROI. It can be noticed that the true axial strain remained homogeneous over the whole specimen's ROI (i.e. approximately same values in all facets) at least up to value of 1%, for all materials and all test speeds. Therefore, the elastic modulus that is calculated with the average axial strain is actually representative of the actual Young modulus of the material.

The Figure V.9 shows the strain-rate dependency of tensile behavior of PLA-PMMA-BS. It can be noted that the tensile strength is multiplied by 1.59 while the strain at break is divided by 1.7 when the engineering strain rate is multiplied by 90 000 (i.e. from displacement rates of 1 mm/min to 1 m/s).

Elastic modulus, maximal axial stress and average true axial strain at break of all materials can be compared in Figure V.10. In that Figure, crosses indicate mean value and vertical lines (ended by points) indicate standard deviations. Detailed results of tensile tests are given in Appendix (Table A1 to A3). Average true axial strain at break is the average of true axial strain computed in all facets of the ROI when rupture occurs (i.e. in the last step of loading). PLA-PMMA-BS presents high value of elastic modulus (about 2.5 GPa in quasi-static loading rates, i.e. from 1 to 100 mm/min, up to about 2.75 GPa at 100 mm.s⁻¹ and 2.9 GPa at 1 m.s⁻¹ - Figure V.10a). These values are similar to those of ABS-PC up to displacement rate of 100 mm.min⁻¹ and higher in dynamic tests (2.75 GPa in average against 2.55 GPa at 100 mm.s⁻¹ and 2.9 GPa against 2.8 GPa at 1 m.s⁻¹). Interestingly, elastic modulus of PLA-PMMA-BS is always higher than that of PLA-BS. Blending PLA with PMMA has therefore a positive effect not only on the

heat resistance of the composition as mentioned in chapter III but also on its rigidity. As expected, axial stress level of all materials increases with test speed because of viscous overstress [8] (Figure V.8 and V.10b). ABS-PC presents the highest tensile strength, followed by PLA-PMMA-BS and PLA-BS, at all test speeds. Finally, average true axial strain at break of PLA-PMMA-BS is always higher than that of ABS-PC including the dynamic range of loading (Figure V.10c). These results confirm the positive influence of the addition of impact modifier BS on PLA ductility, already observed in previous chapters and other studies for quasi-static tensile loadings [9,2]. In addition, efficiency of impact modifier is also demonstrated for high-strain-rate loadings. Compared to binary composition PLA-BS, the addition of PMMA leads to a decrease of strain at break. It is likely to be due to weaker interfacial strength between droplets of BS and PMMA than between BS and PLA. Surprisingly, strain at break of PLA-BS globally increases with the test speed. SEM observations performed on broken specimens of PLA-BS did not reveal significant difference depending on test speeds and this trend remains unexplained at the moment.

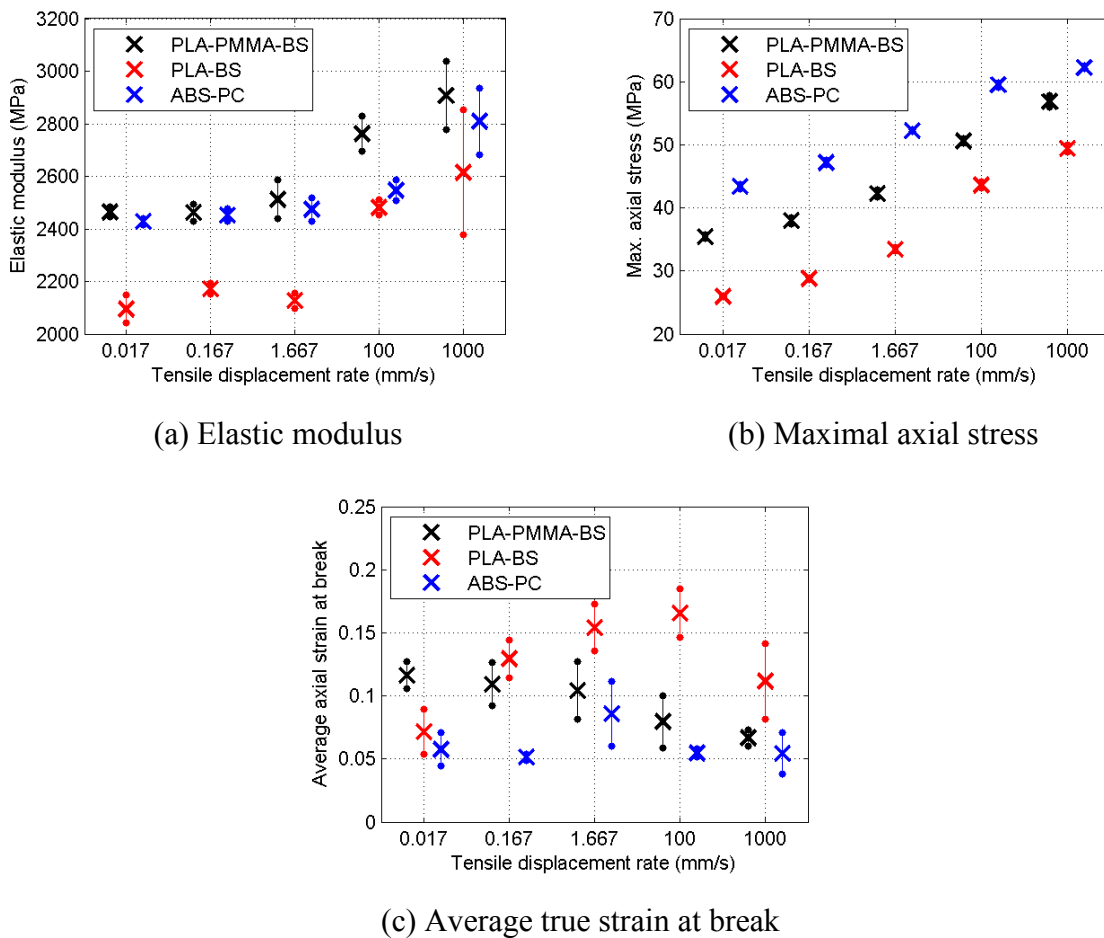


Figure V.10. Tensile properties of PLA-PMMA-BS, PLA-BS and ABS-PC

PLA-PMMA-BS therefore presents appealing tensile properties in quasi-static and dynamic conditions of loading. Comparison with properties of ABS-PC, considered as a reference material for use in technical automotive parts, suggests that this partially-biosourced composition can be suitable for use in technical parts.

However, the simple evaluation of maximal tensile stress and elongation at break is not sufficient in order to assess whether a material can be suitable for use in technical parts subjected to severe loading condition. Indeed, a material must also present a high capacity of energy absorption upon deformation. In fact, if low tensile stress and strain at break are actually prohibitive properties, high values of those parameters do not systematically ensure a high energy of deformation. Indeed, it is not rare that a polymer presents a marked yield peak followed by a significant drop in tensile stress resulting in a post-yield elongation at low stress level [9]. In that case, the polymer is characterized by a high maximal stress and possibly by a high elongation at break but its energy of deformation is quite low. To definitively judge about the potential of PLA-based compositions, their energy of deformation is therefore compared to that of ABS-PC. Volume energy of deformation, E , is computed using Equation (1):

$$E = \int_{\varepsilon=0}^{\varepsilon_{\max}} \sigma d\varepsilon \quad (1)$$

where σ is the nominal axial stress, ε the average true axial strain and ε_{\max} the average true axial strain at break.

The comparison of volume energy of deformation (Figure V.11) definitively confirms that the composition PLA-PMMA-BS is suitable for use in technical parts, even for high-strain-rate loadings. Indeed, capacity of energy absorption of that composition is always higher than that of ABS-PC, from quasi-static to dynamic range of loading speed, although tensile strength of ABS-PC is superior (Figure V.10b). Interestingly, volume deformation energy of PLA-PMMA-BS remains almost constant whichever the test speed, since the decrease of strain at break is offset by the increase in tensile strength. On the contrary, volume deformation energy of PLA-BS globally increases with the test speed, due to the above-mentioned unexplained increase of PLA-BS strain at break (Figure V.10c).

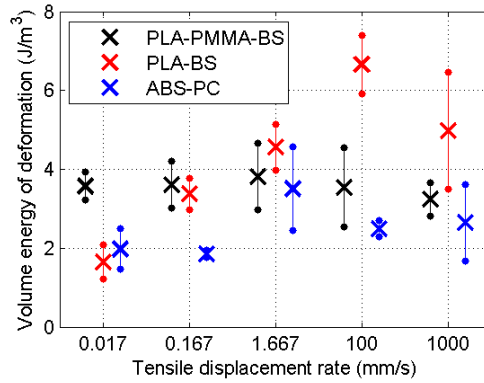
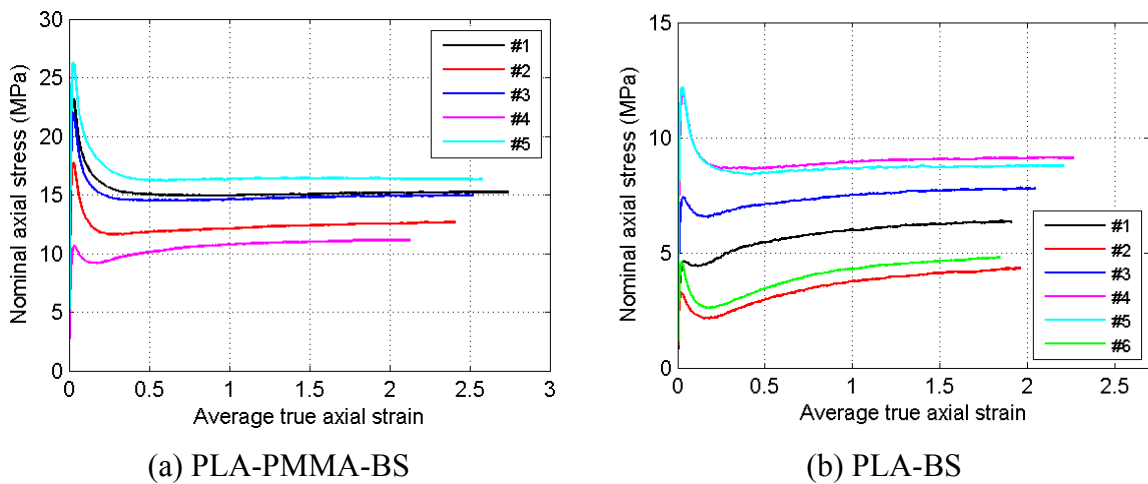
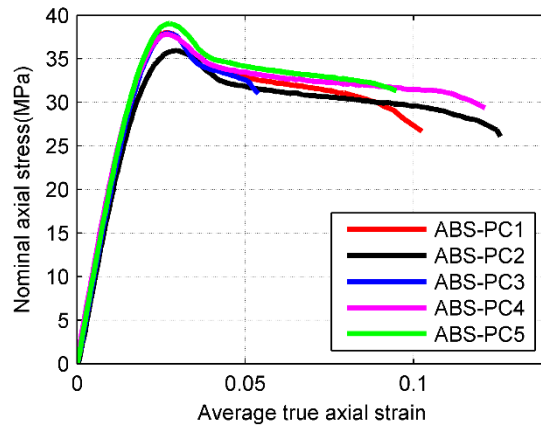


Figure V.11. Volume energy of deformation of PLA-PMMA-BS, PLA-BS and ABS-PC

V.3 Quasi-static tensile tests at high temperature:

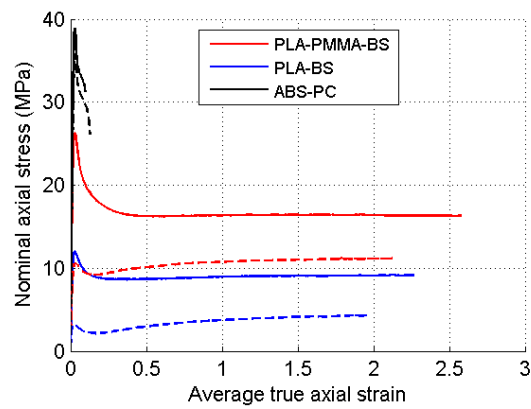
Strain rate and temperature are known to significantly influence the mechanical behavior of polymers. While numerous studies have investigated the influence of strain rate on the constitutive response for several polymers at room temperature [10,11], the influence of temperature on mechanical tensile properties has received much less attention. In the present section, the effect of temperature on the mechanical response of three different compounds was studied. Quasi-static tests were carried out at displacement rates of $10 \text{ mm}\cdot\text{min}^{-1}$ at 50°C (temperature was checked using a non-contact IR thermometer before starting each test). It is noteworthy that during those quasi-static tensile tests at 50°C , both PLA-PMMA-BS and PLA-BS specimens reached the limit of displacement of tensile device without breaking of the sample (except specimen PLPMBS1 due to the presence of a defect on the specimen). Therefore the data represented in stress-strain curves for PLA/PMMA/BS and PLA/BS are limited to the elongation reached at the limit of machine stroke (Figure V.12 a and b).





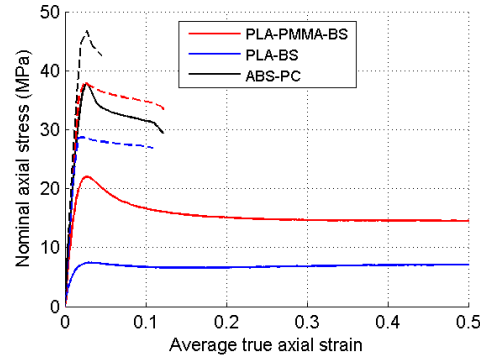
(c) ABS-PC

Figure V.12. Quasi-static behavior of composition ($10\text{mm}\cdot\text{min}^{-1}$) at 50°C



Comparison of tensile behavior of PLA-PMMA-BS, PLA-BS and ABS-PC at 10 mm/min and 50°C (continuous lines: upper bounds of behavior curves; dashed lines: lower bounds)

(a)



Comparison of tensile behavior of PLA-based compositions and ABS-PC at ambient temperature (dashed lines) and 50°C (continuous lines) - 10 mm/min (b)

Figure V.13. Tensile properties of PLA-PMMA-BS, PLA-BS and ABS-PC

PLA-based compositions show high levels of ductility with variable values of tensile strength and rigidity (Figure V.12 a and b). Contrary to the very good reproducibility observed during quasi-static and dynamic tensile tests at ambient temperature, a noticeable variation in the stress–strain curves with variable values of rigidity and yield stress was observed for quasi-static tensile tests at 50°C for both PLA-BS and PLA-PMMA-BS blends (Figure V.12 a and b). In contrast, tensile behavior at 50°C of petro-sourced ABS-PC blend showed low dispersion.

This can be explained by the variation of crystallinity ratio between different samples after heating samples at 50°C (samples with higher crystallinity ratio around 21% present better mechanical properties than samples with lower crystallinity ratio around 17% in quasi-static tensile tests at 50°C).

Table V.3 Tensile properties of PLA-PMMA-BS, PLA-BS and ABS-PC at 10 mm/min, ambient temperature and 50°C (mean \pm standard deviation)

	Temperature	PLA-PMMA-BS	PLA-BS	ABS/PC
Elastic modulus (GPa)	Ambient	2.46 \pm 0.03	2.17 \pm 0.02	2.45 \pm 0.02
	50°C	1.32 \pm 0.38	0.57 \pm 0.27	2.06 \pm 0.05
Maximal stress (MPa)	Ambient	38.0 \pm 0.4	28.8 \pm 0.1	47.1 \pm 0.4
	50°C	20.1 \pm 5.8	7.97 \pm 3.5	37.8 \pm 1.1
Strain at break ^(a)	Ambient	0.109 \pm 0.017	0.129 \pm 0.015	0.052 \pm 0.002
	50°C	Unconcerned	Unconcerned	0.010 \pm 0.029
Volume energy of deformation (mJ/mm ³) ^(b)	Ambient	3.61 \pm 0.59	3.38 \pm 0.40	1.85 \pm 0.09
	50°C	> 29.6 ^(c)	> 12.3 ^(c)	2.99 \pm 0.87

(a) Average of the true axial strains computed by DIC in all facets of specimen ROI at specimen failure.

(b) Volume energy of deformation, e , is defined by $e = \int_{\varepsilon=0}^{\varepsilon_{\max}} \sigma d\varepsilon$ where σ is the nominal axial stress, ε the average true axial strain and ε_{\max} the average true axial strain at break or at the end of test in case of unbroken specimens.

(c) Minimum value attainable because e is computed on unbroken specimens. Given value is the average of all tests.

Tensile behavior of PLA-based compositions at high temperature is compared to that of ABS-PC in Figure V.13. Influence of temperature on elastic modulus and maximal axial stress can be compared in Figure V.13 b and Table V.3. As expected, tensile properties of ABS-PC were slightly affected by the increase of test temperature, thanks to high thermal properties (glass transition temperature of about 125°C and HDT A and B of 99°C and 106°C according to supplier's technical data sheet). Thus, elastic modulus and tensile strength were only divided by a factor 1.19 and 1.2, respectively, between tests at ambient temperature and 50°C. In contrast, properties of PLA-based compositions were significantly affected by the increase of test temperature. Thus, average values of elastic modulus and yield stress of PLA-BS were respectively divided by 3.8 and 3.6. Thanks to the presence of PMMA, these ratios were lower for PLA-PMMA-BS (1.9 for both elastic modulus and yield stress based on average values).

These drops in elastic modulus and tensile stress were directly related to the proximity between glass transition temperature, T_g , of PLA-based compositions (respectively 61.6°C and 62.8°C for PLA-BS and PLA-PMMA-BS following our DSC analyses [Chapter III]) and test temperature. Indeed, the evolution of tensile behavior was characteristic of a transition to rubber behavior with drop in rigidity and strength and spectacular increase of elongation at break. However, it is to note that the addition of PMMA was undoubtedly beneficial for behavior of PLA-PMMA-BS, compared to PLA-BS (Figure V.13b), even if the gain in T_g was quite low (1.2°C). Indeed, PLA-PMMA-BS showed satisfactory properties at 50°C, with rigidity and strength of same order of magnitude of those of a mineral-filled polypropylene [12], for instance, and very high volume energy of deformation, at least of 29.6 mJ/mm³ (minimum attainable value because this figure was computed based on behavior curve of unbroken specimens), to be compared to an average value of about 3 mJ/mm³ for ABS-PC. At the contrary, properties of PLA-BS tested at 50°C were prohibitive for use in technical parts.

V.4 Dynamic mechanical analysis of PLA based materials

Dynamic mechanical analysis (DMA) has been widely employed for investigating viscoelastic behavior of polymeric materials and determining storage and loss modulus and damping characteristics [13,14]. In that work, Instron device Electro Pulse E3000 was employed for dynamic mechanical analysis of the materials. The experiment was performed under cyclic tensile mode with rectangular DMA specimens ($50 \times 10 \times 2.5 \text{ mm}^3$) at a frequency varying from 0.01 to 30 Hz at different temperatures (Table V.4).

Table V.4 DMA tests specifications.

Temperature	20°C	40°C	50°C	60°C
Frequency	(3 tests)	(2tests)	(2 tests)	(2 tests)
Phase 1		3 cycles at 10^{-2} Hz		
Phase 2		3 cycles at $5 \cdot 10^{-2}$ Hz 5 cycles at 0.25 Hz 7 cycles at 0.5 Hz 20 cycles at 1 Hz		
Phase3		100 cycles at 10 Hz 300 cycles at 20 Hz 500 cycles at 30 Hz		

V.4.1 Evolution of dynamic mechanical properties of PLA-PMMA-BS as a function of frequency for all test temperatures

The storage modulus (E'), loss modulus (E'') and $\tan(\delta)$ peaks were determined following dynamic mechanical analyses for PLA based blends and ABS/PC blends. Evolution of dynamic mechanical properties of PLA/PMMA/BS blends are presented in this section for different temperature (from 20 to 60°C, Figure V.13) followed by a comparison with dynamic behavior of PLA-BS and ABS-PC blends.

The storage modulus (E'), loss modulus (E'') and $\tan(\delta)$ peaks have been found to be affected by frequency. The viscoelastic properties of a material are dependent on temperature, time and frequency. If a material is subjected to a constant stress, its elastic modulus will decrease over a period of time. This is due to the fact that the material undergoes molecular rearrangement in an attempt to minimize the localized stresses. Modulus measurements performed over a short time (high frequency) result thus in higher values whereas measurements taken over long times (low frequency) result in lower values [15]. The variation of PLA-PMMA-BS storage modulus with frequency is shown in Figure V.14 a. Increasing frequency has been found to increase the storage modulus value for all test temperature. PLA-PMMA-BS blends present a good thermal stability up to 50°C. At 60 °C and at low frequency,

the material presents a low storage modulus (Figure V.14 a), indicating the vicinity of glass transition temperature. While the loss modulus decreases when increasing frequency at 20°C, 40°C and 50°C, this latter increases when increasing frequency at 60°C (Figure V.14 b). This may be due to a promoted relaxation of polymer molecular chain when it is deformed close to its glass transition temperature ($T_g = 63^\circ\text{C}$), which leads to more pronounced viscous effects in the of the sample. The same trend was observed for PLA-BS but not for ABS-PC, due to higher glass transition temperature (See Appendix A1)). The $\tan \delta$ values measured over a range of frequencies for PLA-PMMA-BS samples are shown in Figure V.14 c. At low frequency, curve of $\tan(\delta)$ shows a peak, which confirms the proximity of T_g for PLA-based blends.

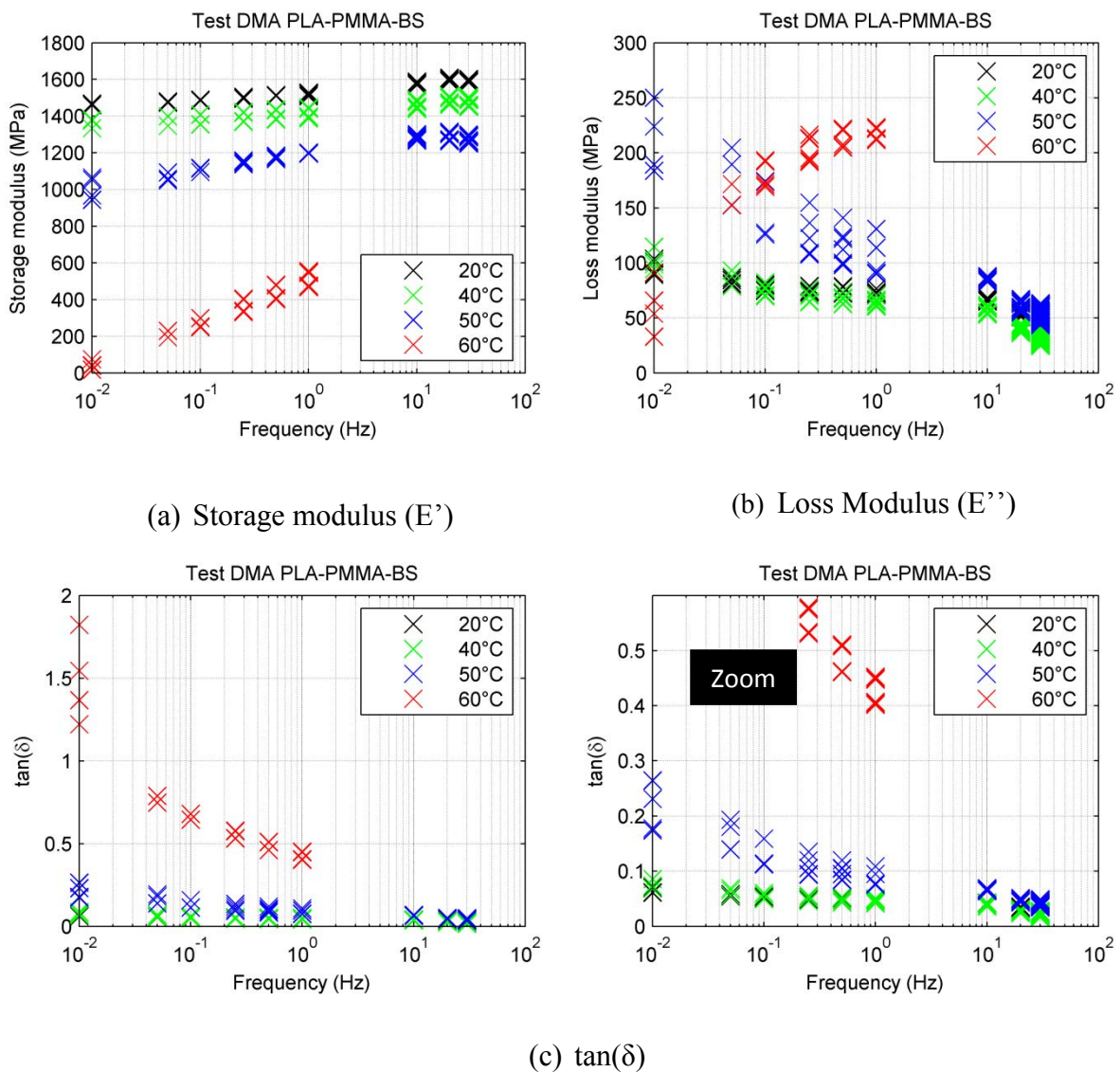


Figure V.14. Viscoelastic parameters of PLA-PMMA-BS blend

V.4.2 Comparison of PLA/PMMA/BS blends with PLA/BS blends

In the same manner and in order to compare dynamic mechanical properties of PLA-PMMA-BS and PLA-BS, the evolution of the storage modulus (E') and $\tan(\delta)$ with loading frequency, at different temperatures, is plotted in Figure V.15.

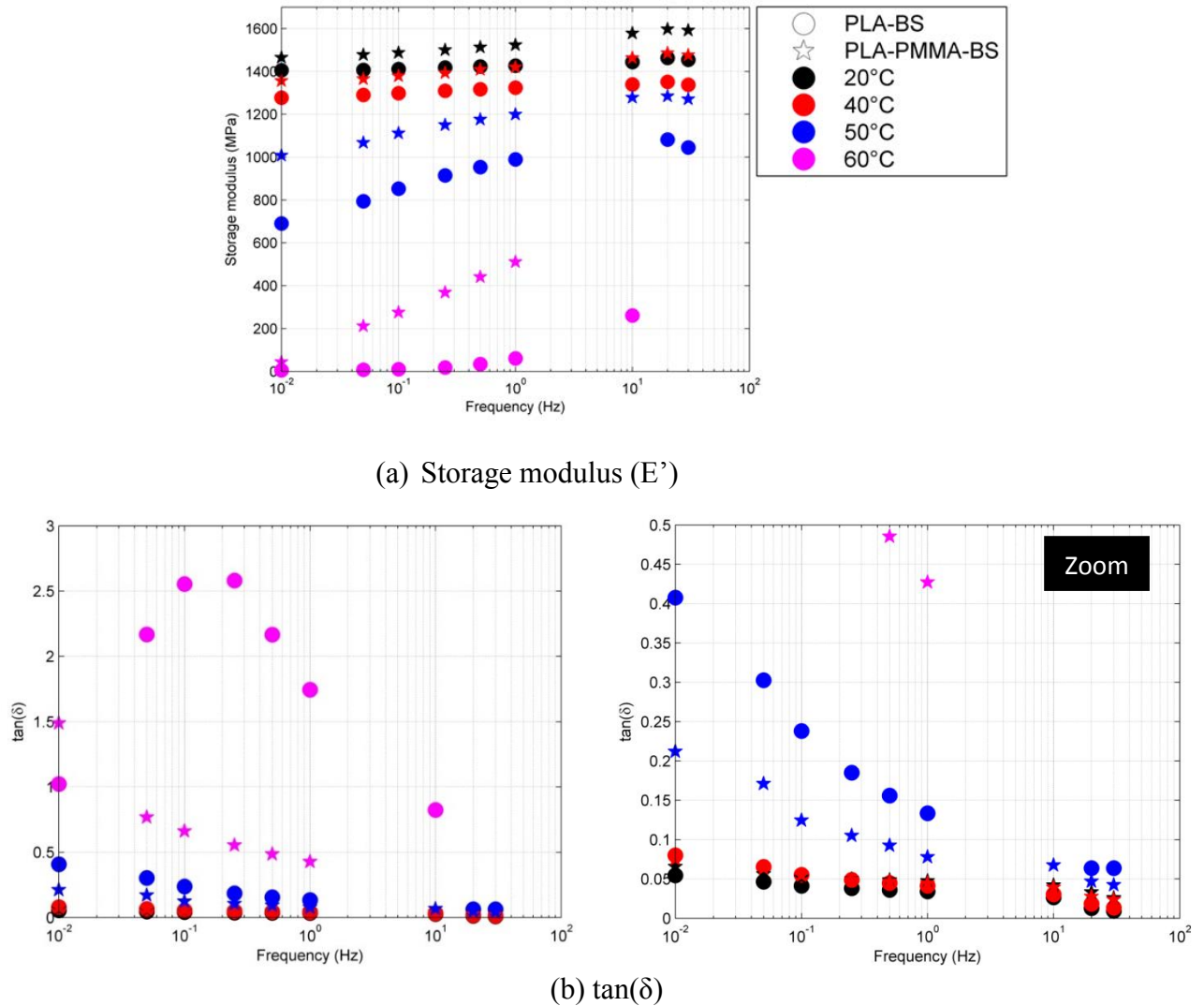


Figure V.15. Dynamic mechanical properties of PLA-PMMA-BS and PLA-BS

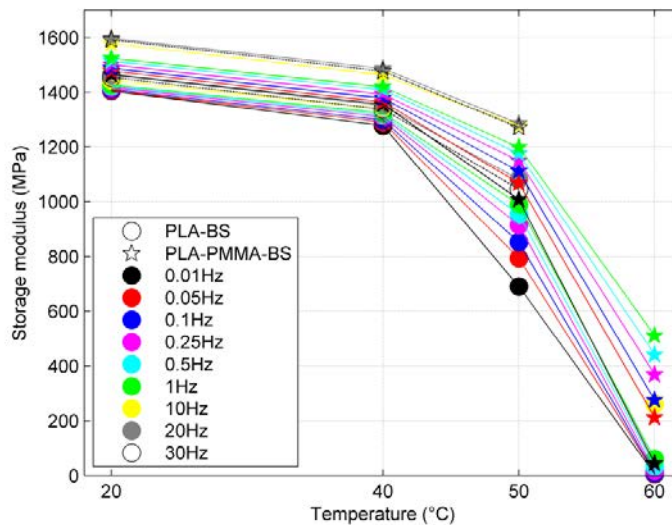
A dramatic drop of storage modulus of PLA-BS blend at 60°C can be observed. Moreover, at 30Hz, it was impossible to maintain the effort at 60°C because of the rubbery behavior of that blend, which led to the buckling of sample whereas it was not the case for PLA-PMMA-BS composition (Figure V.16). For PLA-PMMA-BS blend, the drop of storage modulus was slightly less pronounced except for low frequencies (Figure V.15 a). This can be explained by the fact that an increase of test frequency is equivalent to a decrease of the

temperature "felt" by the material. Then, material behavior is equivalent to the one that could be observed at a temperature below the T_g . Figure V.15 b reveals the presence of a peak of $\tan(\delta)$ for PLA-BS blend localized between 0.1 Hz and 1Hz, which is consistent with the rubbery behavior observed during cyclic tests at high temperature at those frequencies. The peak of $\tan(\delta)$ of PLA-PMMA-BS blends is apparently shifted to lower frequency, indicating a higher T_g .

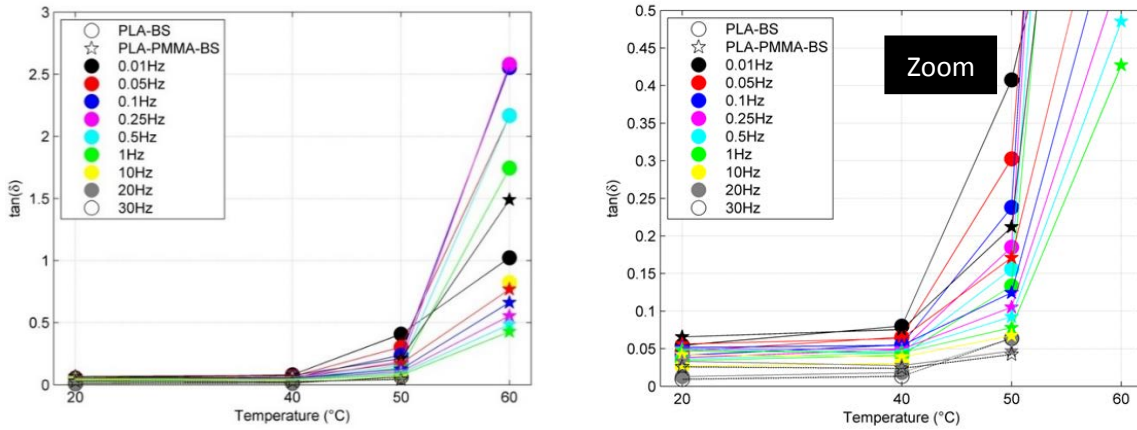


Figure V.16. Buckling of PLA-BS blend during DMA test at 30 Hz and 60 °C

The same results will then presented in other curves showing the storage modulus (E') and $\tan(\delta)$ as a function of temperature at different frequencies (Figure V.17). For all test frequencies, a significant drop in storage modulus (E') is observed when increasing temperature for both PLA-BS and PLA-PMMA-BS blends. However, the drop of E' of PLA-PMMA-BS at high frequency was less pronounced, which suggests again that that material has a higher T_g than PLA-BS.



(a) Storage modulus (E')



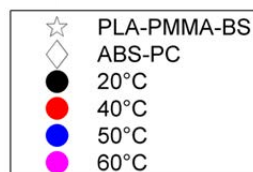
(b) $\tan(\delta)$

Figure V.17. Dynamic mechanical properties of PLA-PMMA-BS and PLA-BS

As a conclusion, the storage modulus of PLA-PMMA-BS is superior to that of PLA-BS, over all frequencies and all temperatures investigated. These results confirm the positive role played by the PMMA on the thermal stability of the material. The peak of $\tan(\delta)$ is absent or starting at lower frequencies for PLA-PMMA-BS, which is consistent with the fact that the material regains stiffness when it is tested at 60 °C once the frequency of sollicitation increases.

V.4.3 Comparison of PLA/PMMA/BS blends with ABS/PC blends

Dynamic mechanical properties of PLA-PMMA-BS and ABS-PC were compared. Thus, the storage modulus (E') and $\tan(\delta)$ of those materials at different DMA frequency and temperature are graphically represented in Figure.V.18.



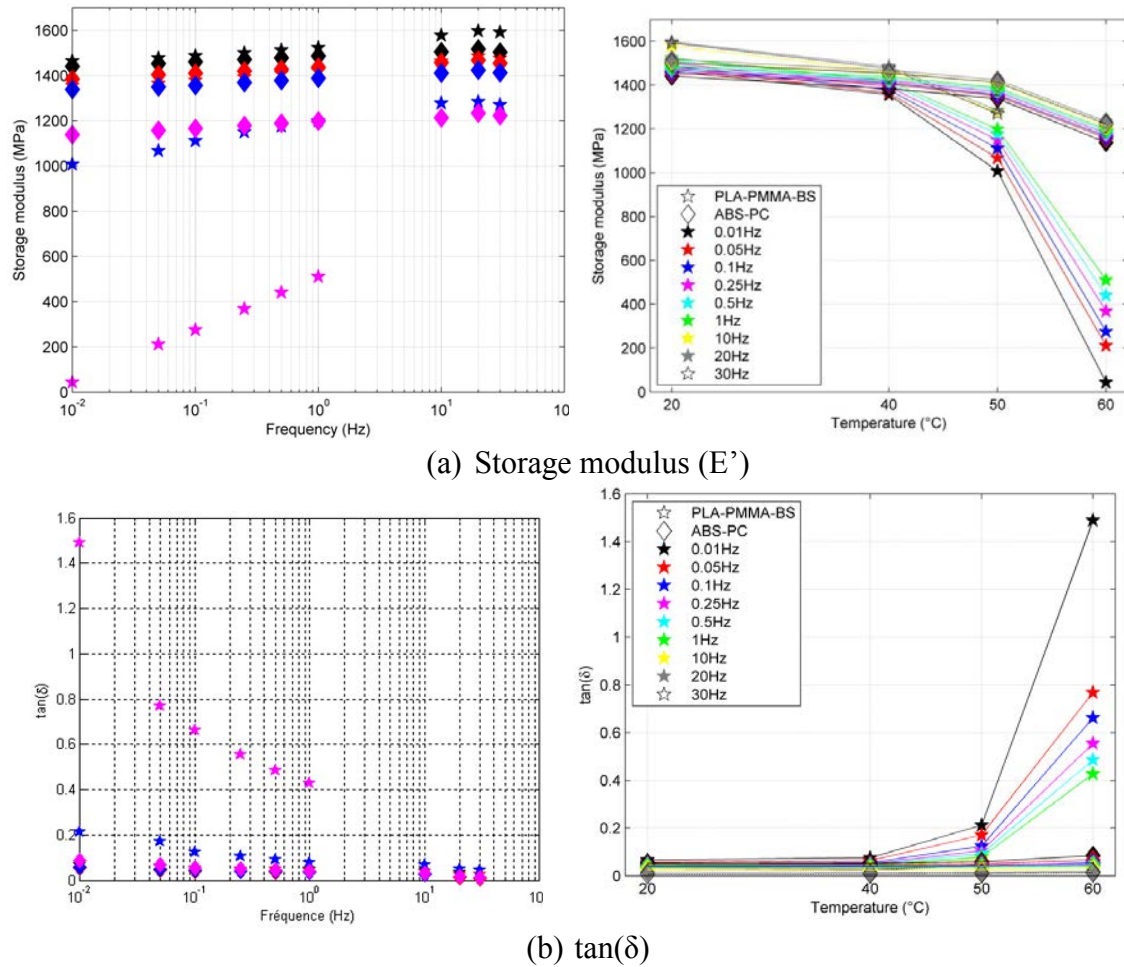


Figure V.18. Dynamic mechanical properties of PLA-PMMA-BS and ABS-PC

PLA-PMMA-BS presents a value of storage modulus (E') comparable to that of ABS-PC until 50°C and E' increases with increasing frequency for both materials (Figure V.18a). ABS-PC shows a good thermal stability without any decrease of storage modulus (E') at all temperatures investigated. At 60°C, E' value of ABS-PC is significantly higher than that of PLA-based materials. Moreover, no remarkable change was observed in the evolution of $\tan(\delta)$ for ABS-PC blend (Figure V.18c and d). Such results were expected since the tests are performed at temperatures, which are far away from the glass transition temperature of ABS/PC ($T_g=107^\circ\text{C}$, 136°C). As a conclusion, dynamic mechanical properties of PLA-based composition are obviously improved by adding PMMA to PLA-BS blends but are still uncompetitive with those of ABS-PC at high temperature.

V.5 Study of durability of PLA based blends:

Since the prepared PLA blends are potentially interesting for automotive applications, it is important to get information concerning their stability or modification upon aging. Accordingly, this study focuses on the characterization of the influence of physical aging under high temperature on the physical properties of PLA blends and, for comparison, of ABS-PC blend.

Injection-molded plates (process conditions described in section V.1.) were placed in a Heraeus 'UT6200' Laboratory oven and SERVATHIN CTH-T-CV008613-P oven. All samples were conditioned at a temperature of 50°C and 85°C. The samples were evaluated initially before conditioning and again after 50, 100, 150 and 250 hours. These conditions were chosen to be aggressive enough to accelerate the degradation that would occur in applications such as automotive interior parts, yet at a temperature below and above the glass transition temperature of PLA based blends (measured at 62°C and 63°C for PLA-BS and PLA-PMMA-BS, respectively).

The initial properties of all samples, including crystallization behavior were evaluated before conditioning.

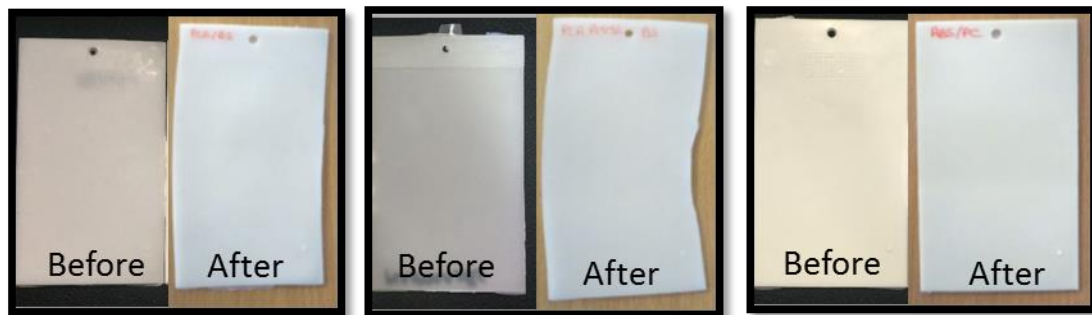


Figure V.19. Shape of PLA-BS((left), PLA-PMMA-BS(middle)and ABS-PC (right) before and after thermal aging at 85°C (different scale image view)

Figure V.19 presents the effect of thermal aging on the shape of material plates after 250 hours at 85°C. As we can see in the figure, the shape of ABS-PC plates is almost unchanged and dimensions are preserved. In contrast, plates of PLA-based blends are highly deformed after thermal ageing, thus confirming that heat resistance of PLA-based blends is still limited (dimensional stability was preserved after thermal ageing at 50°C, i.e. plates remained rectangular and of same dimensions).

The crystalline content of the conditioned samples were monitored over time for both PLA-BS and PLA-PMMA-BS blends (Figure V.20). At 50°C, there is a moderate increase of crystallinity reaching 16% and 12% respectively. At 85°C, the crystallinity drastically increases to reach 47% and 54% for PLA-BS and PLA-PMMA-BS blends, respectively. The increase in crystallinity could be caused by the rearrangement of the amorphous PLA segments into crystalline phase during the degradation of PLA by chain scission, as mentioned in literature [16,17].

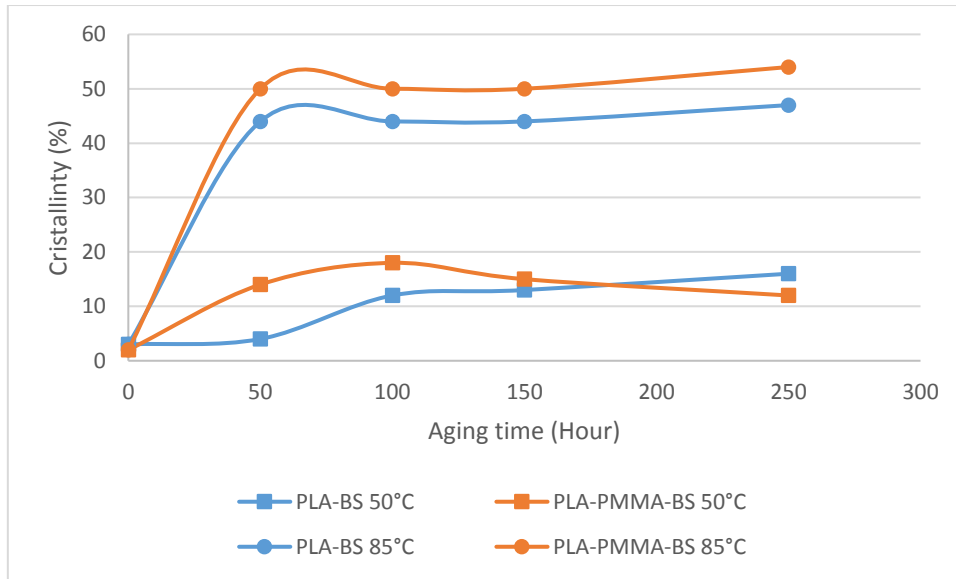


Figure V.20. Evolution of crystallinity of PLA-PMMA-BS and PLA-BS blends after thermal aging at 50°C and 85°C

After thermal aging for 250 hours at 50°C, T_g of both PLA-BS and PLA-PMMA-BS blends slightly increases to reach 64°C and 67°C respectively (Figure V.21). This is due to the increase in the excess enthalpy of relaxation [18] and PLA blends start to degrade causing a small shift in the melting temperature as can be seen in Figure V.21. The enthalpy of cold crystallization (ΔH_{cc}) decreases when increasing aging time at 50°C for both PLA-BS and PLA-PMMA-BS blends. When increasing aging temperature to 85°C, there is no more enthalpy of cold crystallization since PLA-blends reach the full crystallization (Figure V.22 a and b - DSC scans performed during the conditioning period from 0 to 250 hours).

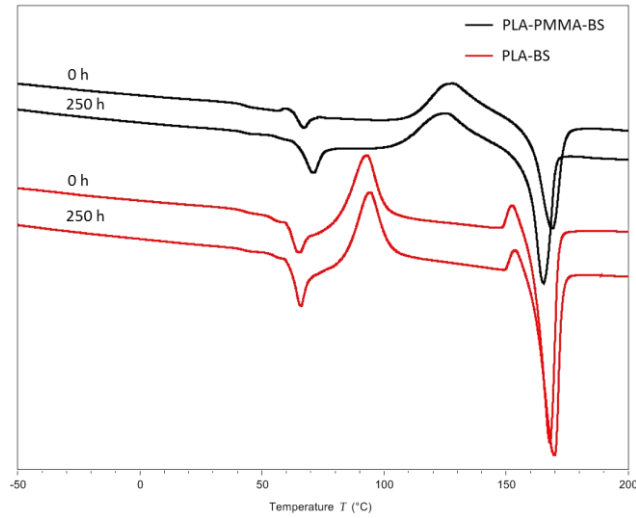
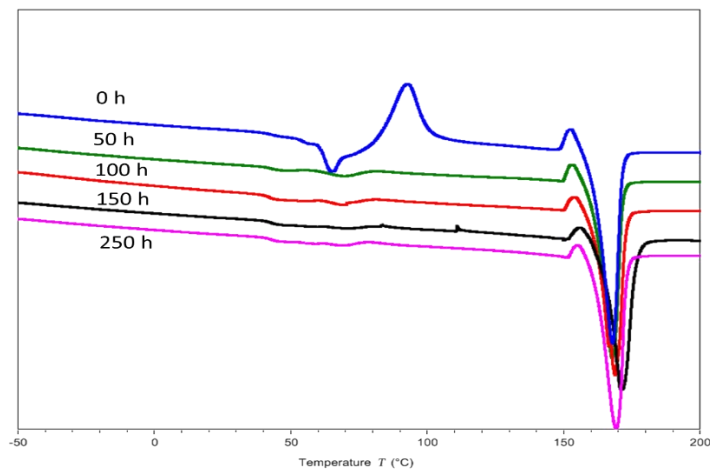
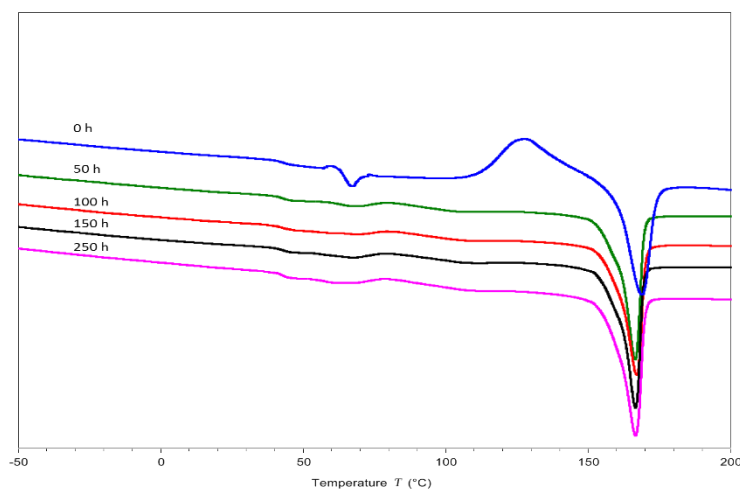


Figure V.21. DSC curves of PLA-BS and PLA-PMMA-BS before and after thermal aging for 250 hours at 50°C



(a) PLA-BS



(b) PLA-PMMA-BS

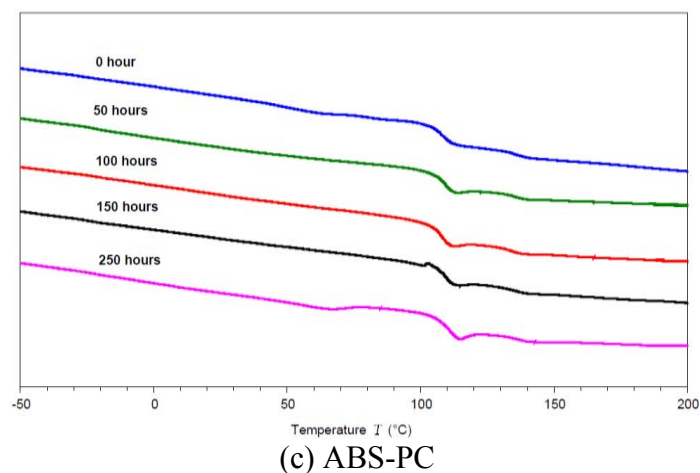


Figure V.22. DSC curves of PLA-BS and PLA-PMMA-BS and ABS-PC before and after thermal aging for 250 hours at 85°C

DSC was also performed on the ABS-PC samples as a control (Figure V.22 c). Figure V.22c shows the DSC traces during the initial heating ramp. Two glass transitions can be seen at $T_{gABS} = 107^{\circ}\text{C}$ and $T_{gPC} = 136^{\circ}\text{C}$. There was very little change in the T_g as a function of conditioning time. No melting endotherm was observed as ABS-PC is an amorphous polymer blend. ABS-PC blends remain thermally stable under thermal aging at 50°C and 85°C.

To complete this study, dynamic mechanical analyses and morphology observation after aging should be performed. They are indeed crucial to study the effect of aging on miscibility of ternary blends, in particular to analyze whether a phase separation may be induced. Furthermore, the effect of thermal aging on mechanical properties of blends should also be studied.

CONCLUSIONS

This chapter focuses on the development of a polylactide (PLA) - poly(methyl methacrylate) (PMMA) - Impact modifier (Biomax Strong - BS) composition for use in technical parts subjected to severe loading conditions. Chapter III has demonstrated the appealing properties of composition 58wt% PLA - 25wt% PMMA - 17wt% BS, in terms of tensile strength and rigidity, elongation at break and impact toughness for material specimens extruded and injection molded at the laboratory scale. Yet, material physical and mechanical properties can be strongly dependent on the manufacturing process, in particular extrusion (feeding rate, screw speed and profile...) and injection molding parameters (mold and melt temperature, pressure...). The first aim of this chapter is therefore to assess whether the good mechanical properties of PLA-based compositions are kept when the material is processed under industrial conditions. It was verified through quasi-static tensile tests of industrially produced PLA-PMMA-BS composition. In particular, tensile tests are characterized by an excellent repeatability and reveal that PLA-based composition has mechanical properties that can compete with those of ABS-PC, a reference blend for use in highly-loaded automotive technical parts. Once the possibility of industrialization of PLA-PMMA-BS processing is attested, next step consists in evaluating its mechanical properties under high strain-rate loadings. To do that, dynamic tensile tests are performed at high loading rate (up to $1 \text{ m}\cdot\text{s}^{-1}$). Results demonstrate again the excellent tensile properties of PLA-PMMA-BS blend, even under high-strain rate loading.

The use of developed PLA-PMMA-BS composition in industrially produced technical parts subjected to high loading rate is therefore validated. In order to evaluate the thermal properties of that composition, for use in parts possibly subjected to a wide range of temperature, mechanical properties of PLA-PMMA-BS under high testing temperature have been studied, using industrially produced specimens. Results confirm that PMMA can improve mechanical properties under high temperature since PLA-PMMA-BS composition shows better rigidity and tensile stress than PLA-BS blends. Dynamic mechanical analyses were also performed under different range of temperature and frequency confirming that dynamic mechanical properties of PLA-PMMA-BS are improved thanks to the addition of PMMA to PLA-BS blends but are still uncompetitive with ABS-PC at high temperature. Finally, a study of durability of PLA based blends under thermal aging was performed, since it is a crucial issue for its use in automotive industry. The results here indicate that PLA-PMMA-BS blends will not be durable

enough for exterior automotive applications at this stage of the development but can be used in numerous interior automotive parts such as door panels, center console etc

REFERENCES

1. Purac C (2013) PLA bioplastics: A driving force in automotive. Corbion Purac. <http://www.corbion.com/bioplastics/pla-markets/automotive>. Accessed 05/01/2016
2. Bouzouita A et al. (2016) Design of highly tough poly(l-lactide)-based ternary blends for automotive applications. *Journal of Applied Polymer Science* 133 (19):n/a-n/a. doi:10.1002/app.43402
3. Samuel C et al. (2013) PLLA/PMMA blends: A shear-induced miscibility with tunable morphologies and properties? *Polymer* 54 (15):3931-3939. doi:<http://dx.doi.org/10.1016/j.polymer.2013.05.021>
4. Eguiburu JL et al. (1998) Blends of amorphous and crystalline polylactides with poly(methyl methacrylate) and poly(methyl acrylate): a miscibility study. *Polymer* 39 (26):6891-6897. doi:[http://dx.doi.org/10.1016/S0032-3861\(98\)00182-7](http://dx.doi.org/10.1016/S0032-3861(98)00182-7)
5. Li S-H, Woo EM (2008) Immiscibility–miscibility phase transitions in blends of poly(L-lactide) with poly(methyl methacrylate). *Polymer International* 57 (11):1242-1251. doi:10.1002/pi.2469
6. Zhang G et al. (2003) Miscibility and phase structure of binary blends of polylactide and poly(methyl methacrylate). *Journal of Polymer Science Part B: Polymer Physics* 41 (1):23-30. doi:10.1002/polb.10353
7. Schreier H et al. (2009) *Image correlation for shape, motion and deformation measurements*. Springer US,
8. Epee A et al. (2011) Constitutive model for a semi-crystalline polymer under dynamic loading. *International Journal of Solids and Structures* 48 (10):1590-1599
9. Notta-Cuvier D et al. (2014) Tailoring polylactide (PLA) properties for automotive applications: Effect of addition of designed additives on main mechanical properties. *Polymer Testing* 36:1-9. doi:<http://dx.doi.org/10.1016/j.polymertesting.2014.03.007>
10. Chocron Benloulou IS et al. (1997) Dynamic tensile testing of aramid and polyethylene fiber composites. *International Journal of Impact Engineering* 19 (2):135-146. doi:[http://dx.doi.org/10.1016/S0734-743X\(96\)00017-6](http://dx.doi.org/10.1016/S0734-743X(96)00017-6)
11. Chen W et al. (2002) Tension and compression tests of two polymers under quasi-static and dynamic loading. *Polymer Testing* 21 (2):113-121. doi:[http://dx.doi.org/10.1016/S0142-9418\(01\)00055-1](http://dx.doi.org/10.1016/S0142-9418(01)00055-1)
12. Notta-Cuvier D et al. (2015) Tailoring Polylactide Properties for Automotive Applications: Effects of Co-Addition of Halloysite Nanotubes and Selected Plasticizer. *Macromolecular Materials and Engineering*:n/a-n/a. doi:10.1002/mame.201500032
13. Pothan LA et al. (2003) Dynamic mechanical analysis of banana fiber reinforced polyester composites. *Composites Science and Technology* 63 (2):283-293. doi:[http://dx.doi.org/10.1016/S0266-3538\(02\)00254-3](http://dx.doi.org/10.1016/S0266-3538(02)00254-3)
14. Oommen Z et al. (2000) Dynamic mechanical and thermal properties of physically compatibilized natural rubber/poly(methyl methacrylate) blends by the addition of natural rubber-graft- poly(methyl methacrylate). *Journal of Polymer Science Part B: Polymer Physics* 38 (4):525-536. doi:10.1002/(sici)1099-0488(20000215)38:4<525::aid-polb4>3.0.co;2-t
15. Murayama T (1978) *Dynamic Mechanical Analysis of Polymeric Material*. vol vol. 1. Elsevier Scientific Publishing Company,
16. Islam MS et al. (2010) Influence of accelerated ageing on the physico-mechanical properties of alkali-treated industrial hemp fibre reinforced poly (lactic acid)(PLA) composites. *Polymer Degradation and Stability* 95 (1):59-65
17. Auras RA et al. (2011) *Poly (lactic acid): synthesis, structures, properties, processing, and applications*, vol 10. John Wiley & Sons,

18. Cai H et al. (1996) *Effects of physical aging, crystallinity, and orientation on the enzymatic degradation of poly(lactic acid)*. *Journal of Polymer Science Part B: Polymer Physics* 34 (16):2701-2708. doi:10.1002/(sici)1099-0488(19961130)34:16<2701::aid-polb2>3.0.co;2-s

APPENDIX: detailed results of tensile tests and dynamic mechanical analysis**Table A1.** Tensile properties of composition PLA-PMMA-BS (ambient temperature)

Displacement rate	Sample code	Elastic modulus (MPa)	Max. nominal axial stress (MPa)	Average true axial strain at break	
1 mm/min	PLPMBS3	2458	35.9	0.128	
	PLPMBS4	2469	35.6	0.127	
	PLPMBS5	2460	35.3	0.113	
	PLPMBS6	2442	35.2	0.104	
	PLPMBS7	2495	35.1	0.110	
	10 mm/min	PLPMBS8	2469	38.4	0.124
		PLPMBS9	2440	38.4	0.108
PLPMBS10		2501	37.7	0.119	
PLPMBS11		2421	37.3	0.115	
PLPMBS12		2484	38.0	0.080	
100 mm/min		PLPMBS13	2607	42.8	0.092
	PLPMBS14	2488	42.0	0.142	
	PLPMBS15	2568	43.0	0.100	
	PLPMBS16	2481	42.0	0.105	
	PLPMBS17	2419	41.6	0.082	
	100 mm/s	PLPMBS1D	2703	50.3	0.109
		PLPMBS2D	2790	50.8	0.065
PLPMBS3D		2851	51.0	0.056	
PLPMBS4D		2665	50.5	0.084	
PLPMBS5D		2789	51.1	0.097	
PLPMBS6D		2776	50.1	0.067	
1 m/s		PLPMBS7D	2924	56.2	0.061
	PLPMBS8D	2802	56.7	0.068	
	PLPMBS9D	2845	57.7	0.075	
	PLPMBS10D	3160	57.2	0.069	
	PLPMBS11D	2830	57.8	0.069	
	PLPMBS12D	2883	55.5	0.057	

Table A2. Tensile properties of composition PLA-BS (ambient temperature)

Displacement rate	Sample code	Elastic modulus (MPa)	Max. nominal axial stress (MPa)	Average true axial strain at break
1 mm/min	PLABS2	2083	25.9	0.082
	PLABS3	2014	25.9	0.074
	PLABS4	2098	26.0	0.050

	PLABS5	2141	25.9	0.058
	PLABS6	2142	26.1	0.094
10 mm/min	PLABS7	2179	28.9	0.113
	PLABS8	2201	29.0	0.146
	PLABS9	2170	28.6	0.127
	PLABS10	2148	28.7	0.118
	PLABS11	2163	28.9	0.143
100 mm/min	PLABS13	2117	33.7	0.159
	PLABS15	2170	33.7	0.170
	PLABS16	2104	33.4	0.159
	PLABS17	2119	33.1	0.128
100 mm/s	PLABS1D	2461	43.3	0.160
	PLABS2D	2459	43.1	0.185
	PLABS3D	2514	43.4	0.166
	PLABS4D	2512	44.2	0.137
	PLABS5D	2460	44.0	0.180
1 m/s	PLABS6D	2192	48.4	0.065
	PLABS7D	2689	49.8	0.106
	PLABS8D	2689	49.8	0.119
	PLABS9D	2763	49.7	0.121
	PLABS10D	2742	49.3	0.147

Table A3. Tensile properties of composition PLA-BS (ambient temperature)

Displacement rate	Sample code	Elastic modulus (MPa)	Max. nominal axial stress (MPa)	Average true axial strain at break
1 mm/min	ABSPC2	2446	43.7	0.077
	ABSPC3	2419	43.7	0.067
	ABSPC4	2421	43.1	0.047
	ABSPC5	2418	43.5	0.052
	ABSPC6	2434	43.0	0.046
	10 mm/min	ABSPC7	2461	47.7
ABSPC8		2461	47.3	0.053
ABSPC9		2419	46.7	0.053
ABSPC10		2483	47.0	0.050
ABSPC11		2440	47.1	0.054
100 mm/min	ABSPC12	2481	52.0	0.069
	ABSPC13	2454	52.3	0.107
	ABSPC14	2436	52.3	0.056
	ABSPC15	2550	52.3	0.080
	ABSPC17	2450	52.2	0.117
	100 mm/s	ABSPC1D	2586	59.2
ABSPC2D		2495	59.0	0.049
ABSPC3D		2581	60.0	0.056
ABSPC4D		2548	59.7	0.054
ABSPC5D		2525	59.4	0.056
1 m/s	ABSPC6D	2767	62.3	0.075

	ABSPC7D	2995	62.3	0.035
	ABSPC8D	2859	62.1	0.040
	ABSPC9D	2658	62.0	0.062
	ABSPC10D	2768	62.5	0.060

Table A4. Tensile properties of PLA based blends and ABS-PC blends under 50°C at 10mm/min

Sample code	Displacement rate	Elastic modulus (MPa)	Max. nominal axial stress (MPa)	Average true axial strain
PLPMBS-1	10 mm/min (50°C)	1076	14.6	2.74
PLPMBS-2		1511	23	-
PLPMBS-3		1218	17.8	-
PLPMBS-4		1449	22	-
PLPMBS-5		713	11.2	-
PLPMBS-6		1697	26.3	-
PLABS-1		416	6.4	-
PLABS-2		280	4.4	-
PLABS-3		525	7.8	-
PLABS-4		859	12	-
PLABS-5		935	12.2	-
PLABS-6		392	4.8	-
ABSPC -1		2076	37.9	0.1
ABSPC -2		1971	35.9	0.12
ABSPC -3		2037	37.9	0.05
ABSPC -4		2095	37.7	0.12
ABSPC -5		2102	39	0.09

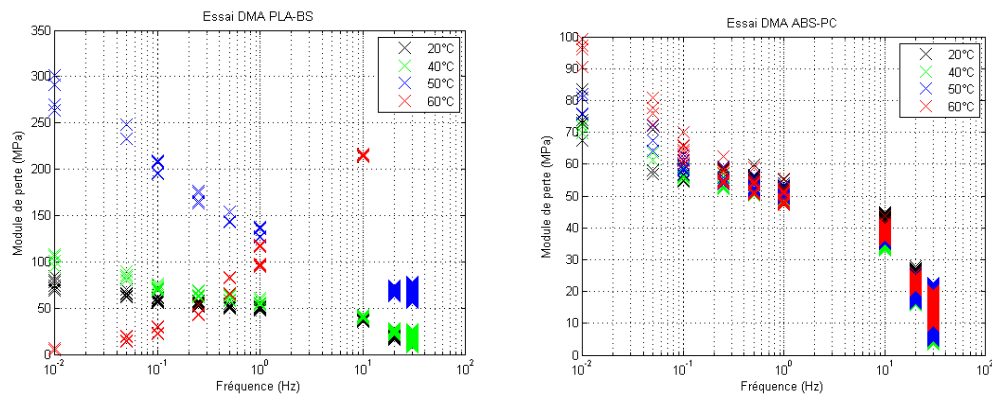


Figure A1. Loss modulus of PLA-BS blends (on the left) and ABS-PC (on the right)

GENERAL CONCLUSION AND OUTLOOKS

General conclusion and outlooks

The interest to use polymeric materials derived from renewable resources continuously increases because of the considerably improved environmental awareness of society and the fear from the depletion of petrochemical based plastics. In this regard, Poly (lactic acid), PLA, seems to be the biopolymer that responds the most successfully to the surge of demands for such materials and can satisfy the requirements of large scale processing and wide range of application at the same time. Interest for PLA can be explained by numerous interesting properties, such as good processability, good mechanical properties (in particular high tensile and flexural strength and rigidity), biodegradability, biocompatibility and relatively low-cost compared to other bio-sourced polymers. However, durable applications of PLA in technical parts are still limited by its inherent brittleness and limited low thermal stability. These parameters therefore need to be improved for PLA industrial application, especially for automotive parts possibly subjected to severe loading and environmental conditions.

The principal aim of this thesis is the design of new bio-based PLA materials for automotive application, through the improvement of thermal and mechanical PLA properties. The work reported in this thesis demonstrated that the properties of PLA-based compositions can be tailored by a careful selection of the polymer blends that compose the matrix (here PLA-PMMA blends) and the incorporation of a specific amount of impact modifier (Biostrong, hereafter called BS). In order to determine the optimal composition of PLA-based material, PLA/PMMA/BS ternary blends with a varying content of PMMA and 17 wt.% BS were prepared using melt blending and injection molding processes. All blends presented improved impact toughness together with a slight decrease in rigidity and tensile strength. The most promising composition, namely PLA70-PMMA30+17 wt% BS (hereafter simply called PLA-PMMA-BS composition), was selected as the one that presented the best balance between ductility and stiffness, while containing at least 50% of bio-sourced polymer in the blend. The comparison of mechanical properties of PLA-PMMA-BS to those of a commercial ABS/PC blend demonstrated that that PLA-based ternary blend could be a very promising bio-sourced alternative for use in automotive applications.

However, still limited heat resistance and crystallization ability of these blends remained inferior to what is required for technical applications (especially for automotive exterior parts that are subjected to harsh thermal conditions) and industrial high-speed processing, for instance, by injection techniques. Three approaches were investigated in this work to overcome

this problem: annealing process, stereocomplexation of PLA and combination with nanoparticles as nucleating agent. Annealing is promoted to improve heat resistance by improving crystallinity ratio. However, time and temperature of pre-heat treatment must be optimized not to affect the ductility of PLA-PMMA-BS blend. In our study, blend annealing for 10 min at 120°C allows improving HDT (up to around 80°C) and impact toughness but affects the ductility of the blend, which therefore loses its capacity to bear severe loading conditions. Additionally, annealing process is expensive and involves longer production time. Therefore, it cannot be seen as a promising solution for mass production characterizing the automotive industry. The second approach was the stereocomplexation of PLLA and PDLA that can theoretically improve heat resistance. Nevertheless, in our case, the results were unsatisfactory with affected impact toughness and unenhanced heat deflection temperature. It is likely that better results could be obtained by optimizing process parameters in order to make complete sc-PLA. To obtain more satisfying results, future works may focus on the control of the stereocomplexation by changing the molecular weight of both PLLA and PDLA in order to perform a full stereocomplexation of high crystallinity degree. The process should be controlled in terms of time of process, speed rotor and order of addition of compounds since these parameters can affect mechanical properties (impact strength). The third approach concerned the enhancement of crystallinity behavior of PLA-PMMA-BS blend thanks to combination with nucleating agent and nanoparticles. In our study, a limited improvement of crystallinity degree (6%) was achieved, but heat-resistance was not improved. Moreover, a migration of silica nanoparticles inside rubber microdomains of impact modifier was noticed. In the future, a deep investigation should be realized in order to understand this phenomenon. In addition, different nature of nanoparticles should be considered in order to improve thermal resistance of PLA-PMMA-BS blends.

Finally, another aspect of this thesis work consists to ensure the scaling up of selected composition PLA-PMMA-BS (without any additional processing or filling) towards industrialization. In particular, it was verified that the material can be processed at an “industrial scale” while keeping interesting thermo-mechanical properties. Indeed, quasi-static tensile tests of industrially produced PLA-PMMA-BS composition were characterized by an excellent repeatability and revealed that PLA-based composition has mechanical properties that can compete with those of ABS-PC, a reference blend for use in highly-loaded automotive technical parts. Once the possibility of industrialization of PLA-PMMA-BS processing is attested, its mechanical properties under high strain-rate loadings was evaluated, based on dynamic tensile

tests at high loading rate (up to 1 m.s^{-1}). The results again demonstrate the excellent tensile properties of PLA-PMMA-BS blend, even under high-strain rate loadings.

The use of developed PLA-PMMA-BS composition in industrially produced technical parts subjected to high loading rate is therefore validated. Another key-point is to evaluate the thermal properties of that composition, for use in parts to be subjected to a wide range of temperature. Mechanical properties of PLA-PMMA-BS under relatively high testing temperature (50°C) have therefore been studied, using industrially produced specimens. The results confirmed that the addition of PMMA can improve mechanical properties of PLA-based materials under high temperature with better tensile strength and rigidity of PLA-PMMA-BS compared to PLA-BS blends. Dynamic mechanical analyses at a wide range of frequency were also performed under different temperatures. The results again showed that dynamic mechanical properties of PLA-PMMA-BS are improved thanks to the addition of PMMA but are still uncompetitive with those of ABS-PC at high temperature.

Finally, a study of durability of PLA based blends under thermal aging was initiated. Aging of biosourced materials sensitive to hydrolysis such as PLA is indeed a crucial issue for a more widespread use in technical applications and is today a significant barrier to the use of PLA in the automotive sector. Further work should focus on a deeper study of thermal, mechanical properties and morphology of blends after weathering and hydrolysis aging, following preliminary results obtained during this thesis.

The results collected in the frame of this work can find extension in several orientations.

Using the actual production process like extrusion and injection molding, it is already possible to process automotive interior parts with PLA-PMMA-BS blends as demonstrated in this thesis. Moreover, several approaches could be considered in a near future to improve thermal properties of PLA-based compositions, which could allow its use even for automotive exterior parts. Then, 3D printing technologies (or additive manufacturing) promises rapid prototyping capabilities with the high-volume throughput of conventional manufacturing in a next future. As this technology evolves, automotive companies are starting to look into the possibilities of 3D printing. If up to now, the 3D technology was used to print rare car parts only, nowadays you can have an entire vehicle printed in 44 hours.

Additive manufacturing enables a continuous factory production for individual parts. Process speed is another factor to be taken into consideration, because a faster process means more continuity in the design and the overall development process. In addition, this technology can offer more flexibility to the design and manufacturers can develop more customized

features, such as lightweight lattice structures, fancier geometries, parts made of more than two materials, etc. While traditionally acrylonitrile-butadiene-styrene (ABS) has been used in 3D printers for industrial applications, these latter have shifted to PLA due to its green reputation, pleasant smell, as well as its low shrinkage and good printability. Therefore, a new project could be aimed at extending our approach to the development of polylactid acid based materials dedicated to additive manufacturing for automotive application. Some tests of 3D printing of PLA-PMMA-BS blend with, e.g., the new Freeformer printing machine should be done. This new device makes easier the printing of numerous materials since standard granulates are used as start material to make prototypes of printed blends, with the possibility to integrate preparation of melt granulates in the process chain in the same way as during injection molding. In addition, the special discharge unit featuring a pulsed nozzle closure marks a new era in industrial processing with the generation of tiny plastic droplets and their application layer-by-layer to produce three-dimensional parts created directly from 3D CAD data. Therefore, it would be amazing to print PLA-PMMA-BS and realize different shapes in order to study the adhesion between layers, mechanical properties of printed samples, the quality of printed objects in terms of shrinkage and contraction, etc.

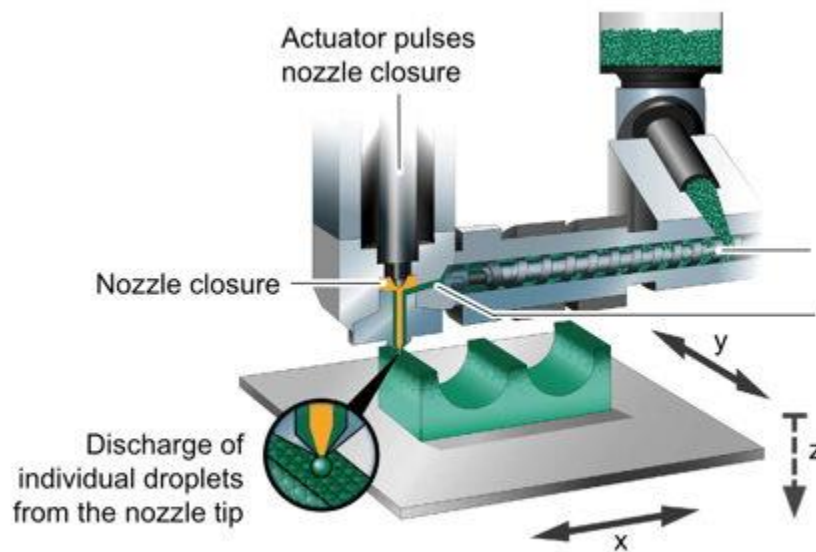


Figure 1. Descriptive diagram of Freeformar 3D printing machine

LIST OF PUBLICATIONS

List of publications

- ❖ Delphine Notta-Cuvier*, Marius Murariu, Jérémy Odent, Rémi Delille, Amani Bouzouita, Jean-Marie Raquez, Franck Lauro, Philippe Dubois. Tailoring Polylactide Properties for Automotive Applications: Effects of Co-Addition of Halloysite Nanotubes and Selected Plasticizer. *Macromolecular Materials and Engineering*, **2015**, 7, 684-698. **(Published paper) [IF= 2.781]**
- ❖ Amani Bouzouita, Cédric Samuel, Delphine Notta-cuvier, Jérémy Odent, Franck Lauro, Philippe Dubois, Jean Marie Raquez*. Design of highly tough poly (L-lactide)-based ternary blends for automotive applications, *J. Appl. Polym. Sci.* **2016**, 133, DOI: 10.1002/app.43402 **(Published paper) [IF=1.768]**
- ❖ D. Notta-Cuviera*, A. Bouzouita, R. Delille, G. Haugou, J.-M. Raquez, F. Lauro, P. Dubois, Design of toughened PLA based material for application in structures subjected to severe loading conditions. Part 1. Quasi-static and dynamic tensile tests at ambient temperature. *Polymer Testing*, **2016 (Submitted paper)**
- ❖ Amani Bouzouita, Delphine Notta-Cuvier, Jean-Marie Raquez, Franck Lauro and Philippe Dubois, Poly(lactic acid)-based materials for automotive applications, *Advances in Polymer Science*, **2016 (Submitted review)**

RÉSUMÉ

L'attractivité des matériaux polymères issus de ressources renouvelables augmente continuellement en raison de la prise de conscience environnementale de la société. Dans ce contexte, l'acide polylactique (PLA) est un biopolymère qui possède d'indéniables atouts (notamment en termes de rigidité et résistance en traction/flexion) permettant d'envisager des applications à grande échelle, par exemple pour l'automobile. Cependant, les applications durables du PLA sont encore considérablement restreintes à cause de sa fragilité et de sa stabilité thermique limitée. Dans cette thèse, nous nous sommes focalisés sur la conception de nouveaux matériaux à base de PLA pour des applications dans l'automobile, en travaillant notamment sur l'amélioration des propriétés thermiques et mécaniques (notamment la ductilité), y compris sous haute vitesse de déformation. Ainsi, la composition optimale permettant d'atteindre le meilleur compromis entre différentes propriétés (ductilité, résistance et rigidité, résilience, stabilité thermique...), tout en étant composée d'au moins 50% de matériaux biosourcés est déterminée. D'autres stratégies visant à améliorer la capacité ou la vitesse de cristallisation des compositions à base de PLA ont également été étudiées. Dans tous ces développements, une attention particulière est portée sur l'étude des interactions entre structure, propriétés et process.

MOTS-CLEFS: Polymères biosourcés; stabilité thermique ; propriétés mécaniques, morphologies ; industrialisation ; application automobile

ABSTRACT

The interest to use polymeric materials derived from renewable resources increases continuously due to considerably improved environmental awareness and the expected depletion of petrochemical resources. In this regard, Poly(lactic acid), PLA, is a biopolymer that can respond to the demand for such materials for a wide range of applications, thanks to interesting mechanical properties such as high tensile/flexural strength and rigidity, in particular. However, in many cases, durable applications of PLA have been significantly limited by its inherent brittleness and limited thermal stability. In this dissertation, we focused on the design of new biobased PLA materials for automotive parts subjected to severe loading and environmental conditions, by improving thermal and mechanical properties, including under high strain rate loadings. Thus, the most promising compound is selected as the one that offers the best balance between different properties (ductility, strength and stiffness, impact toughness, good thermal stability...) with a content of bio-sourced polymer in the blend at least equal to 50%. Other strategies to improve crystallinity of PLA-based compounds are also studied. In all those developments, a particular attention is paid to the study of structure-process-properties interactions.

KEYWORDS: Biopolymers and renewable polymers; heat resistance; mechanical properties; morphology; industrialization; automotive application

Résumé de Thèse de doctorat

Pour obtenir le grade de Docteur de l'Université de

VALENCIENNES ET DU HAINAUT-CAMBRESIS

et l'Université de MONS

Discipline, spécialité selon la liste des spécialités pour lesquelles l'Ecole Doctorale est accréditée :
Sciences et Mécanique

Ecole doctorale :

Sciences Pour l'Ingénieur (SPI)

Laboratoires :

Laboratoire d'Automatique, de Mécanique et d'Informatique Industrielles et Humaines (LAMIH)
Service des Matériaux Polymères et Composites (SMPC)

Elaboration des matériaux à base de l'acide polylactique pour application automobile: Etude des interactions entre structure-process-propriétés

par Amani BOUZOUITA

Soutenu le 12/10/2016, à Valenciennes, devant le Jury composé de :

Rapporteurs

- Mme Sandra Domenek, Professeure des Universités, Agro ParisTech.
- M. Yves Grohens, Professeur des Universités, LIMATB.

Examineurs

- M. Marius Murariu, Chercheur Senior, centre de recherche Materia Nova.
- M. Philippe Dubois, Professeur, centre de recherche LIST.
- M. Cyrille Sollogoub, Maître de conférences, Art et Métiers PariTech CNAM.

Directeurs de thèse

- M. Franck Lauro, Professeur des Universités, Université de Valenciennes - LAMIH
- M. Jean-Marie Raquez, Chercheur qualifié FNRS, Université de Mons - SMPC

Co-encadrante :

- Mme Delphine Notta-Cuvier, Maître de Conférences, Université de Valenciennes - LAMIH

L'attractivité des matériaux polymères issus de ressources renouvelables augmente continuellement en raison de la prise de conscience environnementale de la société. Dans ce contexte, l'acide polylactique (PLA) est un biopolymère qui possède d'indéniables atouts (notamment en termes de rigidité et résistance en traction/flexion) permettant d'envisager des applications à grande échelle, par exemple pour l'automobile. Cependant, les applications durables du PLA sont encore considérablement restreintes à cause de sa fragilité et de sa stabilité thermique limitée. Dans cette thèse, nous nous sommes focalisés sur la conception de nouveaux matériaux à base de PLA pour des applications dans l'automobile, en travaillant notamment sur l'amélioration des propriétés thermiques et mécaniques (notamment la ductilité), y compris sous haute vitesse de déformation. Ainsi, la composition optimale permettant d'atteindre le meilleur compromis entre différentes propriétés (ductilité, résistance et rigidité, résilience, stabilité thermique...), tout en étant composée d'au moins 50% de matériaux biosourcés est déterminée. D'autres stratégies visant à améliorer la capacité ou la vitesse de cristallisation des compositions à base de PLA ont également été étudiées. Dans tous ces développements, une attention particulière est portée sur l'étude des interactions entre structure, propriétés et process.

L'objectif de recherche consiste à élaborer des matériaux biosourcés à base de poly (acide) lactique (PLA) pour des applications intérieures ou extérieures pour l'automobile. Ce matériau biosourcé à base de (PLA) doit répondre aux différentes exigences du secteur automobile tel qu'une bonne stabilité thermomécaniques, une bonne rigidité, une meilleure ductilité et une bonne résistance à l'impact. Ce qui n'est pas le cas pour le (PLA) que certes il est biodégradable, recyclable et présente des bonnes propriétés mécaniques (haute rigidité), néanmoins il est fragile et représente une faible stabilité thermomécaniques au-delà de sa température de transition vitreuse (T_g) ce qui limite son domaine d'application techniques. D'où l'objectif de notre thèse qui consiste à l'amélioration des propriétés du PLA pour qu'il soit apte à être

utilisé dans l'industrie automobile et qui peut remplacer les polymères pétrosourcés comme l'ABS/PC.

Pour cela, les deux premiers chapitres positionnent les attendus du travail de thèse dans un contexte de production et d'utilisation du PLA, par rapport aux autres plastiques, aujourd'hui et dans le futur. L'introduction générale situe le champ de recherche et la pertinence de l'objectif de la thèse, à savoir développer des matériaux biosourcés (à base de PLA) pour des applications durables dans le domaine de l'automobile. Le choix du PLA comme polymère d'étude est clairement expliqué et défendu. Après l'introduction générale, le deuxième chapitre « Etat de l'art » présente les différentes techniques utilisées pour l'augmentation de la ductilité en gardant une bonne rigidité à savoir l'ajout des plastifiants, des modificateurs d'impact et le post-traitement de recuit ; l'amélioration de la stabilité thermique (température de fléchissement sous charge, heat deflection temperature HDT) en développant des nanocomposites à base de PLA suivie d'un processus de recuit, en mélangeant le PLA avec un matériau à base de ressource pétrolière de haute résistance thermomécanique ou créer des stéréocomplexes par l'ajout du PDLA au PLLA ; et finalement l'amélioration de l'injectabilité via le contrôle de la cristallinité par l'ajout des agents nucléants tel que le talc ou la création des stéréocomplexes qui permettent ainsi de réduire le temps de demi cristallisation, améliorer la cristallinité et améliorer la processabilité.

Ces différentes techniques existantes sont présentées et une discussion plus en détail des résultats liés à la formulation du PLA, la cristallisation et la fabrication de mélanges de polymères pour l'augmentation notamment de la HDT et la ténacité a été choisie. Ce choix introduit bien l'étude expérimentale qui a été menée. De plus, le choix du PMMA comme partenaire du PLA pour la formulation des mélanges dans la thèse est expliqué.

Dans le troisième chapitre qui consiste à développer un matériau biosourcés à base de PLA hautement ductile avec une stabilité thermomécanique améliorée, différentes compositions de matériaux ont été étudiés, basés sur une matrice (PLA/PMMA) et différents types de modificateurs d'impact

(biousourcés et pétrosourcés). En se basant sur la littérature, l'ajout du PMMA permet d'améliorer la stabilité thermomécanique en augmentant la valeur de (T_g) alors que l'ajout du modificateur d'impact permet d'apporter au mélange une meilleure résistance aux chocs. Le choix du meilleur modificateur d'impact (BS) a été confirmé après des tests mécaniques sur les différents mélanges. Le BS est un modificateur d'impact commercial qui permet la distribution de micro-domaines caoutchoutiques dans le polymère. Ces micro-domaines ont la capacité d'absorber et dissiper une partie de l'énergie de l'impact.

Sept mélanges ternaires ont été réalisés à l'échelle laboratoire à base d'une matrice PLA/PMMA (rapport variant) et un modificateur d'impact Biomax Strong (BS) (taux fixe 17%). Des caractérisations thermiques, thermodynamiques, mécaniques et morphologiques ont été réalisées sur des éprouvettes injectées et montrant que les mélanges obtenus ont une matrice PLA/PMMA miscibles et un modificateur d'impact immiscible. En augmentant le taux de PMMA, la stabilité thermomécanique s'améliore suite à l'augmentation de la valeur de T_g (Figure1). Pour les propriétés mécaniques, l'ajout du modificateur d'impact a permis d'améliorer la résistance au choc (de 3 kJ/M² jusqu'à 44 kJ/M²) une valeur optimum pour un rapport de 70/30 de PLA/PMMA et avoir une bonne ductilité sans altérer la bonne rigidité du PLA.

Tableau.1 Température de transition vitreuse, taux de cristallinité, température de relaxation et valeurs de HDT pour les mélanges PLLA/PMMA/BS déterminés à partir des analyses de DSC et DMTA.

Sample Code	T_g^* (°C)	X_c^* (%)	$T_{\tan\delta 1}^{**}$ (°C)	$T_{\tan\delta 2}^{**}$ (°C)	HDT ^{**} (°C)
Neat PLA	61	3	57	-42	54
PLA/BS	61.6	19	60	-42	53
PLA80/PMMA20/BS	61.8	9	64	-43	57
PLA70/PMMA30/BS	62.8	3	67	-43	58
PLA50/PMMA50/BS	66	-	76	-40	63
PLA30/PMMA70/BS	89	-	93	-40	70

Sample Code	T _g [*] (°C)	X _c [*] (%)	T _{tanδ1} ^{**} (°C)	T _{tanδ2} ^{**} (°C)	HDT ^{**} (°C)
PLA20/PMMA80/BS	97	-	100	-33	72
PMMA/BS	117	-	115	-	84
Neat PMMA	116	-	118	-	-
Neat BS	-	-	-	-35	-

* Déterminés par DSC

** Déterminés par DMTA

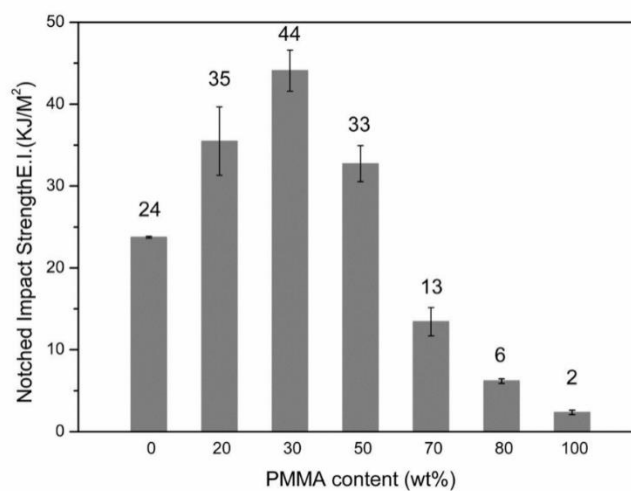


Figure 1. Effet du taux de PMMA sur la résistance aux chocs des mélanges PLA/PMMA/BS

Suite à des analyses morphologiques, des images de la surface des éprouvettes fracturées montrent qu'il existe une relation entre la taille des particules du BS immiscible dans la matrice et la résistance aux chocs. En augmentant le taux de PMMA, la distribution des particules devient plus large ainsi que les diamètres et pour avoir une meilleure résistance aux chocs il faut respecter la valeur optimale des diamètres des particules qui est aux alentours de 0.5 µm.

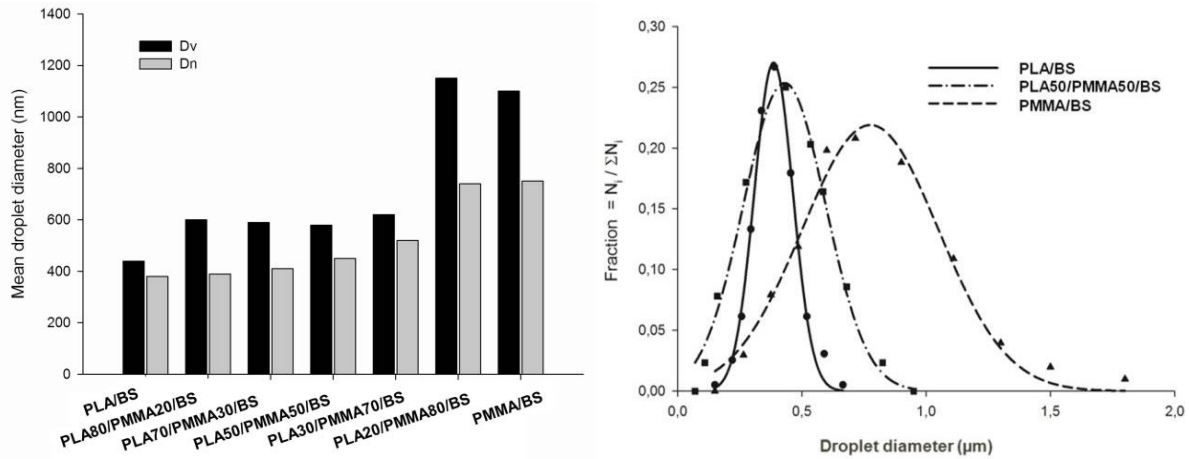


Figure 2. Diamètres des particules de BS en fonction de taux de PMMA content (à gauche) et la taille de distribution des microdomaines caoutchoutiques de BS (à droite) pour différents mélanges de PLA/PMMA/BS.

BS semble être plus compatible avec le PLA qu'avec le PMMA. La taille des gouttelettes de BS dans le PLA est plus faible et leur distribution plus homogène. Ceci permet l'augmentation de l'élongation à la rupture et de la ténacité. Cette augmentation de la ductilité pourrait être liée à des effets de décohérence entre phase PLA et BS, création de fibrilles, craquelage et cisaillement et de la formation in-situ de copolymères greffés PLA/BS. En effet, BS et PLA possèdent de groupements réactifs qui pourront réagir et ainsi produire de polymères comptabilisant les deux phases

Enfin, un seul mélange a été sélectionné pour la suite des recherches de rapport de matrice PLA 70/PMMA30, ce mélange a été choisi suite à ces performances qui offrent un équilibre entre la bonne rigidité, une meilleure ductilité, une excellente résistance aux chocs et le caractère biosourcé (+50% de polymère biosourcé). Une comparaison du matériau alternatif par rapport à l'ABS/PC qui est utilisé dans le secteur automobile et qui a un coût comparable au mélange ternaire, montre que le matériau biosourcé alternatif a de meilleures propriétés mécaniques que celles de l'ABS/PC mais les propriétés thermomécaniques restent encore à développer suite à une légère amélioration.

Pour cela, dans le quatrième chapitre qui consiste à améliorer la résistance thermomécanique de la composition optimale PLA70/PMMA30/BS via le contrôle de la cristallinité, autres solutions ont été étudiés pour l'amélioration de la stabilité thermomécanique en se référant à la littérature. L'idée essentielle est que la cristallisation du PLA pourrait améliorer la HDT, la rigidité et la résistance mécaniques des mélanges. Trois techniques sont testées : le post traitement de recuit, la stéréocomplexation et la cristallisation à l'aide d'un agent nucléant et de nanoparticules de silicium (EBS/SiO₂). Un post traitement de recuit (120°C pendant 10, 20 et 30 min) a été réalisé sur le mélange ternaire PLA/PMMA/BS et sur le mélange binaire PLA/BS considéré comme référence. Les résultats montrent que indépendamment de temps de recuit il y a une amélioration de la stabilité thermomécanique (\uparrow HDT, \uparrow Tang δ) suite à l'amélioration de la cristallinité (figure 3). Le process de recuit maintien la ductilité des mélanges avec une faible baisse de l'allongement à la rupture mais une amélioration de la rigidité. Le process de recuit n'a aucun effet sur la résistance aux chocs pour le mélange ternaire. Le post traitement de recuit semblait être la technique la plus efficace en termes d'augmentation de HDT. Elle permet l'obtention du taux de cristallinité le plus haut. La T_g des mélanges recristallisés augmente jusqu'à 100 °C.

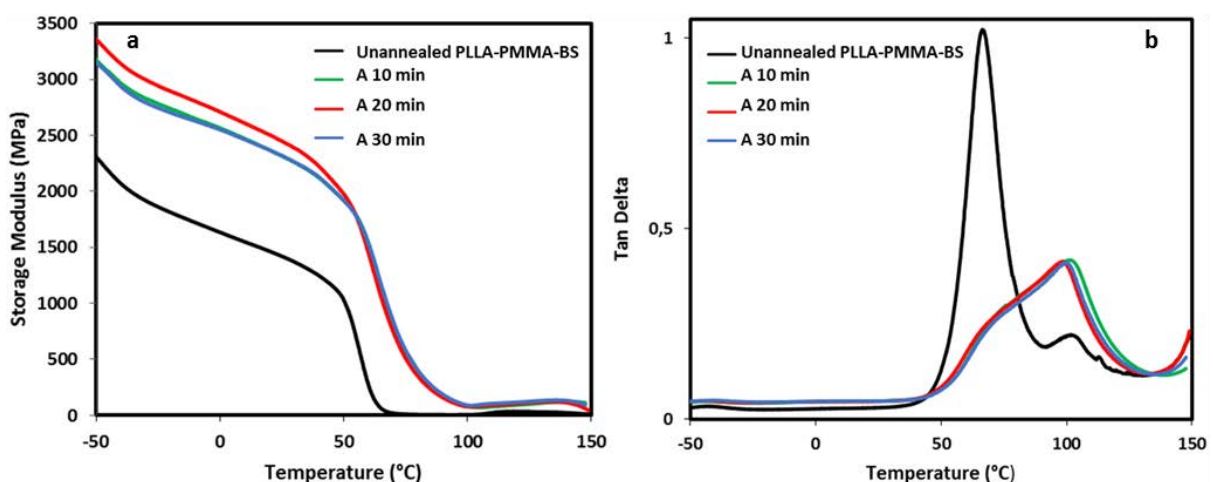


Figure 1. Courbes DMTA de PLLA-PMMA-BS non recuit et recuit après différents temps

de recuit (a) Comparaison du module de stockage des mélanges à base de PLLA (b) Comparaison de $\tan\delta$ des mélanges à base de PLLA.

Les courbes de $\tan\delta$ montrent un pic légèrement déformé au contraire des pics observés pour les mélanges PLA/PMMA/BS amorphes. Mais cette technique n'est pas utilisable dans le secteur automobile puisque elle peut engendrer un temps et un coût supplémentaire sur la production ce qui peut affecter la productivité dans l'industrie automobile.

La deuxième technique appliquée, c'est la formation des stéréocomplexes pour améliorer la cristallinité des mélanges. Pour cela, des mélanges à base de PLLA/PDLA/PMMA/BS ont été élaborés avec différents taux de PDLA (5, 10, 30, 50) et les mêmes caractérisations ont été réalisées et qui montrent qu'il y a une légère amélioration de la cristallinité ainsi qu'une meilleure résistance aux chocs en maintenant des bonnes propriétés mécaniques (rigidité, ductilité). Cette amélioration de la cristallinité était beaucoup plus faible de ce que se trouve dans la littérature, ce qui peut déduire que le processus d'élaboration de ce mélange n'était pas le plus adapté. Le mélange PLLA/PDLA (90/10) permettait une augmentation de la ténacité. Afin d'obtenir des résultats équivalents avec le mélange ternaire (+ PMMA) le procédé d'incorporation des stéréocomplexes a été optimisé. Cependant, le degré de cristallinité obtenu par stéréocomplexe reste inférieur au degré obtenu par traitement thermique simple et donc l'effet sur l'HDT reste faible. Dans les perspectives une proposition d'une étude plus approfondie sur la stéréocomplexation et notamment en utilisant des PDLA avec des masses molaires différentes a été proposé.

La troisième technique utilisée pour l'amélioration de la cristallinité c'est la voie d'utilisation du mélange EBS/SiO₂ qui permettait un gain dans la ténacité mais pas l'augmentation de l'HDT à cause d'une faible cristallinité du mélange. La raison semble la migration des nanoparticules favorable dans phase BS, ce qui les retire donc de la matrice et minimise leurs effets (Figure 4). En conclusion,

ces deux chapitres de résultats aboutissent à une formulation pertinente du PLA en vue de l'augmentation de l'HDT et la ténacité. Elles permettent aussi d'écartier des pistes de travail moins performantes et constituent une avancée dans les connaissances dans le domaine.

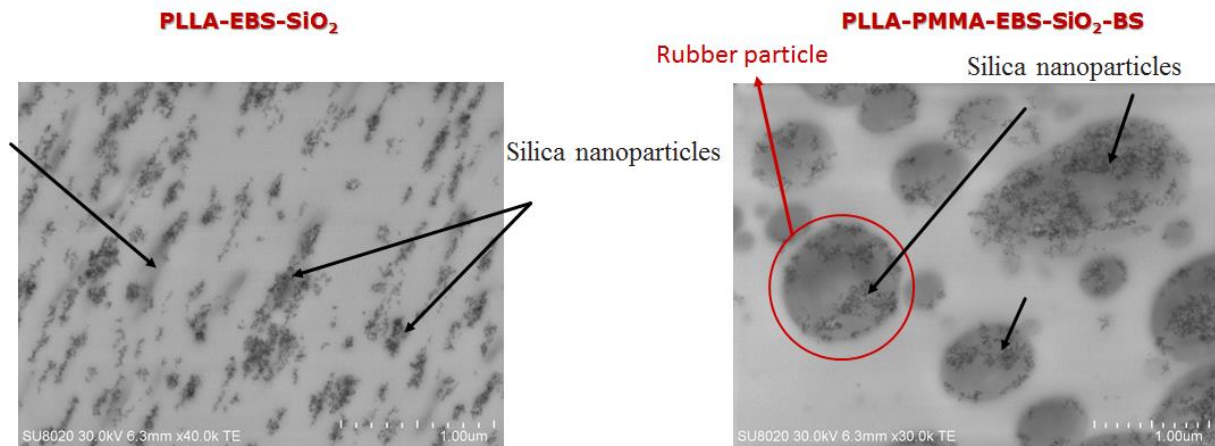


Figure 4. TEM des surfaces fracturées des mélanges à base de PLLA

Le dernier chapitre concerne la mise à l'échelle industrielle de la production des échantillons avec la formulation du mélange retenue (PLA70/PMMA30/BS). Pour l'extrapolation des résultats obtenus à grande échelle, le mélange ternaire PLA/PMMA/BS a été sélectionné pour une extrusion à grande échelle afin de vérifier la possibilité d'industrialisation du mélange élaboré et l'obtention des performances semblables à celles obtenus à l'échelle laboratoire. Une étude sur le temps de séjour du matériau à l'intérieur de l'extrudeuse a été étudié et montre que plus le temps est important plus les propriétés mécaniques de mélanges sont meilleurs (Figure 5).

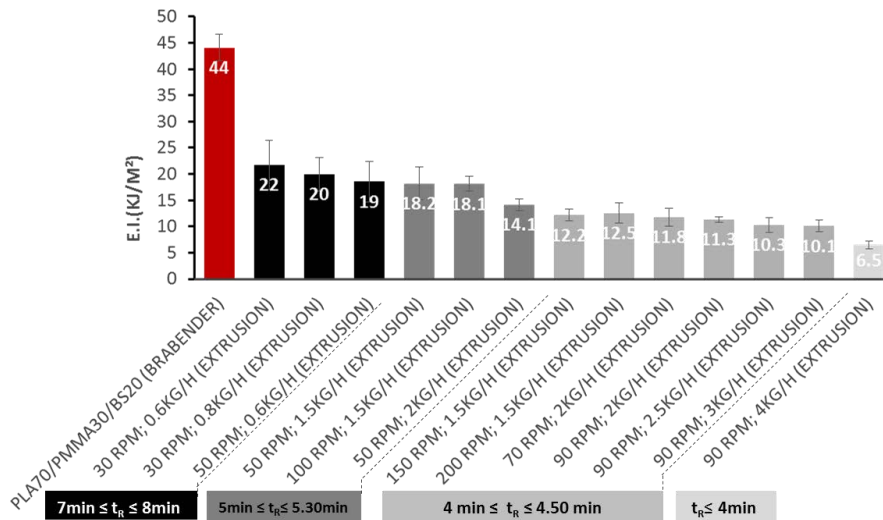


Figure 5. Evolution de la résistance aux chocs du mélange PLA70-PMMA30-BS20 en fonction du temps de séjour à l'intérieure de l'extrudeuse

Un choix de vitesse de rotation de vis et de débit de matière a été sélectionné pour avoir une importante quantité de matière permettant par la suite d'injecter des plaques avec la collaboration de l'industrie automobile. Une étude dynamique, quasi-statiques et thermodynamiques en traction ont été réalisés sur des éprouvettes à l'aide du logiciel de la corrélation d'image.

Les propriétés des matériaux obtenus sont comparées aux propriétés des mélanges ABS/PC utilisés aujourd'hui par l'industrie automobile. La ductilité des matériaux partiellement biosourcés est supérieure aux matériaux pétrochimiques, cependant la perte de rigidité aux températures de 50 et 60 °C est toujours supérieure.

Le chapitre se conclut sur une étude de la durabilité des mélanges PLA/PMMA/BS en comparaison à celle de l'ABS/PC sous conditions de vieillissement accéléré. Les résultats montrent qu'une utilisation du matériau biosourcé à l'intérieur du véhicule peut être envisagée, mais que sa durabilité pour des pièces extérieures n'est pas suffisante pour l'instant.

En perspective, le vieillissement hydrolytiques et sous UV sont aussi envisagés puisque le PLA est très sensible aux UV. Une continuation du développement des matériaux à base de PLA en ajoutant des fibres naturelles telque le Kenaf pour augmenter la stabilité thermique du PLA a été proposée. Une possibilité

d'impression 3D sera étudié comme perspectives afin d'élargir le domaine d'application de mélange avec une nouvelle technologie d'impression 3D « le Freeformer » (Figure 6). Une nécessité d'étudier l'adhésion entre les couches imprimées et les propriétés mécaniques des pièces est aussi indispensable.

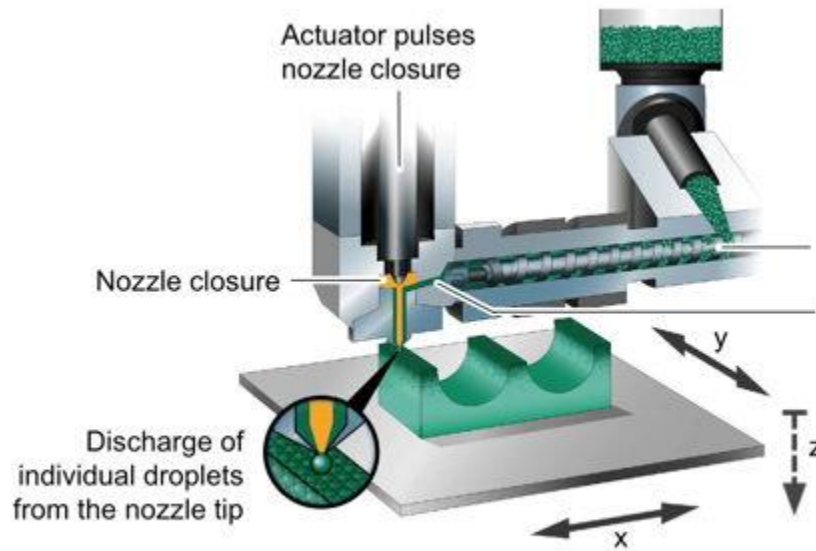


Figure 6. Diagramme descriptif de la machine d'impression 3D Freeformer